CATALOGING THE GENETIC DIVERSITY OF BATS (ORDER: CHIROPTERA) IN TURKEY

by

Zirve Yiğit

BS. in Biology, METU, 2008

Submitted to the Institute of Environmental Sciences in partial fulfillment of the requirements for the degree of

Master of Science

in

Environmental Sciences

Boğaziçi University

2012

DEDICATION

This project is dedicated to my mother, Zeliha Zengin, who has never failed to give me financial and moral support, for providing for all my needs during the time I worked on my thesis, and for teaching me the importance of hard work and higher education.

ACKNOWLEDGEMENTS

I would like to thank my supervisor, Assist Prof. Raşit Bilgin, for the patient guidance, encouragement and advice he has provided throughout my time working on this thesis. He also supplied all the necessary laboratory resources and documents for this project. I have been very blessed to have such a supervisor who cared so much about my work and responded to my questions so patiently. I would like to thank Assoc. Prof. Ahmet Karataş from Niğde University for sending those invaluable samples for this work. I would also like to thank Öncü Maracı, Evrim Kalkan and Emrah Çoraman at Boğaziçi University who helped me, especially with laboratory skills in my supervisor's absence. In particular, I would like to thank Prof. Andrzej Furman and Prof. Nüzhet Dalfes for the valuable contributions and suggestions they had for this work.

I am very thankful to my family; my mother and my brother for their love and understanding. I must also express my gratitude to Bill Bremmer for his willingness to proofread all the pages of this work.

Finally, I would like to thank the Research Fund of Boğaziçi University (No: 6183) for providing the funding which allowed me to undertake this research.

ABSTRACT

CATALOGING THE GENETIC DIVERSITY OF BATS (ORDER: CHIROPTERA) IN TURKEY

In this study, 26 bat species from Turkey and surroundings were investigated with the cytochrome-oxidase subunit I (CO1) barcoding method. Twelve CO1 sequences from Barcode of Life Database (BOLD) and Genbank and 134 specimens from Turkey and surroundings were analyzed. Neighbor-joining (NJ) and maximum-likelihood (ML) trees were generated and haplotype networks were prepared. For each species sequences were identified in BOLD, and a BOLD tree of each species was obtained for intraspecific and interspecific comparisons. Previous studies regarding Turkish bat fauna were reviewed to make species classifications based on morphological taxonomy. We found that at least six species have high intraspecific divergence and are good candidates for discovery of cryptic species or subspecies for the Turkish population. We found two species show high intraspecific divergence between the Turkish population and other populations. We conclude that, at least for bats, CO1 barcoding is a promising method for discovery of new taxa, as well as being a quick and efficient identification method.

ÖZET

TÜRKİYE'DE BULUNAN YARASA (ORDER: CHIROPTERA) TÜRLERİNİN GENETİK ÇEŞİTLİLİĞİNİN KATALOGLANMASI

Bu çalışmada, Türkiye ve yakın çevresinde bulunan 26 yarasa türü, cytochrome-oxidase subunit I (CO1) barkodlaması yöntemiyle incelenmiştir. Yaşam Barkodu Veri Tabanı (BOLD) ve Gen Bankası'ndan elde edilen 12 CO1 sekansı ve ayrıca Türkiye ve yakın çevresinden alınan 134 adet örnek analiz edildi. Neighbor-joining (NJ) ve maximum-likelihood (ML) ağaçları oluşturuldu ve haplotip ağları hazırlandı. Herbir türün sekansı BOLD aracılığıyla tanımlandı. Tür-içi ve türler arası karşılaştırmalar yapmak için BOLD ağaçları çalışmaya eklendi. Türkiye yarasalarının morfolojik taksonomi bilgilerini gözden geçirerek tür sınıflandırması yapmak için önceki bilimsel makaleler değerlendirildi. Çalışmamızdaki en az altı yarasa türünde yüksek tür-içi farklılıkları gözlendiği için bu türler gelecekteki kriptik ya da alt tür çalışmaları için iyi birer aday olarak gösterilebilirler. Ayrıca Türk yarasa popülâsyonu ve diğer popülâsyonlar arası tür içi farklılıkları olan iki tür gözlemledik. Özet olarak, CO1 barkodlama metodunun, en azından yarasalar için, çabuk ve yeterli bir sistem olmasının yanı sıra yeni sınıflandırma düzeylerinin bulunmasında da iyi bir rol oynadığını düşünüyoruz.

TABLE OF CONTENTS

LIST OF TABLES

LIST OF FIGURES

LIST OF SYMBOLS/ABBREVIATIONS

Symbol	Explanation
BOLD	Barcode of Life Database
bp	Base pair
COI, CO1	Cytochrome oxidase I
DNA	Deoxyribonucleic Acid
DNTP	Deoxyribonucleotide triphosphate
EDTA	Ethylenediaminetetraacetic acid
H	Haplotype
IUCN	International Union for Conservation of Nature
mtDNA	Mitochondrial DNA
ML	Maximum-likelihood
NJ	Neighbor-joining
PCR	Polymerase chain reaction
TBE	Tris base boric acid, EDTA

1. INTRODUCTION

1.1. DNA Barcoding

DNA barcoding is a method that uses a standard barcode sequence to identify an organism by comparing it to a known database of sequences. For animals and many other eukaryotes, variations in the 650-bp fragment of the mitochondrial cytochrome-oxidase subunit I (CO1) gene are investigated for DNA barcoding. According to Hebert et al. (2003) and Saccone et al. (1999), mitochondrial genes instead of nuclear genes should be used for barcoding purposes since animal mitochondrial genome lacks introns, is exposed to limited recombination and is haploid. Similarly, mitochondrial genes encoding ribosomal (12S, 16S) DNA have insertions and deletions (indels) that can complicate the alignments (Hebert et al. 2003, Doyle and Gaut 2000). Hence 13 protein-coding genes are better suited for DNA barcoding since indels are relatively uncommon in them. In addition, the third-positions of mitochondrial genes exhibit a comparatively high rate of base substitutions, and have a rate of molecular evolution about three times higher than that of 12S or 16S rDNA (Knowlton and Weight 1998). This shows that the CO1 gene evolves fast enough to discriminate not only closely related species, but also phylogeograhic groups within a single species.

The CO1 gene has two important advantages over other 12 protein-coding mitochondrial genes. First, there are many universal primers for this gene, and second, changes in its amino acid sequence occur more slowly than any other mitochondrial gene. As a result, any unidentified organism may be assigned to a higher taxonomic group before examining nucleotide substitutions to determine its species identity (Hebert et al. 2003).

A number of studies have shown that CO1 sequence variability within a species is very low (generally less than 1-2%) and having higher intraspecific divergence may be a sign of a species complex. According to Hebert et al. (2003), DNA barcoding has four main advantages over morphological identification. First, it eliminates incorrect identifications caused by phenotypic plasticity and genetic variability. Phenotypic

plasticity is the production of multiple phenotypes from a single genotype, depending on environmental conditions (Miner et al. 2005), and genetic variability is a measure of the tendency of individual genotypes in a population to vary from one another (e.g., Mendel's experiments). Second, DNA barcoding can provide insights when cryptic species are studied. Third, genetic identification is not limited to particular life stages or the sex of certain species. Lastly, a high level of expertise is not needed for species identification. Usually, CO1 itself is enough to identify a species, but in case it remains inefficient for certain groups, additional genes may also be sequenced.

Dry museum specimens can also be sequenced with great success to assemble a comprehensive DNA barcode library (Hebert et al. 2004a). Museum specimens, however, may be lacking the 650 bp-length mitochondrial DNA region; therefore, in order to improve sequencing from museum specimens, mini-barcodes have been shown to be effective (Hajibabaei et al. 2006). However, obtaining full-length barcodes instead of mini-barcodes increases the resolution (Hajibabaei et al. 2007).

1.2. Bats as Target Species

Bats are the only mammals that can fly. Most of them have fur or hair, they give birth to live young, and they feed milk to their newborn. While most bats feed mainly on insects, others feed on leaves, fruit and/or nectar and pollen. Some bats eat fish, frogs, birds and other bats. Vampire bats feed only on blood. Approximately 20% of all mammal species belong to the order Chiroptera (Wilson and Reeder 2005). Bats are arranged into two major categories (suborders); the Megachiroptera, or large bats, and the Microchiroptera, or small bats. Bats occupy a wide range of habitats, such as wetlands, woodlands, farmlands, and urban areas. They have a relatively long life-span, produce low numbers of offspring (usually one offspring once or twice a year), migrate (10% of the known bat species) and they live in stable, predictable habitats with populations close to their carrying capacity. Bat communities are, therefore, resource limited and competition-based groups (Findley 1993).

Bats are key species in their particular environments; they are top predators of common insects. They are sensitive to land use practices, construction and changes in water quality. Fenton et al. (1992) showed that there is a high difference in species diversity between disturbed and undisturbed sites (deforestation) in their study of Phyllostomid bats in the Neotropics. Monitoring nocturnal bats also helps scientists understand the effects of generally undetectable minor environmental changes such as light pollution.

Species identification is a vital part of biodiversity studies. Although most mammal species are thought to have been described (Wilson and Reeder, 2005), bats remain one of the problematic groups due to their cryptic behavior and morphology.

1.2.1. Morphological Identification of Bats

The first step in identifying a captured bat is determining whether it is a male or a female. In some bats, this is easy bacuse the penises of bats are apparent but in others, it might be hard to distinguish since they have excessive fur around their genitals.

Age determination is the next step. Because bats generally grow rapidly, the forearms of the young are as long as those of adults by the time they can fly. Therefore, it is difficult to tell the difference between an adult-sized young and an adult. In many bats, young have dark, blackish fur compared to lighter colored fur in adults. Finger joints are also good indicators. Adult bats have knobby finger joints, while young bats have smooth ones. Differences in finger joints can be seen when the wing of the bat is back-lit. Other than these methods, no other non-lethal procedures have yet been developed by biologists.

After determining its sex and age, the next problem is determining the species of the bat in hand. The first step is deciding which of the 19 living families it belongs to. Biologists use “keys” to identify organisms. These are logical, stepwise morphological features presented to help determine the species identity of a bat. In some cases, bat detectors can also help to recognize different species by their calls. Sattler et al. (2007) show that, echolocation studies coupled with habitat data help to recognize cryptic species *Pipistrellus pipistrellus* and *Pipistrellus pygmaeus* in Europe.

1.3. Cryptic Species and DNA Barcoding

Since the introduction of binomial nomenclature by Linnaeus, present taxonomic information is highly built on morphological data. However, morphologically cryptic taxa are very common in many groups, which can lead to misleading classifications. Cryptic species are two or more genetically distinct but morphologically similar species that are classified as a single species (Pfenninger and Schwenk, 2007). The evolution of the CO1 gene is rapid enough to discriminate phylogeographic groups and putative species within a single species complex (Cox and Hebert 2001, Wares and Cunningham 2001).

Mayer and von Helversen's (2001) work is worth mentioning for our study. Instead of using the CO1 mitochondrial gene region, they preferred another mitochondrial gene region, namely NADH dehydrogenase, subunit 1 (ND1). In their study, they observe that convergent adaptive evolution may result in morphological similarity among distantly related species if they live in similar niches. They also state that closely related species may differ in their ecology but not necessarily in their morphology. They conclude that both morphological and genetic analyses are necessary for species identification.

Mayer et al. (2007) show that DNA barcodes are helpful in describing a high number of undiscovered species. For the Western Palaearctic realm, 37 vespertilionid bat species were defined prior to mitochondrial ND1 sequencing. After the study, a total of 51 species were distinguished. They also discovered that species pairs *Eptesicus serotinus*/*Eptesicus nilssonii*, *Myotis myotis/M. oxygnathus* and *Pipistrellus kuhlii/P. deserti* are genetically very similar, although they are morphologically very different. Recent speciation or introgressions of mitochondrial haplotypes are likely explanations for these three species pairs. Although *Hypsugo ariel* and *H. bodenheimeri* are previously recorded as different species, they are treated as one species in Mayer et al.'s (2007) study as morphological differences are restricted to an additional cusp at the second upper incisor in *H. bodenheimeri.*

Clare et al. (2006) investigated 87 species of bats from Guyana, six which showed divergent intraspecific lineages, indicating that they represent species complexes. The authors believe that the assembly of a DNA barcode library will not only help recognition

of cryptic species, but will also lead to the development of an automated identification system.

2. THESIS OBJECTIVES

CO1 sequence differences between closely related species are higher than differences within species. Hebert et al. (2004b) proposes a standard sequence threshold of ten times the mean intraspecific variation for a particular group under investigation. Using this threshold approach, studying groups like bats, which have not received intensive taxonomic analysis, can give new insights on unidentified species.

Because obtaining full-length barcodes instead of mini-barcodes increases the resolution (Hajibabaei et al. 2007), full-length barcodes are used in our study to help clarify the taxonomic status of some cryptic bat species within Turkey.

In a recent study, DNA barcodes from nearly 1900 specimens representing 165 mammalian species in Southeast Asia showed that the approach can aid conservation by determining species groups needing more detailed analysis for conservation planning in biodiversity hotspots (Francis et al. 2010). Cryptic species identification in Turkey will provide a clearer picture of species distribution in this region and define subspecies-specific measures to be taken in order to conserve certain threatened Turkish bats. A better knowledge of species diversity of bats will help us understand the phylogeography of the species in Turkey.

A high level of intraspecific variation implies that there might be cryptic species within the group being investigated. According to Clare et al. (2006), CO1 divergence of conspecifics greater than 2.5% will provide an idea of potential cryptic species because in previous studies of bats, sequence diversity in cytochrome b is shown to be less than 2.5% and rates of evolution in cytochrome b and CO1 are similar.

It is also important to evaluate nuclear genetic markers before drawing conclusions through genetic identification methods (Berthier et al. 2006). Evaluating historical as well as contemporary factors through the use of mitochondrial and nuclear markers helped researchers determine the complete picture in evolution of *Myotis myotis* and *Myotis blythii*. Therefore, our study will reveal a part of the big picture by using

single-gene (CO1) sequences. Mayer and von Helversen (2001) had a similar task in their attempt to study cryptic bat species in Europe. They concluded that neither morphological nor mitochondrial DNA sequence analysis alone can be guaranteed to identify species.

Hence, from this perspective, the main objective of this thesis is to investigate the mitochondrial CO1 region to help clarify the presence of cryptic species within Turkey by comparing our results with the literature.

3. MATERIALS AND METHODS

3.1. Sample Information

In this project, a total of 134 bat samples from 26 species were collected and analyzed. The species that were barcoded, with their corresponding localities from Turkey and a few samples from its neighbors, are shown in Appendix A.

3.2. Laboratory Methods

3.2.1. DNA Extraction

ROCHE DNA Extraction Kits (Mannheim, Germany) were used for the DNA extraction of bat tissue samples. Manufacturer's protocol was followed with one modification. In the first step of the protocol, the incubation time of sample tissue with Lysis Buffer and Proteinase K was increased to 24 hours to enhance the lysis of the cell membranes.

The isolated DNA strands were checked in electrophoresis. In order to prepare agarose gels, 1% agar was prepared in 1X TBE (Tris base, boric acid, EDTA) buffer with Ethidium bromide. 3 µl of isolated DNA mixed with 3 µl of 1X loading dye (Fermentas) were loaded on the gel for each reaction. Samples were run at 90 V for 45 minutes. The band images were taken under ultraviolet light by Biorad Gel Doc Imaging System.

3.2.2. PCR Amplification

In order to amplify the CO1 region of the bat species mentioned above (Table 3.1), the polymerase chain reaction (PCR) was performed according to the procedures described in Hajibabaei et al. (2005) with some modifications after optimizations. These included 2.5 µL 10X NH4 (MgCl2 free) PCR buffer, 2.5 µL (2.5 mM) MgCl2, 3.125 µL (10 µM) forward and reverse primer cocktail, 0.5 µL (10 µM) DNTPs, 0.3 µL *Taq* polymerase and 1 µL template DNA in a total volume of 25 µL. PCRs were run under the

following thermal cycle conditions: 1 min at 94°C followed by 10 cycles of 30 s at 94°C, 40 s at 50°C, and 1 min at 72°C, followed by 35 cycles of 30 s at 94°C, 40 s at 55°C, and 1 min at 72°C, and finally 10 min at 72°C (Clare et al. 2006). Primer cocktails for PCRs are obtained from Ivanova et al. (2006) and given in Table 3.1.

Table 3.1. Primer cocktails (Ivanova et al. 2006).

PCR Cocktail	Primers
Cocktail 1 F	**VF1 5'-TTCTCAACCAACCACAAAGACATTGG-3'**
	VF1d 5'-TTCTCAACCAACCACAARGAYATYGG-3'
	VF1i 5'-TTCTCAACCAACCAIAAIGAIATIGG-3'
Cocktail 1 R	**VR1 5'-TAGACTTCTGGGTGGCCAAAGAATCA-3'**
	VR1d 5'-TAGACTTCTGGGTGGCCRAARAAYCA-3'
	VR1i 5'-TAGACTTCTGGGTGICCIAAIAAICA-3'
Cocktail 2 F	**LepF1_t1 5'TGTAAAACGACGGCCAGTATTCAACCAATCATAAAGATATTGG-3'**
	VF1_t1 5'-TGTAAAACGACGGCCAGTTCTCAACCAACCACAAAGACATTGG-3'
	VF1d_t1 5'-TGTAAAACGACGGCCAGTTCTCAACCAACCACAARGAYATYGG-3'
	VF1i_t1 5'-TGTAAAACGACGGCCAGTTCTCAACCAACCAIAAIGAIATIGG-3'
Cocktail 2 R	**LepR1_t1 5'-CAGGAAACAGCTATGACTAAACTTCTGGATGTCCAAAAAATCA-3'**
	VR1_t1 5'- CAGGAAACAGCTATGACTAGACTTCTGGGTGGCCAAAGAATCA-3'
	VR1d_t1 5'-CAGGAAACAGCTATGACTAGACTTCTGGGTGGCCRAARAAYCA-3'
	VR1i_t1 5'- CAGGAAACAGCTATGACTAGACTTCTGGGTGICCIAAIAAICA-3'

Cocktail 1 primers with a concentration of 10 pmol/mL were mixed in a 1:1:2 ratio (VF1 : VF1d : VF1i for the forward cocktail; VR1 : VR1d : VR1i for reverse). Cocktail 2 (C_VF1LFt1/C_VR1LRt1), was an improved version including M13-tailed versions of the primers and an additional primer pair, LepF1_t1 and LepRI_t1 in the following ratio; 10 pmol/μL, VF1_t1: VF1d_t1: LepF1_t1: VF1i_t1 (1:1:1:3) or VR1_t1: VR1d_t1: LepRI_t1: VR1i_t1 (1:1:1:3) (Ivanova et al. 2006).

3.2.3. Gel Electrophoresis

1% agarose gels were prepared in 1X TBE (Tris base, boric acid, EDTA) buffer with Ethidium bromide to check the PCR products. 3 µl of the PCR product mixed with 3 µl of 1X loading dye (Fermantas) were loaded on the gel for each reaction. Samples were run at 90 V for 45 minutes and then the gels images were taken under ultraviolet light by the Biorad Gel Doc Imaging System. Specimens giving intense PCR product bands were selected for sequencing.

3.2.4. PCR Sequencing

PCR products were sent to Macrogen Inc. in South Korea for commercial sequencing. Samples producing single clear amplicons from cocktail 1 were sequenced with VF1d and VR1d and samples producing single clear amplicons from cocktail 2 were sequenced with M13F (-21) 5'- TGTAAAACGACGGCCAGT-3' and M13R (-27) 5'-CAGGAAACAGCTATGAC-3' (Norrander et al. 1983, Ivanova et al. 2006, Electronic Appendix 1 BOLD web site: Primer cocktail sequences).

3.3. Analytical Methods

3.3.1. Species Identification

Taxonomic keys were used for morphologic identification by Ahmet Karataş of Niğde University prior to using the BOLD specimen identification tool and our CO1 sequences.

3.3.2. Sequence Analysis

Phylogenetic trees were constructed using neighbor-joining and maximum likelihood methods. The MEGA program version 5.05 (Tamura et al. 2011) was used for constructing trees. Neighbor-joining trees were prepared using Kimura 2-parameter distances and bootstrap method with 1000 bootstrap replicates. Maximum-likelihood trees were prepared again with 1000 bootstrap replicates to assess branch support. CO1

sequences partititoned in Maximum-likelihood according to General Time Reversible model with Gamma-distributed with Invariant Sites (G+I) (Tanner et al. 2011).

Intraspecific and interspecific distances were calculated by MEGA using Kimura 2-parameter distances. DnaSP5 (Librado and Rozas 2009) and TCS1.21 (Clement et al. 2000) programs were used for building haplotype data file and preparing haplotype networks, respectively. All specimens were identified in BOLD using the “identify specimen” tool. According to intraspecific tree results, at least one individual from each clade was compared with BOLD barcodes, and the results are presented in the “Results” section below.

4. RESULTS

In our study, 134 CO1 sequences from 26 different species were generated. The mean intraspecific divergence for the CO1 sequences was 1.1%. The mean interspecific distance was 20.5%. A plot of the frequency of intraspecific and interspecific distances can be seen in Figure 4.1.

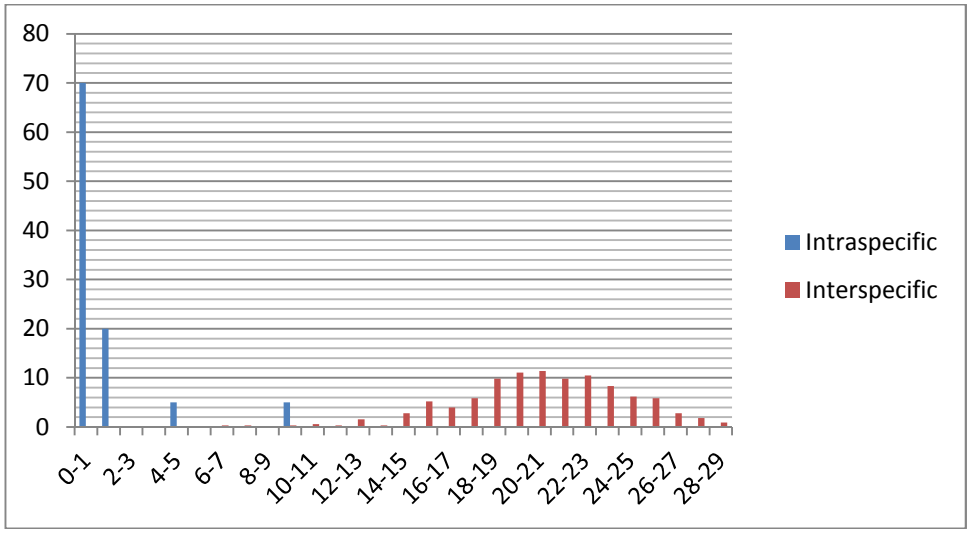

Figure 4.1: Frequency distribution of mean divergences for CO1 sequences for 134 samples, calculated by the Kimura 2-parameter model. Two taxonomic levels are represented: within species (blue bars) and between species (red bars).

For each species, intraspecific neighbor-joining and maximum likelihood trees, a haplotype network, and a BOLD tree (neighbor-joining) were prepared. In the haplotype network, the different colors which were used to indicate different regions are shown in Table 4.1.

Table 4.1. Colors that were used to indicate different regions in the haplotype networks.

REGION	Color
Black Sea	Light green
Mediterranean	Dark green
Central Anatolia	Yellow
Marmara	Purple
East Anatolia	Pink
Aegean	Blue
Southeast Anatolia	Orange
Syria	Light gray
Iran	Dark gray
BOLD+Genbank sequences (unknown)	White

4.1. *Rhinolophus euryale*

Fourteen CO1 sequences were analyzed for *Rhinolophus euryale*. The sequences were obtained from four regions; three individuals from the Black Sea region (two from Zonguldak, one from Sinop), four individuals from the Marmara region (two from Kocaeli, Balıkesir, Kırklareli), one individual from the Aegean region (Denizli) and six individuals from the Mediterranean region (four from Mersin, two from Hatay) (Figure 4.2).

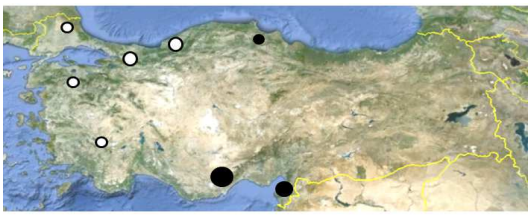

Figure 4.2. The sampling locations for *Rhinolophus euryale*. The circles are proportional to the number of individuals. The black color indicates sampling locations for the first group and the white color indicates sampling locations for the second group in the intraspecific trees (Figure 4.3).

Intraspecific trees for *Rhinolophus euryale* are shown in Figure 4.3. All CO1 sequences generated two groups/clades, and individuals in Group One (samples 77, 36, 72, 17, 37, 70, and 67) were seen in the Black Sea and the Mediterranean regions. The individuals that are coded as samples 69, 16, 34, 200, 68, 71, 35 formed their own clade (Group Two) and were collected from the Aegean, the Black Sea and the Marmara regions.

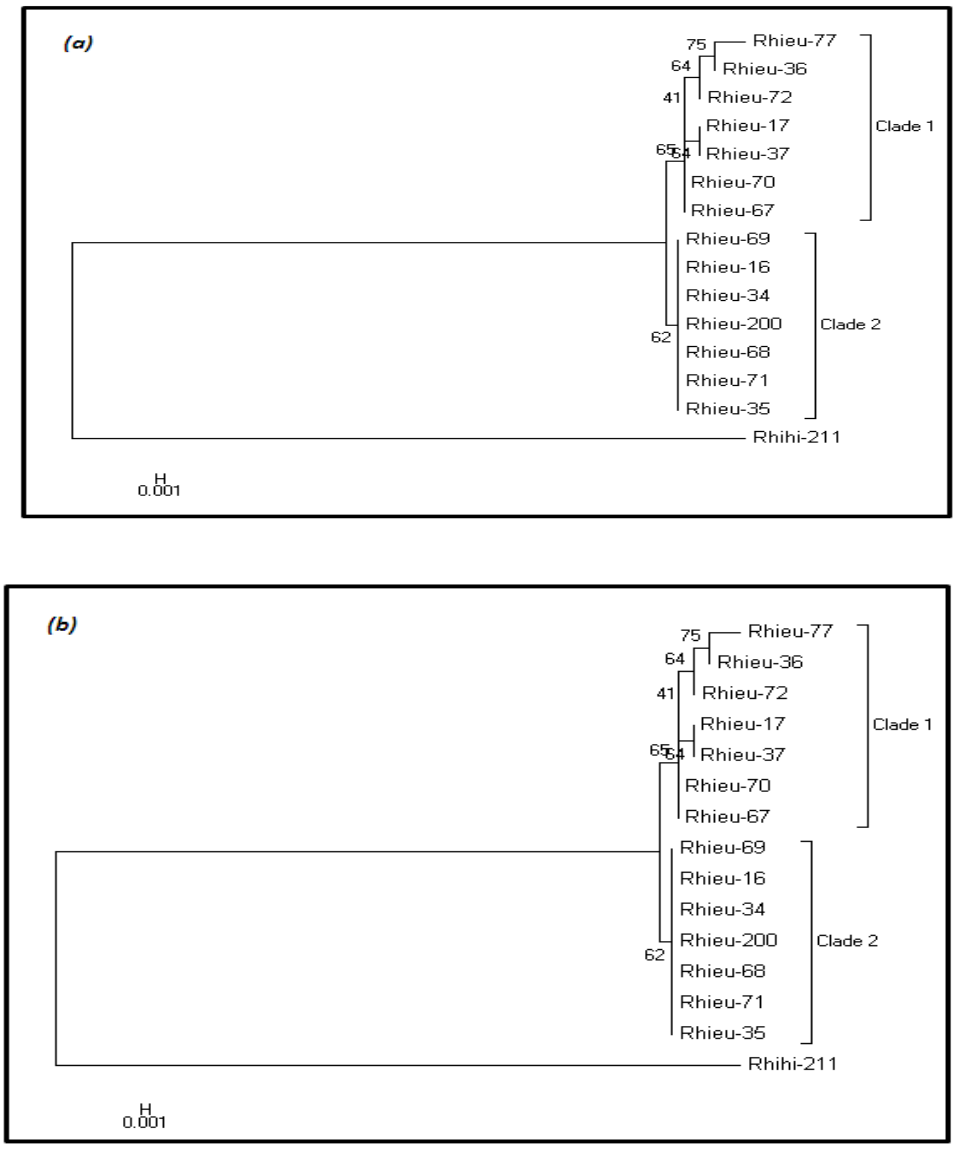

Figure 4.3. Intraspecific trees for *Rhinolophus euryale*. (a) NJ tree and (b) ML tree.

There were six different haplotypes in this species as shown in the haplotype network and the haplotype network table (Figure 4.4 and Appendix B). H2 was the most

common haplotype (seven individuals), and was found in the Aegean region, the Black sea region and had its highest frequency in the Marmara region within the data set.

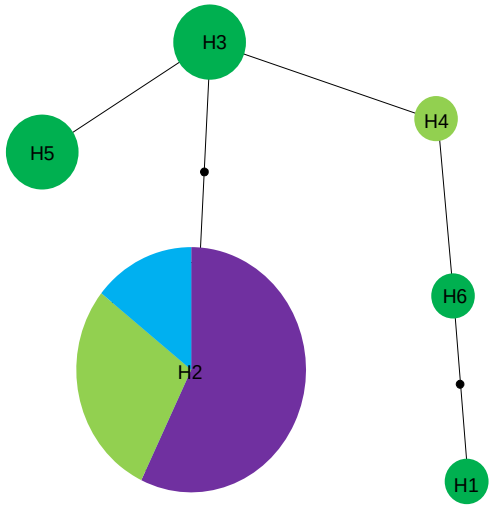

Figure 4.4. Haplotype network for *Rhinolophus euryale*. The sizes of the circles are proportional to the number of individuals. See Table 4.1 for the key to the color codes of the geographic positioning of the haplotypes.

Next, we compared the sequences of the individuals from each clade to those available in BOLD. From Group One we selected one representative individual, 77, and comparing it with the data from BOLD, the closest match to this sample was *Rhinolophus euryale* with a specimen similarity of 99.01%. Comparing the sequence of an individual from Group Two, *Rhinolophus euryale* 200, with the matches that were taken from BOLD, the closest match of *Rhinolophus euryale* 200 was *Rhinolophus euryale* again with a specimen similarity of 100%.

The neighbor-joining tree for *Rhinolophus euryale*, created with BOLD, using one individual belonging to Group One, *Rhinolophus euryale*-77, is shown in Figure 4.5. In the tree, the barcoded individual from Turkey clustered with *Rhinolophus euryale* barcodes in BOLD. The neighbor-joining tree from BOLD for *Rhinolophus euryale* 200 from Group Two is also shown in Figure 4.6. Notably, *Rhinolophus euryale* 200 fell within the same branch but a little bit closer than the *Rhinolophus euryale* 77 to the rest of the samples of *R. euryale* found in BOLD.

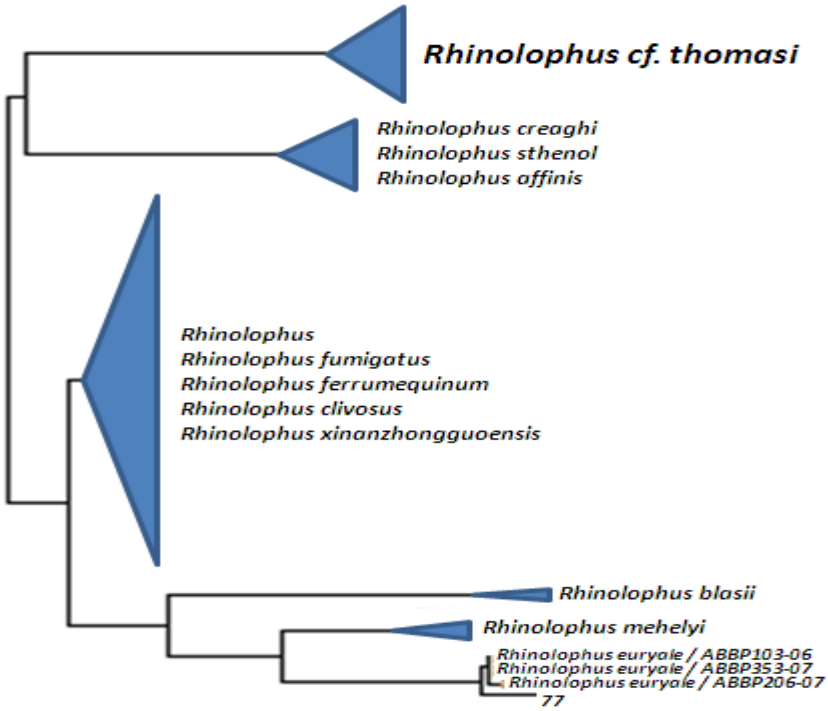

Figure 4.5. Neighbor-joining tree for one of our *Rhinolophus euryale* sequences, sample 77, constructed based on BOLD. The sizes of the triangles are proportional to the number of sequences in BOLD for that species.

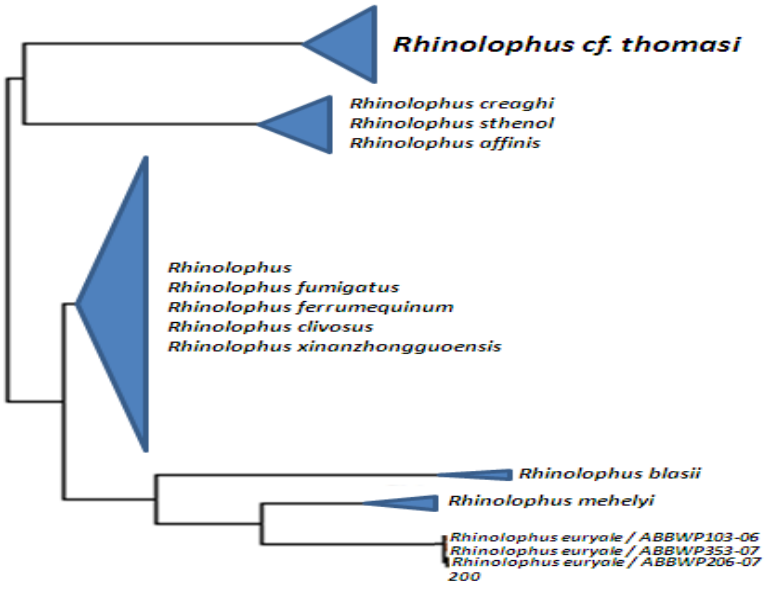

Figure 4.6. Neighbor-joining tree for one of our *Rhinolophus euryale* sequences, sample 200, construvted based on BOLD. The sizes of the triangles are proportional to the number of sequences in BOLD for that species.

4.2. *Rhinolophus ferrumequinum*

Fifteen CO1 sequences were analyzed for *Rhinolophus ferrumequinum*. The sequences were obtained from six regions; two individuals from the East Anatolia region (Kars, Van), four individuals from the Southeast Anatolia region (two from Gaziantep, Şanlıurfa, Mardin), three individuals from the Marmara region (Kırklareli, Çanakkale, Balıkesir), three individuals from the Black Sea region (Rize, Karabük, Zonguldak), one individual from the Mediterranean region (Hatay) and two individuals from the Central Anatolia region (Niğde) (Figure 4.7).

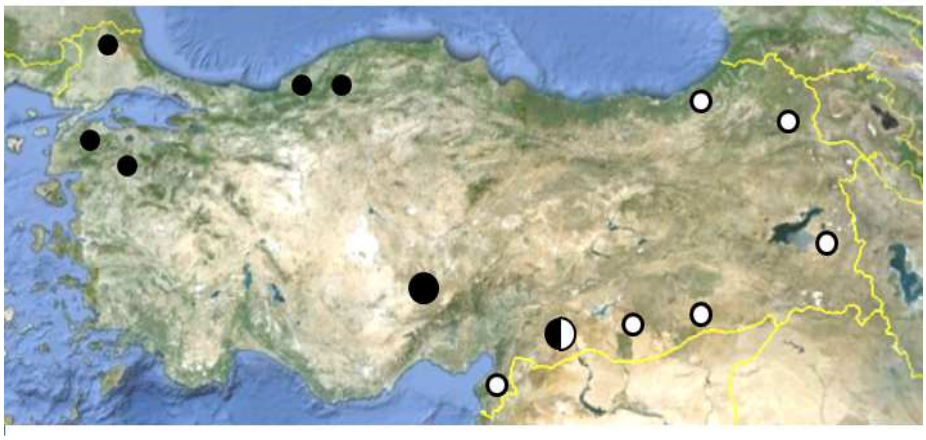

Figure 4.7. The sampling locations for *Rhinolophus ferrumequinum*. The circles are proportional to the number of individuals. The black color indicates sampling locations for the first group and the white color indicates sampling locations for the second group in the intraspecific trees (Figure 4.8).

Intraspecific trees for *Rhinolophus ferrumequinum* are shown in Figure 4.8. All CO1 sequences generated two clades; Group One (samples 2, 26, 76, 136, 174, 184, 202, and 205) was seen in the Southeast Anatolia region, the Marmara region, the Central Anatolia region and the Black Sea region. Group Two (samples 1, 3, 27, 73, 74, 75 and 81) was seen in the East Anatolia region, the Southeast Anatolia region, the Black Sea region and the Mediterranean region.

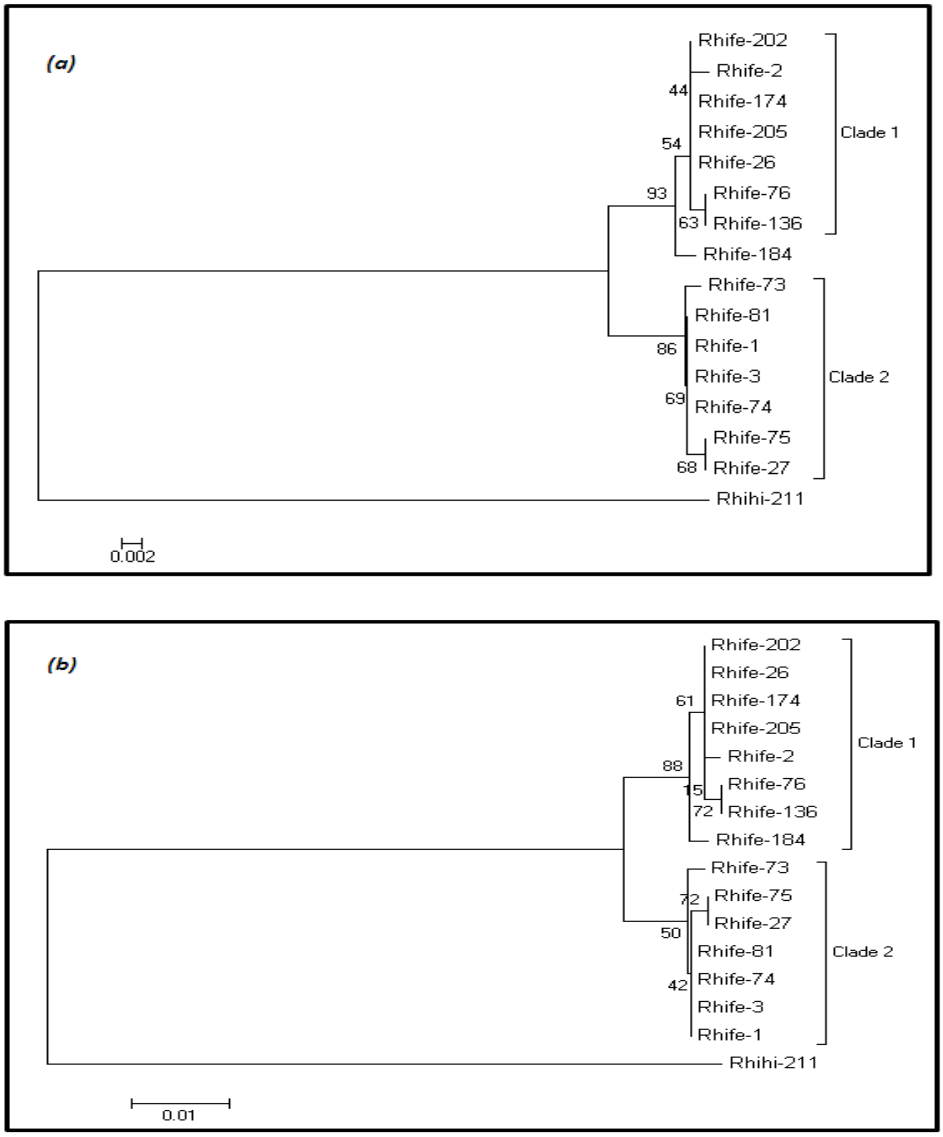

Figure 4.8. Intraspecific trees for *Rhinolophus ferrumequinum*. (a) NJ tree and (b) ML tree.

There were eight different haplotypes in this species as seen in the haplotype network and the haplotype network table (Figure 4.9 and Appendix B). H3 was the most common haplotype (found in four individuals), and was found in the Marmara region and the Black Sea region. Haplotypes H1, H3, H7 and H8 formed one group (Group One), which was separated by eight/nine base pairs from Group Two (Haplotypes H2, H4, H5 and H6). Groups One and Two outlined through the haplotype network matched exactly with the groups that were created by using intraspecific trees.

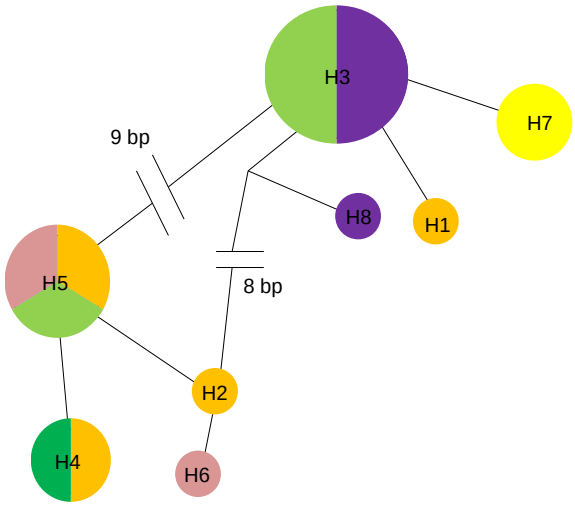

Figure 4.9. Haplotype network for *Rhinolophus ferrumequinum*. The sizes of the circles are proportional to the number of individuals. See Table 4.1 for the key to the color codes of the geographic positioning of the haplotypes.

As a next step, we compared the sequences of the individuals from each clade to those available in BOLD. From Group One, we selected one representative individual, 76, and comparing it with the data from BOLD, the first closest match to sample 76 was *Rhinolophus ferrumequinum* with a specimen similarity range of 99.84-98.01%, the second was *Rhinolophus clivosus* with a specimen similarity of 97.04% and the third was *Rhinolophus* with a specimen similarity range of 95.89-95.07%. From Group Two, we selected one representative individual, 27, and comparing the sequence with the data from BOLD, the first closest match was *Rhinolophus ferrumequinum* with a specimen similarity range of 100-98.19%, the second was *Rhinolophus clivosus* with a specimen similarity of 97.37% and the third was Rhinolophus with a specimen similarity range of 95.89-95.24%.

The neighbor-joining tree for *Rhinolophus ferrumequinum*, created with BOLD, using two individuals (samples 76, 184) belonging to Group One and two individuals (samples 27, 73) belonging to Group Two is shown in Figure 4.10. In the tree, the barcoded individuals from Group One clustered with one clade of *Rhinolophus ferrumequinum* barcodes whereas the barcoded individuals from Group Two clustered with another clade of *Rhinolophus ferrumequinum* barcodes in BOLD. The BOLD tree showed three *Rhinolophus ferrumequinum* clades in total. One individual belonging to *Rhinolophus clivosus* was observed among *Rhinolophus ferrumequinum* clades. There were three other

unidentified *Rhinolophus* clades forming a large monophyletic branch, including *Rhinolophus ferrumequinum* and *Rhinolophus clivosus*.

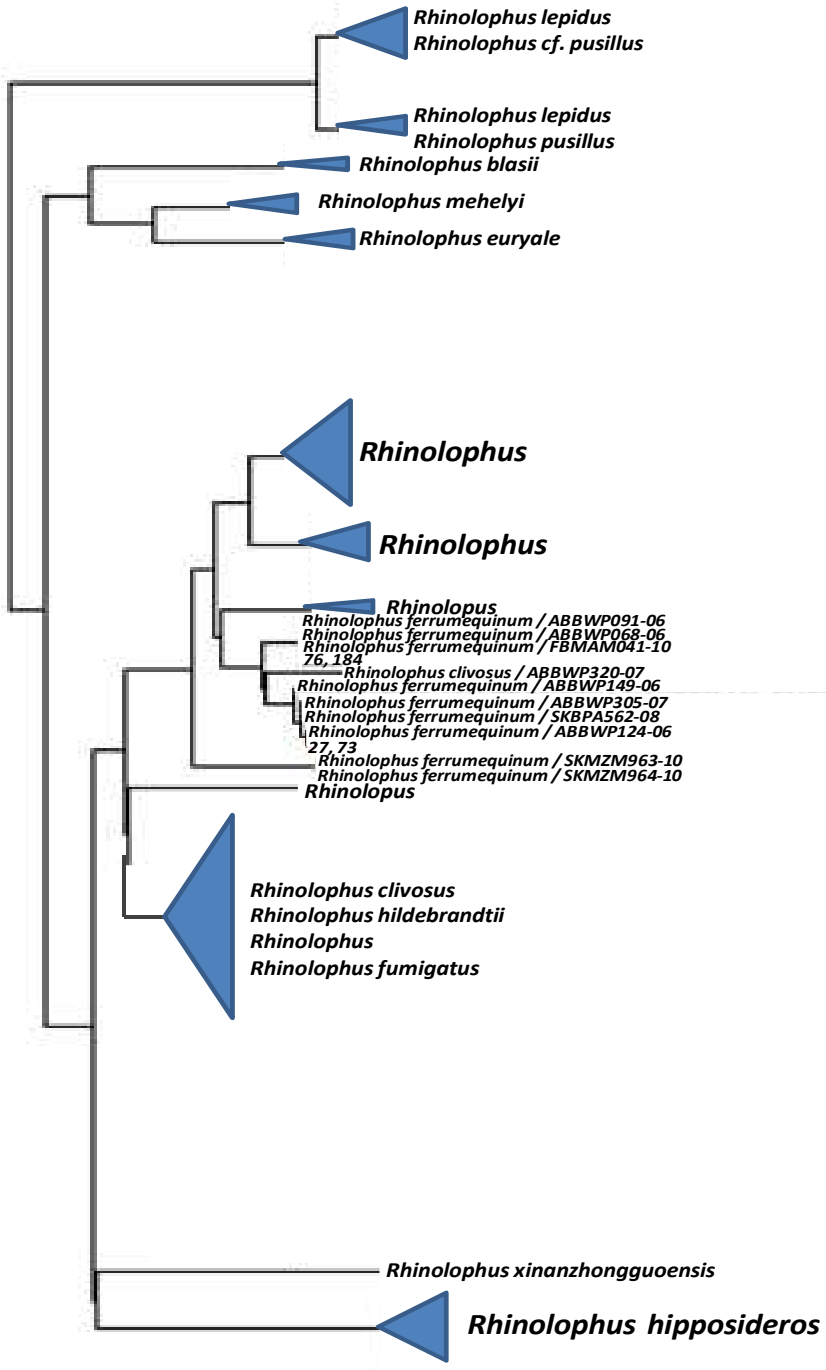

Figure 4.10. Neighbor-joining tree for four of our *Rhinolophus ferrumequinum* sequences (samples 76, 184, 27, 73) constructed based on BOLD. The sizes of the triangles are proportional to the number of sequences in BOLD for that species.

4.3. *Rhinolophus hipposideros*

Fifteen CO1 sequences were analyzed for *Rhinolophus hipposideros*. The sequences were obtained from six regions: one individual from the East Anatolia region (Erzincan), one individual from the Southeast Anatolia region (Şanlıurfa), two individuals from the Marmara region (Balıkesir, Bursa), eight individuals from the Black Sea region (three from Zonguldak, Ordu, Bartın, Sinop, Trabzon, Karabük), one individual from the Mediterranean region (Antalya) and two individuals from the Central Anatolia region (Niğde, Sivas) (Figure 4.11).

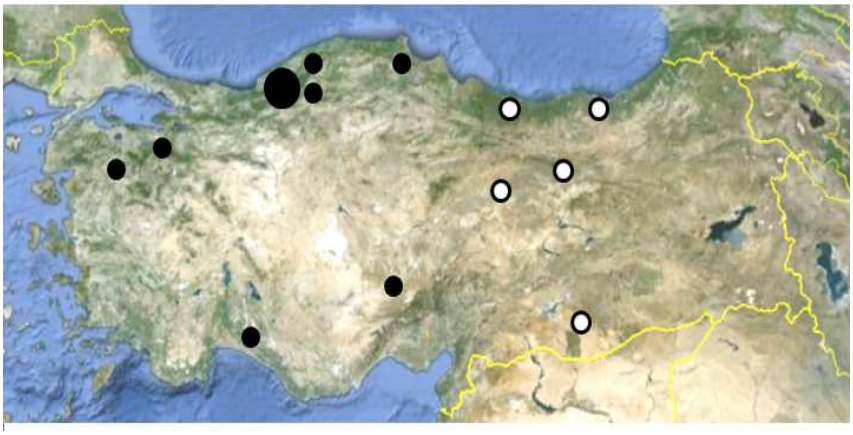

Figure 4.11. The sampling locations for *Rhinolophus hipposideros*. The circles are proportional to the number of individuals. The black color indicates sampling locations for the first group and the white color indicates sampling locations for the second group in the intraspecific trees (Figure 4.12).

Intraspecific trees for *Rhinolophus hipposideros* are shown in Figure 4.12. All CO1 sequences generated two clades; Group One (samples 195, 208, 197, 235, 196, 204, 182, 245, 161 and 144) was seen in the Black Sea region, the Marmara region, the Mediterranean region and the Central Anatolia whereas Group Two (samples 191, 188, 190, 211 and 139) was seen in the Southeast Anatolia region, the Central Anatolia region, the East Anatolia region and the Black Sea region.

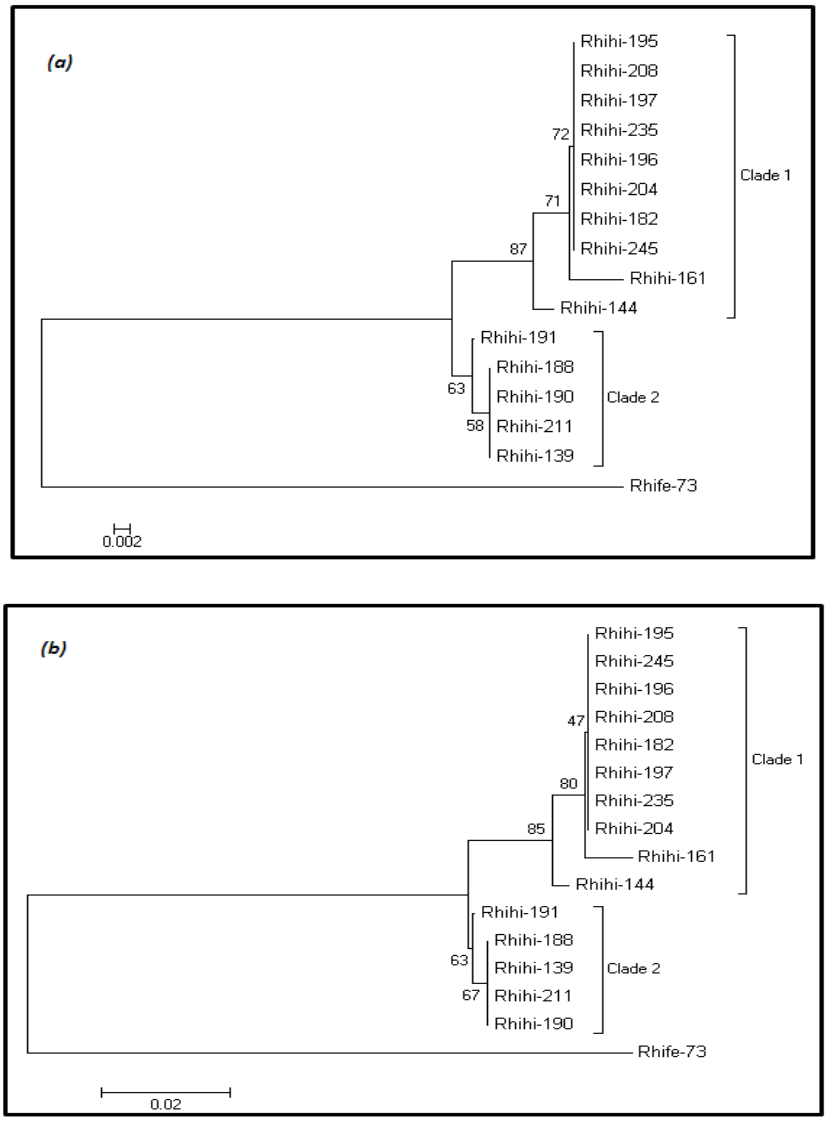

Figure 4.12. Intraspecific trees for *Rhinolophus hipposideros*. (a) NJ tree and (b) ML tree.

There were seven different haplotypes in this species as seen in the haplotype network and the haplotype network table (Figure 4.13 and Appendix B). H1 was the most common haplotype (found in seven individuals), and was found in the Marmara region and had its highest frequency in the Black Sea region within the data set. A comparison of intraspecific trees and the haplotype network showed that haplotypes H1, H3, H4 and H5 formed one group (Group One in the intraspecific tree), which was separated by six base pairs from Group Two (haplotypes H2, H6 and H7). In addition, H3 (individual 161) and H4 (individual 144) were separated by three and four base pairs, respectively from H1 in Group One.

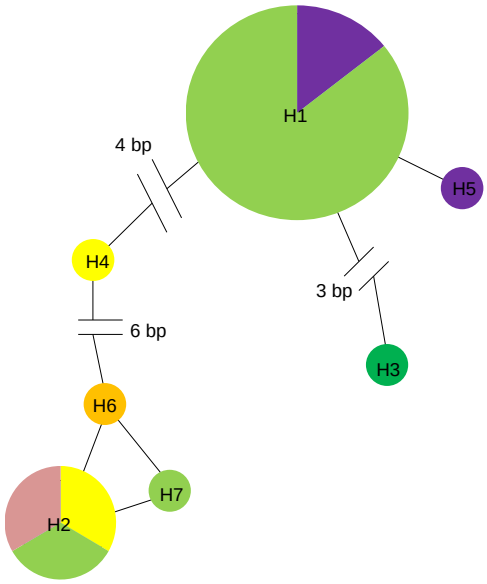

Figure 4.13. Haplotype network for *Rhinolophus hipposideros*. The sizes of the circles are proportional to the number of individuals. See Table 4.1 for the key to the color codes of the geographic positioning of the haplotypes.

Next, we compared the sequences of the individuals from each clade to those available in BOLD. From Group One we selected one representative individual, 161, and comparing it with the data from BOLD, the closest match to this sample was *Rhinolophus hipposideros* with a specimen similarity range of 98.82-95.19%. Comparing the sequence of an individual from Group Two, *Rhinolophus hipposideros* 190, with the matches that were taken from BOLD, the closest match to this sample was *Rhinolophus hipposideros* with a specimen similarity range of 100-96.37%.

The neighbor-joining tree for *Rhinolophus hipposideros*, created with BOLD, using three individuals belonging to Group One, *Rhinolophus hipposideros* 144 (Haplotype H4), 161 (Haplotype H3) and 245 (Haplotype H1) is shown in Figure 4.14. In the tree, the barcoded individuals from Turkey clustered closely with one of the five *Rhinolophus hipposideros* barcodes in BOLD. The neighbor-joining tree from BOLD for *Rhinolophus hipposideros* 190 is also shown in Figure 4.15. Notably, *Rhinolophus hipposideros* 190 fell onto another branch but into the same general *Rhinolophus hipposideros* clade with all other *Rhinolophus hipposideros* CO1 sequences. Hence the grouping that we observed in the intraspecific trees was in conformation with that in the BOLD tree.

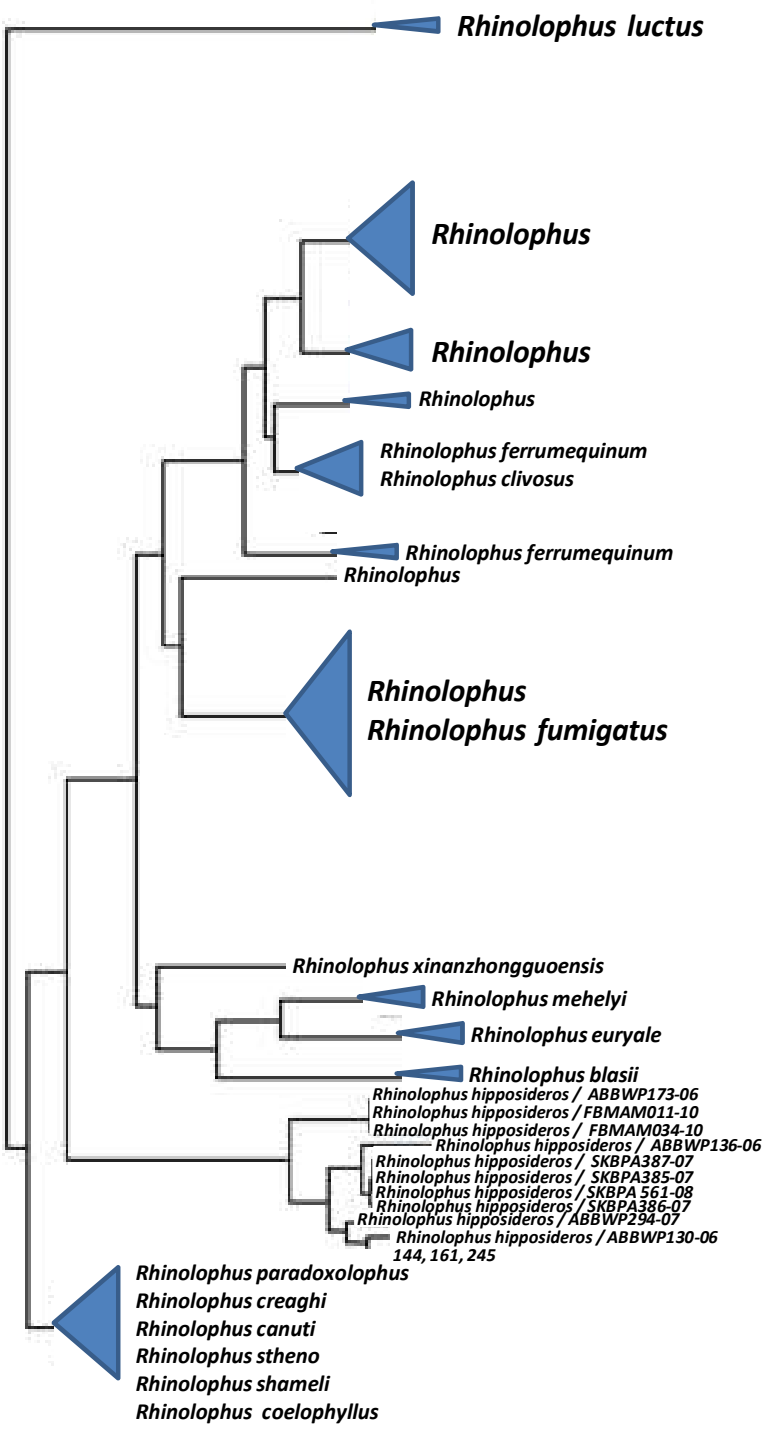

Figure 4.14. Neighbor-joining tree for one of our *Rhinolophus hipposideros* sequences, sample 161, constructed based on BOLD. The sizes of the triangles are proportional to the number of sequences in BOLD for that species.

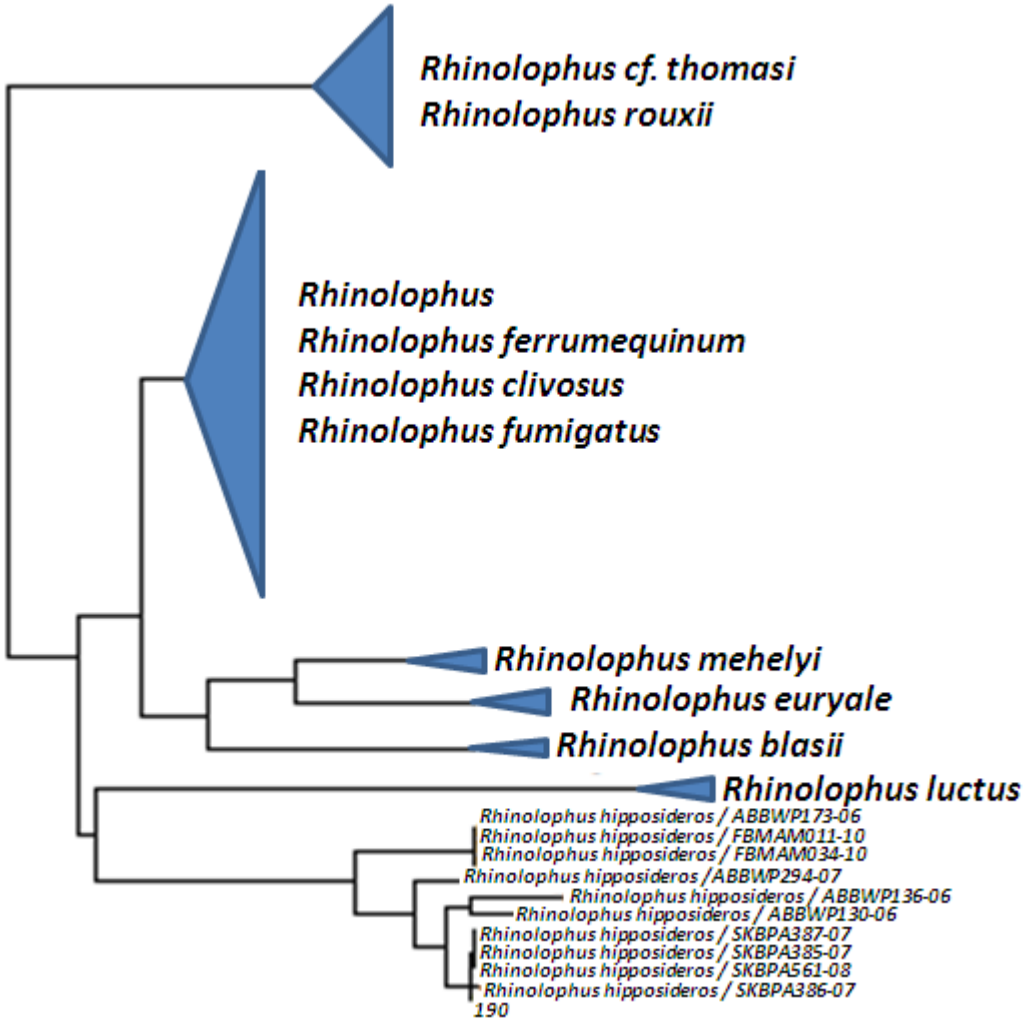

Figure 4.15. Neighbor-joining tree for one of our *Rhinolophus hipposideros* sequences, sample 190, constructed based on BOLD. The sizes of the triangles are proportional to the number of sequences in BOLD for that species.

4.4. *Asellia tridens*

Two sequences were analyzed for *Asellia tridens*. Samples were collected from Ilam, Iran (Figure 4.16). A haplotype network, intraspecific neighbor-joining and maximum-likelihood trees could not be prepared as there were only two sequences and they had the same haplotype.

Figure 4.16. The sampling location for *Asellia tridens*.

We compared our haplotype to those available in BOLD. The closest match to this sample was *Asellia tridens* with a specimen similarity range of 100-97.7%.

The neighbor-joining tree for *Asellia tridens*, constructed with BOLD is shown in Figure 4.17. The samples that were barcoded from Iran (255 & 263) fell within the *Asellia* clade. Our samples collected from Iran clustered closely with two other *Asellia tridens* species from an unknown area. There was one other clade in this tree, sister to the clade containing our sample.

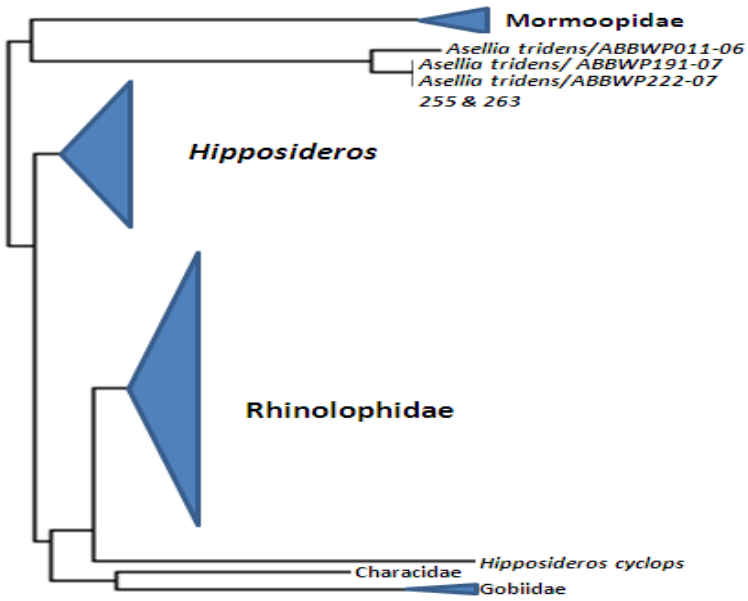

Figure 4.17. Neighbor-joining tree for our *Asellia tridens* sequences (255 & 263) constructed based on BOLD. The size of the triangles are proportional to the number of sequences in BOLD for that species.

4.5. *Taphozous nudiventris*

Three CO1 sequences from Turkey were analyzed for *Taphozous nudiventris*. The samples were collected from the Southeast Anatolia region (Nizip, Gaziantep) (Figure 4.18). A haplotype network could not be prepared as there was only one haplotype for this species. Intraspecific trees were not made for the same reason.

Figure 4.18. The sampling location for *Taphozous nudiventris*.

We compared our haplotype to those available in BOLD. The first closest match to this sample was *Taphozous nudiventris* with a specimen similarity of 100%, the second was an unspecified species from the genus *Taphozous* with a specimen similarity range of 99.33-97.15%, and the third was *Taphozous nudiventris* with a specimen similarity range of 97-96.98%.

The neighbor-joining tree for *Taphozous nudiventris*, created with BOLD, using *Taphozous nudiventris* 177 is shown in Figure 4.19. In the tree, the barcoded individual from Turkey clustered with one of the two branches of *Taphozous nudiventris* barcodes in BOLD.

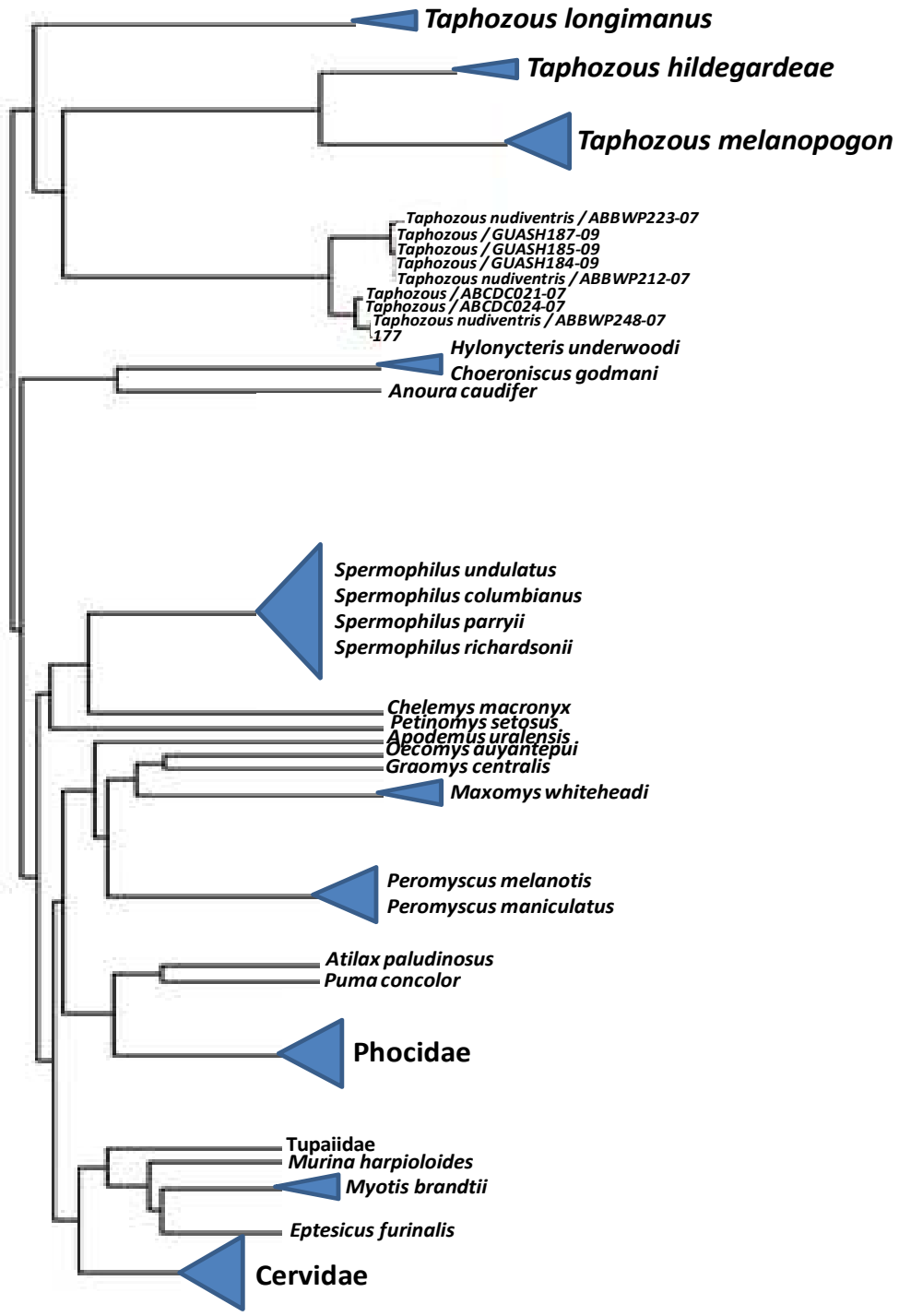

Figure 4.19. Neighbor-joining tree for *Taphozous nudiventris* sequences, using sample 177, constructed based on BOLD. The sizes of the triangles are proportional to the number of sequences in BOLD for that species.

4.6. *Tadarida teniotis*

Nine CO1 sequences were analyzed for *Tadarida teniotis*. The sequences were obtained from two regions; two individuals from the Southeast Anatolia region (Adıyaman, Urfa) and one individual from the Central Anatolia region (Aksaray) (Figure 4.20). Also three sequences from Genbank and three sequences from BOLD were included in the analysis.

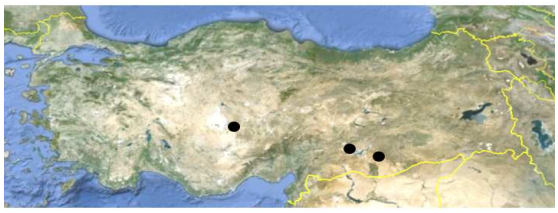

Figure 4.20. The sampling locations for *Tadarida teniotis*. The sizes of the circles are proportional to the number of individuals.

Intraspecific trees for *Tadarida teniotis* are shown in Figure 4.21. All CO1 sequences generated two clades; Group One included only the sequences from BOLD and Genbank whereas Group Two included our CO1 sequences from Turkey.

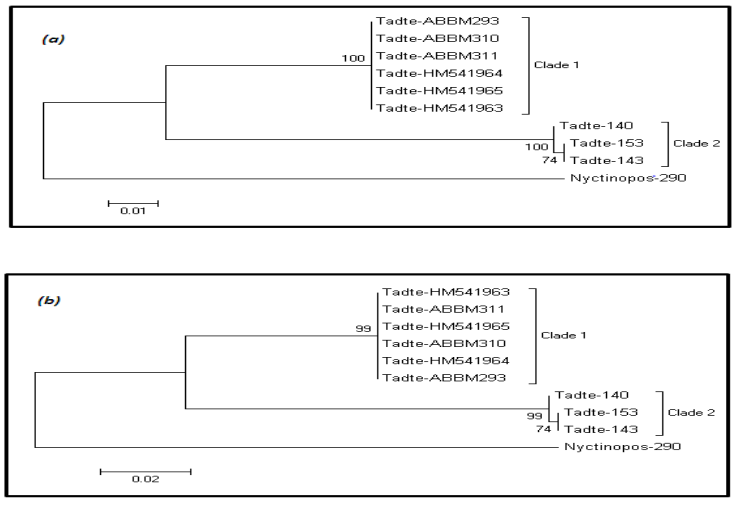

Figure 4.21. Intraspecific trees for *Tadarida teniotis*. (a) NJ tree and (b) ML tree. The codes that begin with ABBM are taken from BOLD. The codes that begin with HM are taken from Genbank.

There were three different haplotypes in this species as seen in the haplotype network and the haplotype network table (Figure 4.22 and Appendix B). H1 was the most common haplotype (found in six individuals) and all samples having haplotype H1 were taken from Genbank and BOLD. Haplotypes H2 and H3, found in Turkey formed one group, which was separated by 63 base pairs from H1.

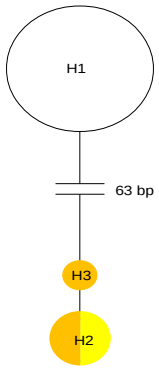

Figure 4.22. Haplotype network for *Tadarida teniotis*. The sizes of the circles are proportional to the number of individual. See Table 4.1 for the key to the color codes of the geographic positioning of the haplotypes.

Next, we compared the sequences of the individuals from each clade to those available in BOLD. From Group One we selected one representative individual, HM541965, and comparing it with the data from BOLD, the closest match to this sample was *Tadarida teniotis* with a specimen similarity range of 100-88.37%. Comparing the sequence of an individual from Group Two, *Tadarida teniotis* 153, with the matches that were taken from BOLD, the closest match to this sample was *Tadarida teniotis* with a specimen similarity range of 100-89.11%.

The neighbor-joining tree for *Tadarida teniotis*, created with BOLD, using one individual belonging to Group One, *Tadarida teniotis* HM541965, is shown in Figure 4.23. In the tree, the barcoded individual from Genbank clustered closely with a clade of *Tadarida teniotis* barcodes in BOLD. The neighbor-joining tree from BOLD for *Tadarida teniotis* 153 is also shown in Figure 4.24. *Tadarida teniotis* 153 fell within the reciprocal clade that contained HM541965. Hence, the two clades retrieved for this species in our intraspecific trees, and the two clades observed in the BOLD tree were in conformation.

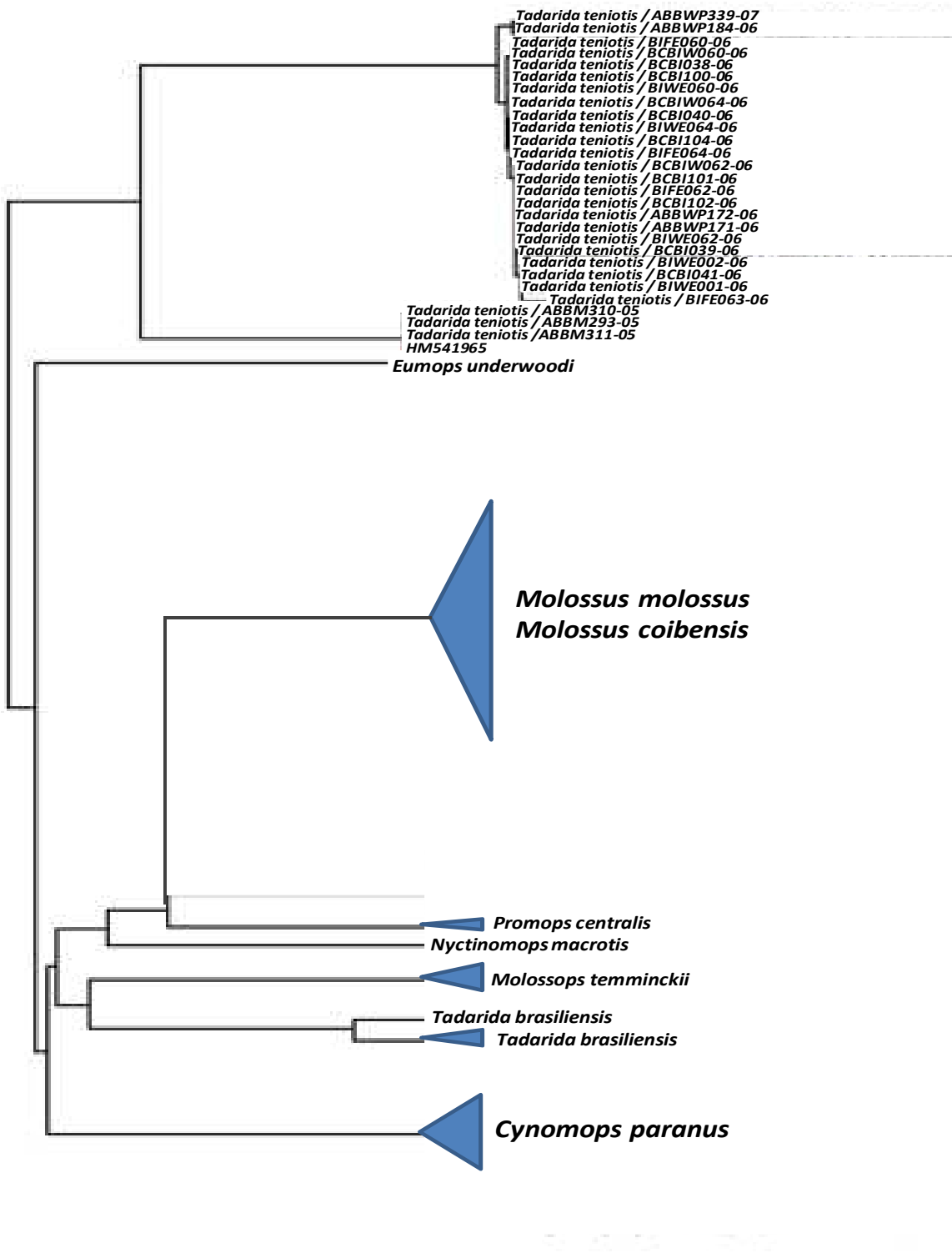

Figure 4.23. Neighbor-joining tree for one of our *Tadarida teniotis* sequences, sample HM541965, constructed based on BOLD. The sizes of the triangles are proportional to the number of sequences in BOLD for that species.

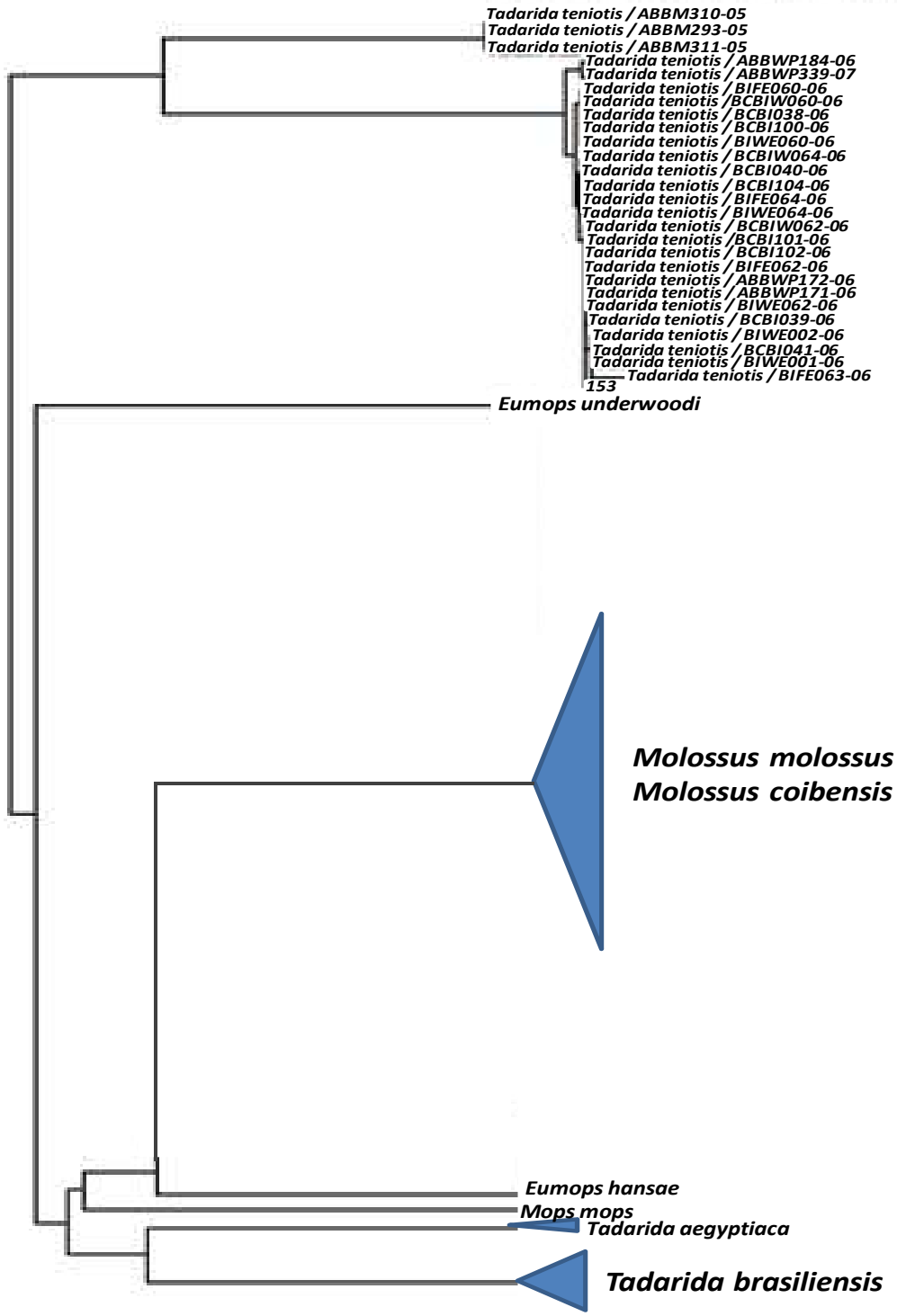

Figure 4.24. Neighbor-joining tree for one of our *Tadarida teniotis* sequences, sample 153, constructed based on BOLD. The sizes of the triangles are proportional to the number of sequences in BOLD for that species.

4.7. *Eptesicus serotinus*

Ten sequences were analyzed for *Eptesicus serotinus*. The sequences were obtained from four locations; one from Syria, one from the Black Sea region (Zonguldak) and two from the Mediterranean region (Elmalı and Beşkonak, Antalya) (Figure 4.25). Also three sequences from Genbank and three from BOLD were included in the analysis.

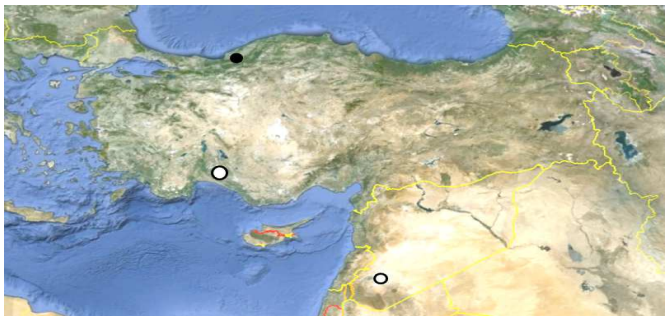

Figure 4.25. The sampling locations for *Eptesicus serotinus*. The circles are proportional to the number of individuals. The black color indicates sampling location for the first group and the white color indicates sampling locations for the second group in the intraspecific trees (Figure 4.26).

Intraspecific trees for *Eptesicus serotinus* are shown in Figure 4.26. All CO1 sequences generated three clades. The first clade consisted of BOLD and Genbank sequences entirely. The second clade had only one sample, *Eptesicus serotinus* 203 from Zonguldak, the Black Sea region. The third clade had *Eptesicus serotinus* 163, 269 and 270. Samples 269 and 270 were both from Antalya whereas sample 163 was from Syria.

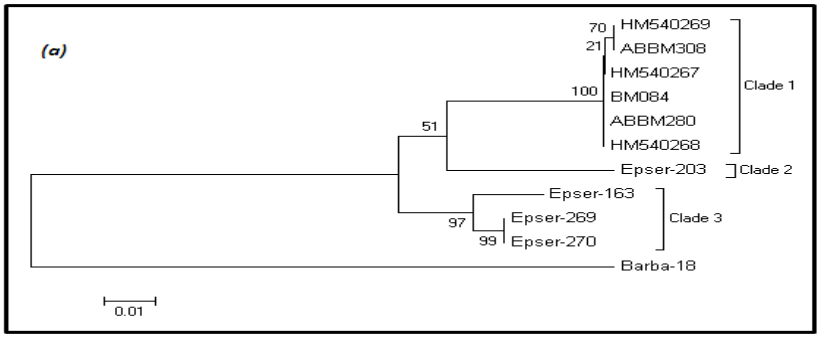

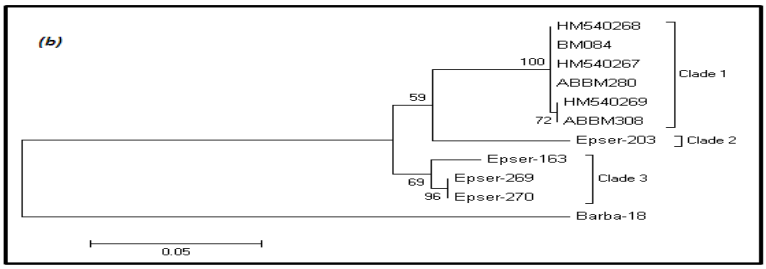

Figure 4.26. Intraspecific trees for *Eptesicus serotinus*. (a) Neighbor-joining tree and (b) Maximum-likelihood tree. The codes that begin with HM, ABBM and BM were taken from BOLD and Genbank.

There were five different haplotypes in this species as seen in the haplotype network and the haplotype network table (Figure 4.27 and Appendix B). The H1 haplotype was found in four of the six individuals obtained from BOLD and Genbank, with the codes HM540267, BM084, ABBM280 and HM540268. Haplotype H2 was different from H1 by a single base pair and was found in the other two individuals obtained from BOLD and Genbank, with the codes HM540269 and ABBM308, respectively. Haplotype H4 was found in one individual from the Black Sea region and was separated by 21 base pairs from the rest of the individuals, forming a separate clade (Figure 4.27). Although H3 and H5 were separated by 11 base pairs in the haplotype network, they were included on the same branch in the BOLD tree (Figure 4.28). H3 was found in two individuals from Antalya (the Mediterranean region), whereas H5 was found in one individual from Syria.

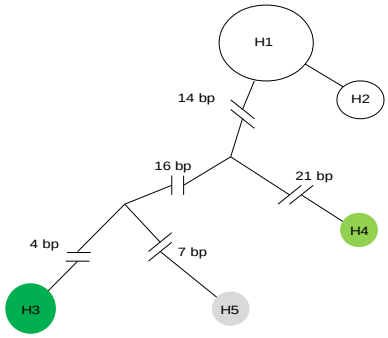

Figure 4.27. Haplotype network for *Eptesicus serotinus*. The sizes of the circles are proportional to the number of individuals. See Table 4.1 for the key to the color codes of the geographic positioning of the haplotypes.

As a next step, we compared the sequences of the individuals from each clade to those available in BOLD. Between haplotypes H1 and H2 we selected one representative individual, HM540269, and comparing it with the data from BOLD, the first closest match to this sample was *Eptesicus serotinus* with a specimen similarity range of 100-98.16%, the second was *Eptesicus nilssonii* with a specimen similarity of 94.29% and the third was an unknown bat species with a specimen similarity of 94.24%. Comparing an individual with the haplotype H3, *Eptesicus serotinus* 270, to the three matches taken from BOLD, the first closest match of *Eptesicus serotinus* 270 was to *Eptesicus serotinus* with a specimen similarity of 98.22%, the second was *Eptesicus bottae* with a specimen similarity of 95.47% and the third was again *Eptesicus serotinus* with a specimen similarity of 95.31%. Comparing another individual with haplotype H4, *Eptesicus serotinus* 203, to the three matches taken from BOLD, the first closest match of *Eptesicus serotinus* 203 was *Eptesicus serotinus* with a specimen similarity of 100%, the second was *Eptesicus nilssonii* with a specimen similarity range of 99.29-97.86% and the third was again *Eptesicus serotinus* with a specimen similarity range of 93.91-93.57%. Finally, *Eptesicus serotinus* 163, with haplotype H5 was compared to the three matches that were taken from BOLD, and the first closest match was *Eptesicus serotinus* with a specimen similarity range of 99.11-95.04%, the second was *Eptesicus bottae* with a specimen similarity of 95.04%, and third was again *Eptesicus serotinus* with a specimen similarity range of 94.86-94.83%.

The neighbor-joining tree for *Eptesicus serotinus*, created with BOLD is shown in Figure 4.28. Sample 203 from Zonguldak (the Black Sea region) clustered with *Eptesicus serotinus* and *Eptesicus nilssoni* as a separate group. HM540269 clustered with another group as expected from both haplotype network and intraspecific trees. Although *Eptesicus serotinus* 163 and *Eptesicus serotinus* 270 formed different clades in the intraspecific trees (Figure 4.26) and had 11 base pair difference in the haplotype network (Figure 4.27), they appeared in the same clade in the BOLD tree. Specimen 163 was from Syria and specimen 270, which separated from the rest of the samples, was from Antalya, along the Mediterranean coast of Turkey.

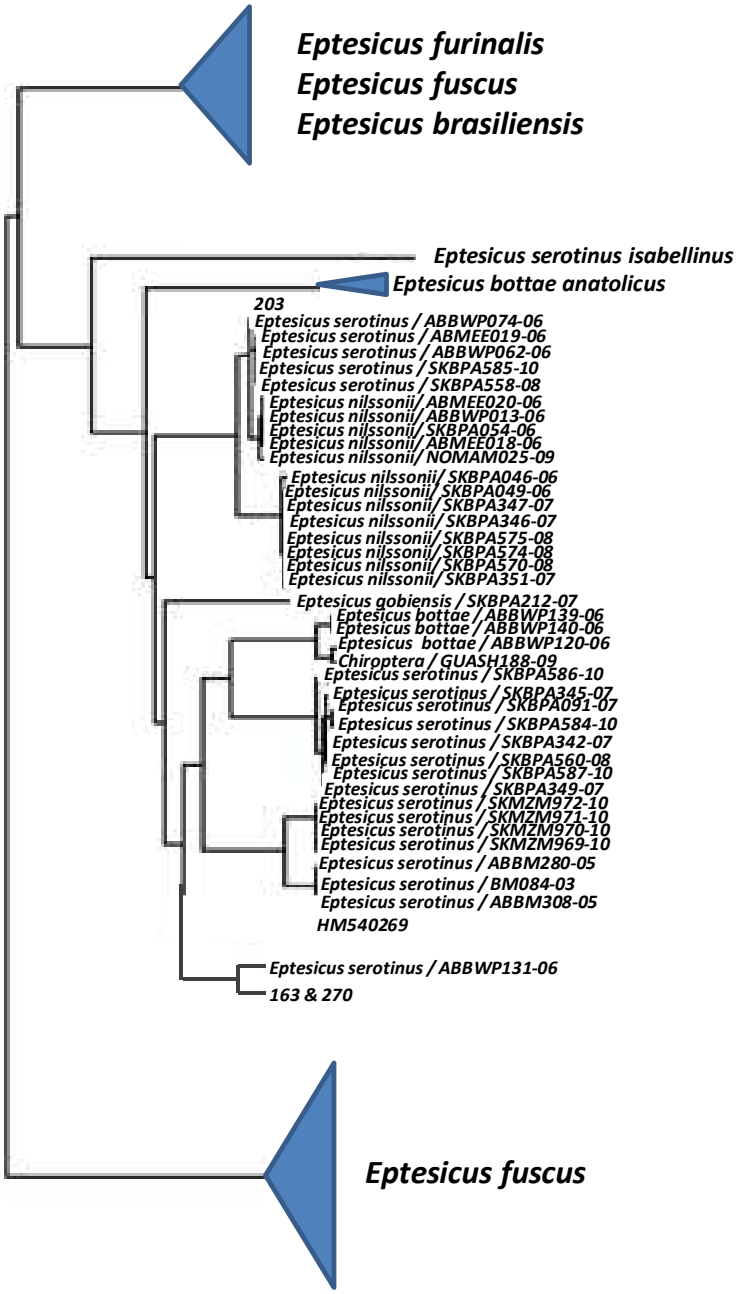

Figure 4.28. Neighbor-joining tree for *Eptesicus serotinus*, based on BOLD tree. The sizes of the triangles are proportional to the number of sequences in BOLD for that species.

4.8. *Nyctalus lasiopterus*

One CO1 sequence from Turkey was analyzed for *Nyctalus lasiopterus*. The sample was collected from the Mediterranean region (Antalya) (Figure 4.29). A haplotype network and intraspecific trees could not be prepared as there was only one sample for this species.

Figure 4.29. The sampling location for *Nyctalus lasiopterus*.

We compared the sequence of our individual to those available in BOLD. The closest match to this sample was *Nyctalus lasiopterus* with a specimen similarity range of 100-99.84%.

The neighbor-joining tree for *Nyctalus lasiopterus*, created with BOLD, using our individual, *Nyctalus lasiopterus* 271, is shown in Figure 4.30. In the tree, the barcoded individual from Turkey clustered closely with the *Nyctalus lasiopterus* barcodes in BOLD, in a single clade.

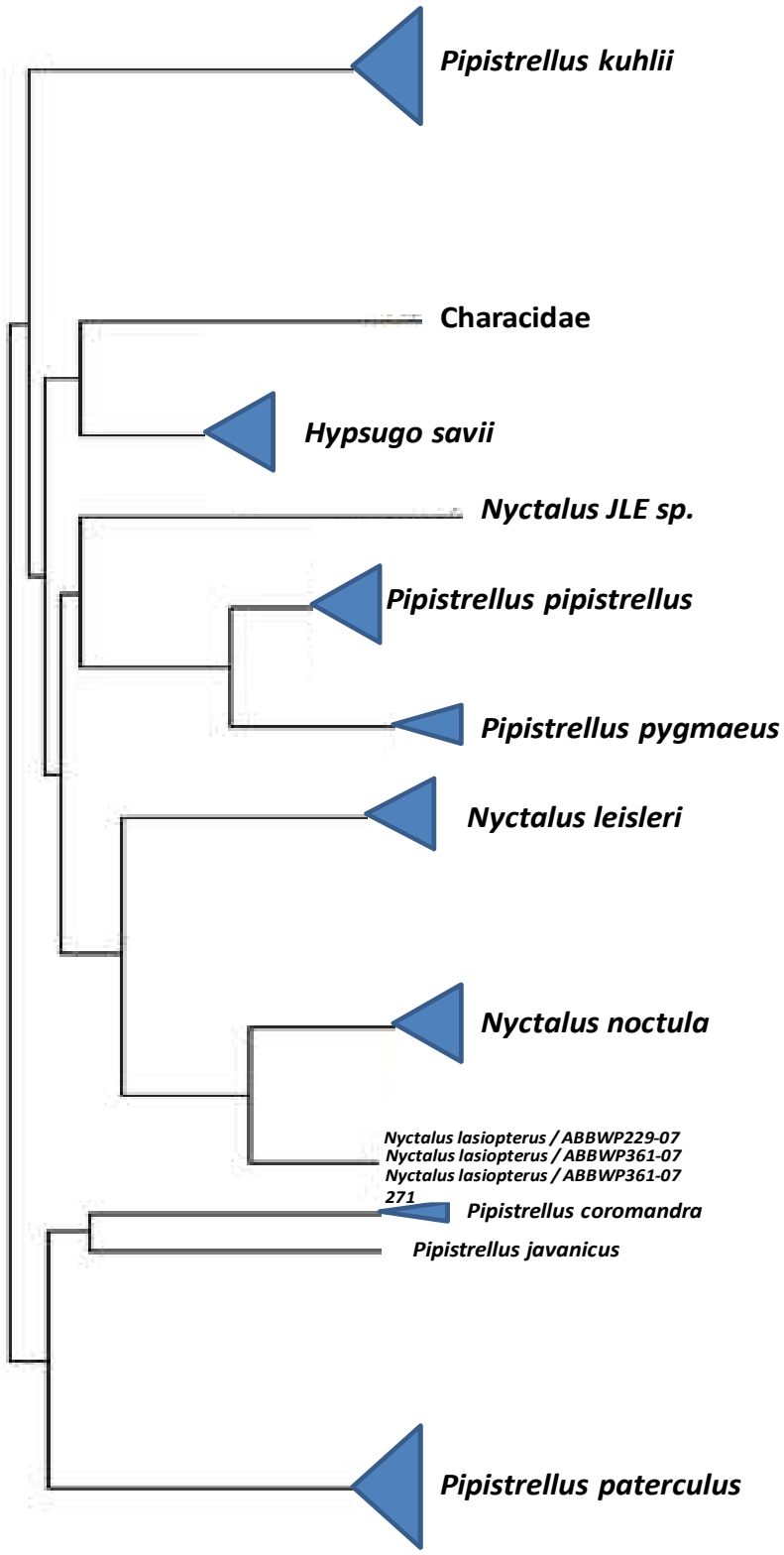

Figure 4.30. Neighbor-joining tree for our *Nyctalus lasiopterus* sequence, sample 271, constructed based on BOLD. The sizes of the triangles are proportional to the number of sequences in BOLD for that species.

4.9. *Nyctalus leisleri*

Five CO1 sequences from Turkey were analyzed for *Nyctalus leisleri*. The samples were collected from the Marmara region (Kırklareli), the Black Sea region (Trabzon) and the Mediterranean region (Antalya) (Figure 4.31). A haplotype network could not be prepared as there was one haplotype for this species. Intraspecific trees were also not prepared for the same reason.

Figure 4.31. The sampling locations for *Nyctalus leisleri*. The circles are proportional to the number of individuals.

We compared our haplotype to those available in BOLD. Comparing it with the data from BOLD, the closest match to this sample was *Nyctalus leisleri* with a specimen similarity range of 100-99.29%

The neighbor joining tree for *Nyctalus leisleri*, created with BOLD, using the same haplotype, is shown in Figure 4.32. In the tree, the barcoded individual from Trabzon clustered closely with *Nyctalus leisleri* barcodes in BOLD, in a single clade.

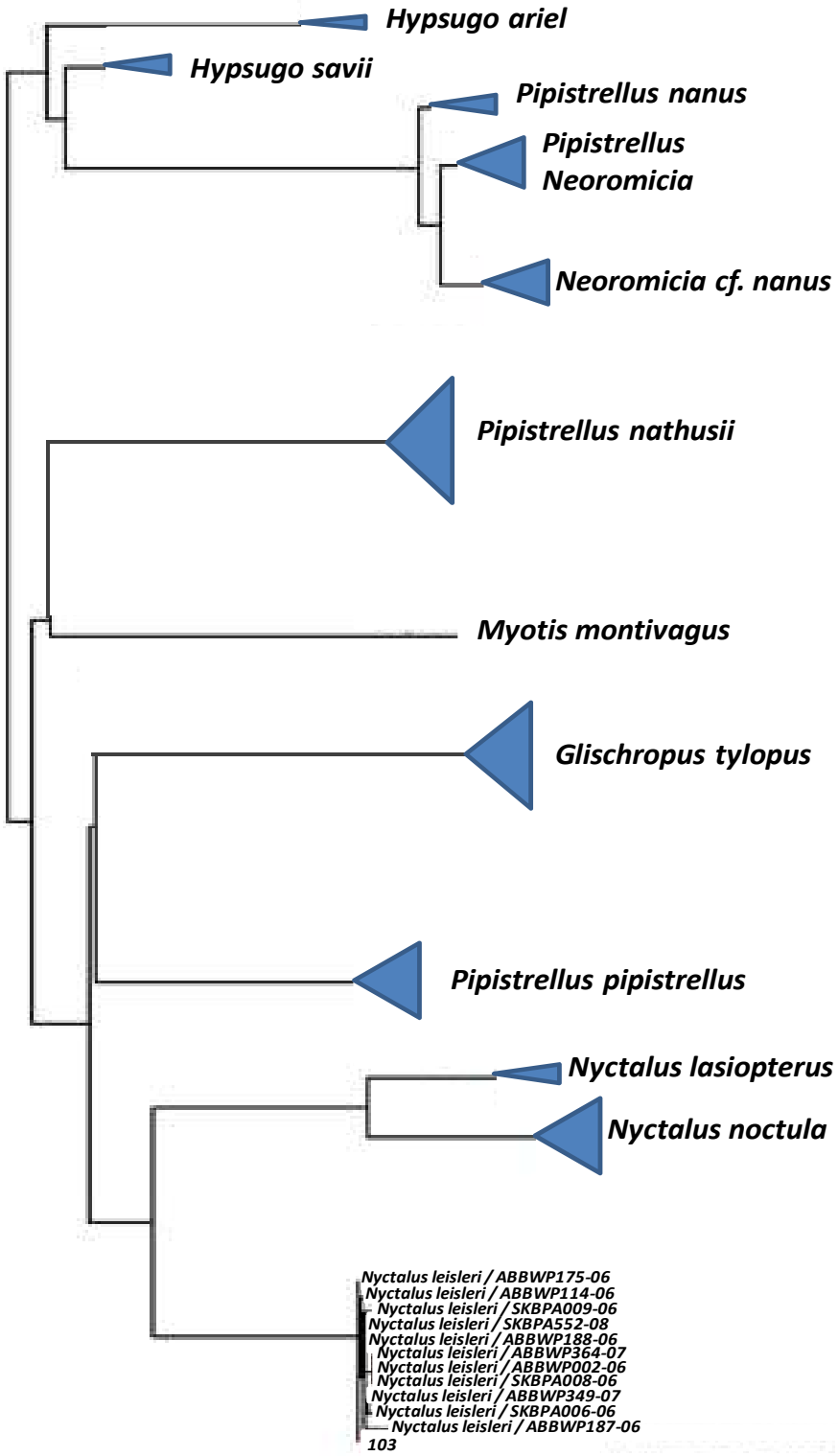

Figure 4.32. Neighbor-joining tree for our *Nyctalus leisleri* sequences, using sample 103, constructed based on BOLD. The sizes of the triangles are proportional to the number of sequences in BOLD for that species.

4.10. *Nyctalus noctula*

Two CO1 sequences from Turkey were analyzed for *Nyctalus noctula*. The samples were collected from the Marmara region (Kırklareli) and the Mediterranean region (Osmaniye) (Figure 4.33). Intraspecific trees could not be prepared as there were only two samples for this species.

Figure 4.33. The sampling locations for *Nyctalus noctula*. The circles are proportional to the number of individuals.

There were two haplotypes in this species as seen in the haplotype network and the haplotype network table (Figure 4.34 and Appendix B). H1 was found in the Marmara region whereas H2 was found in the Mediterranean region. H1 was separated by two base pairs from H2.

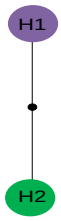

Figure 4.34. Haplotype network for *Nyctalus noctula*. The sizes of the circles are proportional to the number of individuals. See Table 4.1 for the key to the color-codes of the geographic positioning of the haplotypes.

As the next step, we compared the sequence of one of our individuals to those available in BOLD. We used sample 199, and comparing it with the data from BOLD, the closest match to this sample was *Nyctalus noctula* with a specimen similarity range of 100-99.68%.

The neighbor-joining tree for *Nyctalus noctula*, created with BOLD, using the same individual, *Nyctalus noctula* 199, is shown in Figure 4.35. In the tree, the barcoded individual from Turkey clustered closely with *Nyctalus noctula* barcodes in BOLD, forming a single clade. We obtained location information for two of the BOLD barcodes in this clade, which were Ploen, Germany and Lebensau, Germany.

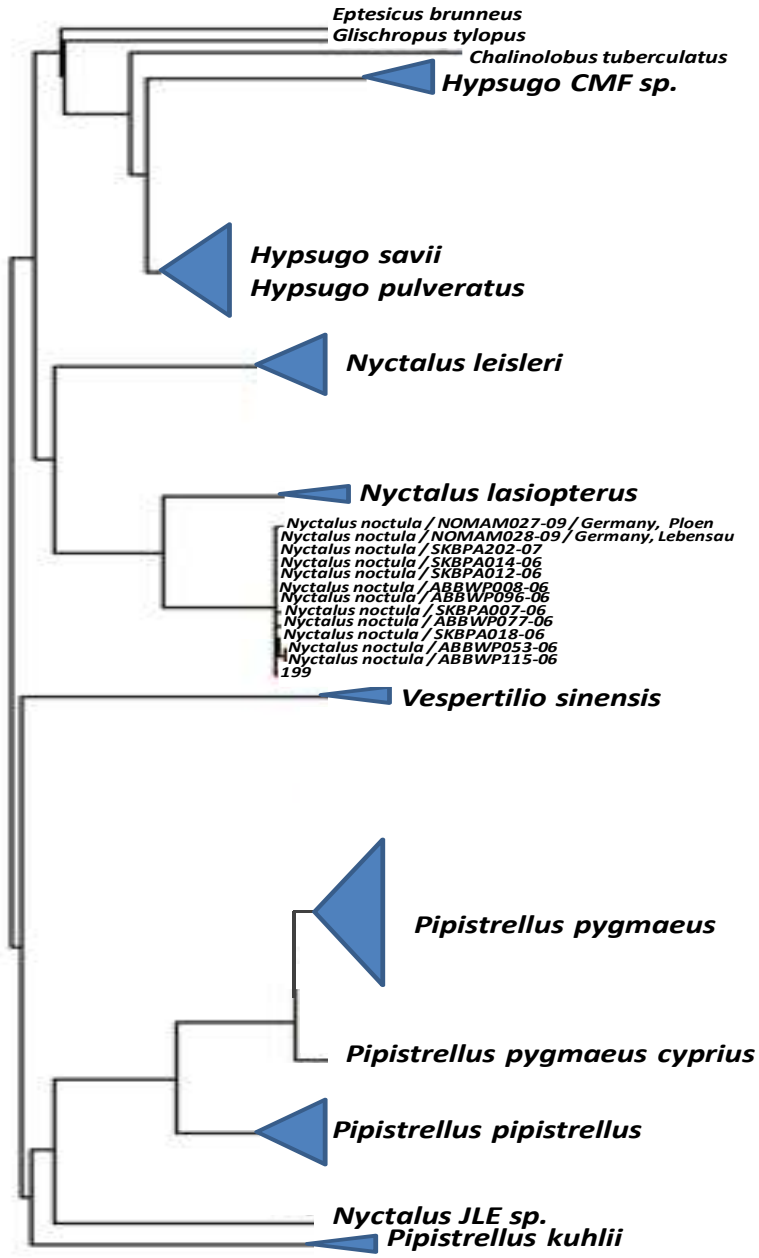

Figure 4.35. Neighbor-joining tree for one of our *Nyctalus noctula* sequences, sample 199, constructed based on BOLD. The sizes of the triangles are proportional to the number of sequences in BOLD for that species.

4.11. *Pipistrellus kuhlii*

Eleven CO1 sequences were analyzed for *Pipistrellus kuhlii*. The sequences were obtained from three regions; two from the Mediterranean region (Mersin, Kahramanmaraş), one from the East Anatolia region (Iğdır) and nine from the Southeast Anatolia region (two from Urfa, two from Gaziantep, two from Adıyaman, one each from Diyarbakır and Mardin) (Figure 4.36).

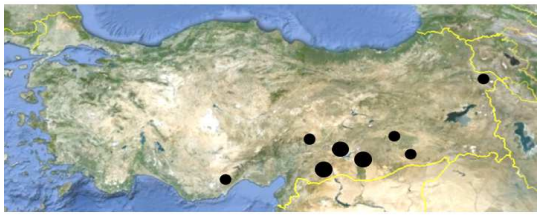

Figure 4.36. The sampling locations for *Pipistrellus kuhlii*. The circles are proportional to the number of individuals.

Intraspecific trees for *Pipistrellus kuhlii* are shown in Figure 4.37. Our CO1 sequences did not generate distinctive clades; however, *Pipistrellus kuhlii* 223 and 228 formed a separate group.

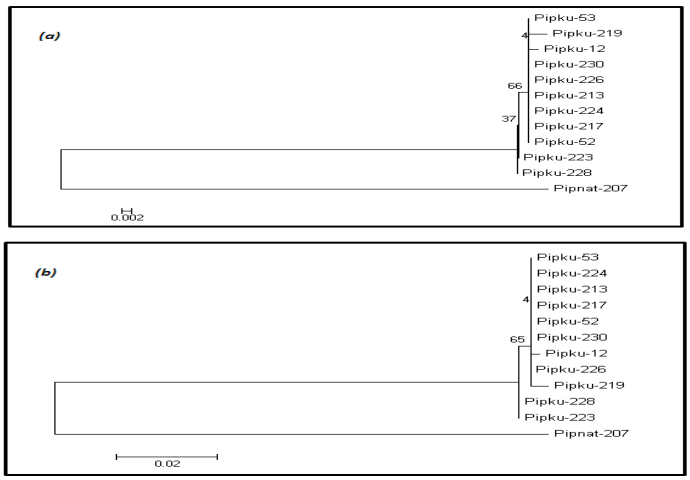

Figure 4.37. Intraspecific trees for *Pipistrellus kuhlii*. (a) NJ tree and (b) ML tree.

There were four different haplotypes in this species as seen in the haplotype network and the haplotype network table (Figure 4.38 and Appendix B). H1 was the most common haplotype (found in seven individuals), and was found in the Marmara region and had its highest frequency in the Southeastern Turkey. Haplotypes H2 and H3 were separated by one base pair from H1. Haplotype H4 was separated by two base pairs from H1 and was found in the Mediterranean region.

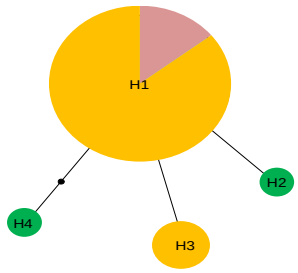

Figure 4.38. Haplotype network for *Pipistrellus kuhlii*. The sizes of the circles are proportional to the number of individuals. See Table 4.1 for the key to the color codes of the geographic positioning of the haplotypes.

Next, we compared the sequences of our individuals from each group in intraspecific trees (Figure 4.37) to those available in BOLD. From the main clade, we selected one representative individual, 224, and comparing it with the data from BOLD, the first closest match to this sample was *Pipistrellus kuhlii* with a specimen similarity range of 100-95.7%, the second was *Pipistrellus deserti* with a specimen similarity range of 95.7-95.16% and the third was *Pipistrellus kuhlii* with a specimen similarity range of 94.98-94.24%. Comparing an individual from the smaller group, *Pipistrellus kuhlii* 223, with the matches taken from BOLD, the first closest match of this sample was *Pipistrellus kuhlii* with a specimen similarity range of 99.83-95.26%, the second was *Pipistrellus deserti* with a specimen similarity range of 95.26-94.75% and the third was *Pipistrellus kuhlii* again with a specimen similarity range of 94.59-93.87%.

The neighbor-joining tree for *Pipistrellus kuhlii*, created with BOLD, using two individuals belonging to the small and the main groups in intraspecific trees, *Pipistrellus kuhlii* 223 and 224 are shown in Figure 4.39. In the tree, the barcoded individuals from Turkey clustered closely with one of the three main *Pipistrellus kuhlii* clades in BOLD.

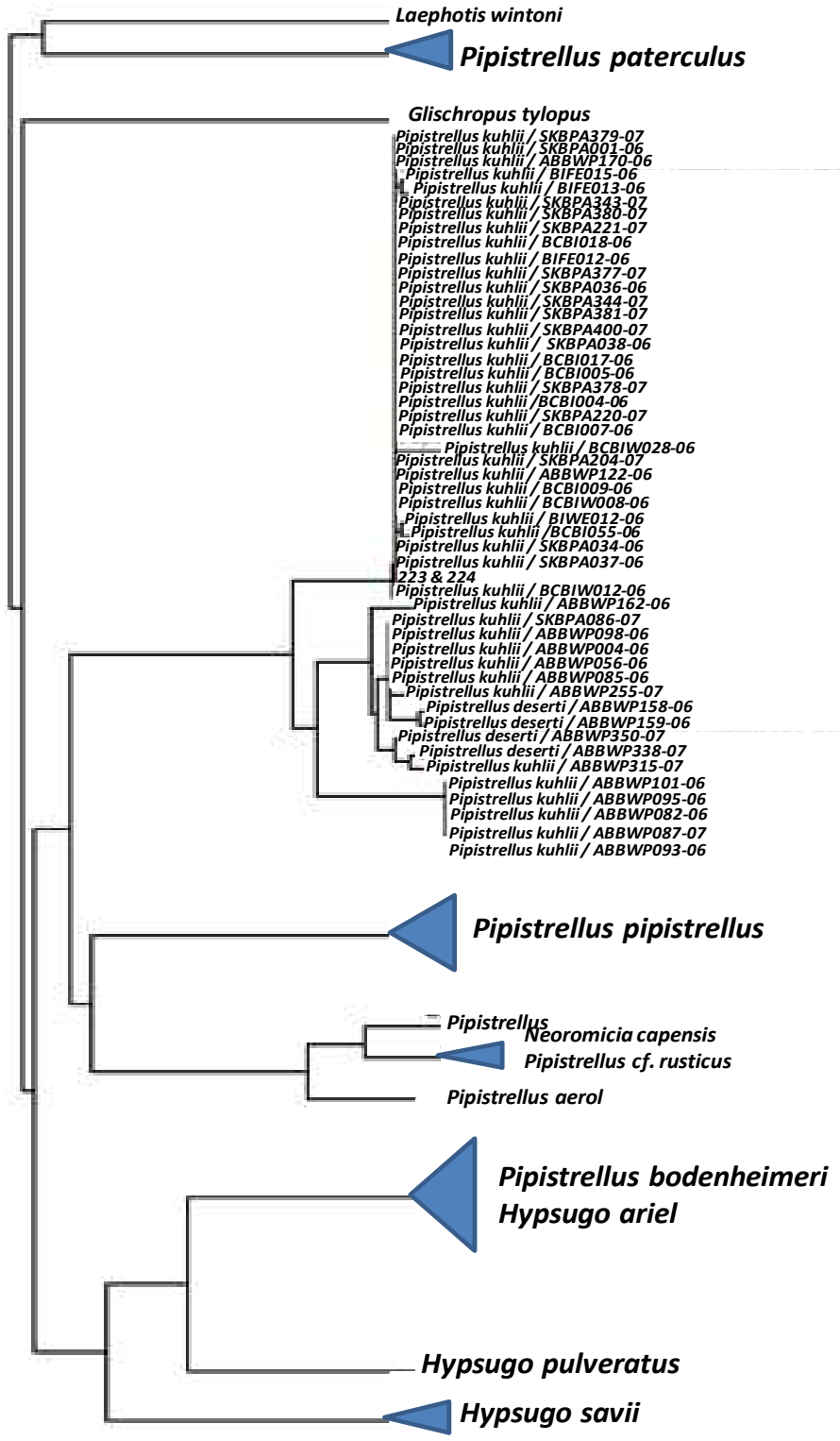

Figure 4.39. Neighbor-joining tree for two of our *Pipistrellus kuhlii* sequences, samples 223 and 224, constructed based on BOLD. The sizes of the triangles are proportional to the number of sequences in BOLD for that species.

4.12. *Pipistrellus nathusii*

Three CO1 sequences from Turkey were analyzed for *Pipistrellus nathusii*. The samples were collected from two locations; the Aegean region (Afyon) and the Marmara region (Balıkesir) (Figure 4.40). A haplotype network could not be prepared as there was only one haplotype for this species. Intraspecific trees were not made for the same reason.

Figure 4.40. The sampling locations for *Pipistrellus nathusii*. The circles are proportional to the number of individuals.

We compared the sequences of our individuals to those available in BOLD. Comparing it with the data from BOLD, the closest match to our haplotype was *Pipistrellus nathusii* with a specimen similarity range of 100-99.66%

The neighbor-joining tree for *Pipistrellus nathusii*, created with BOLD, using the same haplotype, is shown in Figure 4.41. In the tree, the barcoded individual from Balıkesir (Kuş cenneti, Manyas) clustered closely with other *Pipistrellus nathusii* barcodes in BOLD, forming a single clade.

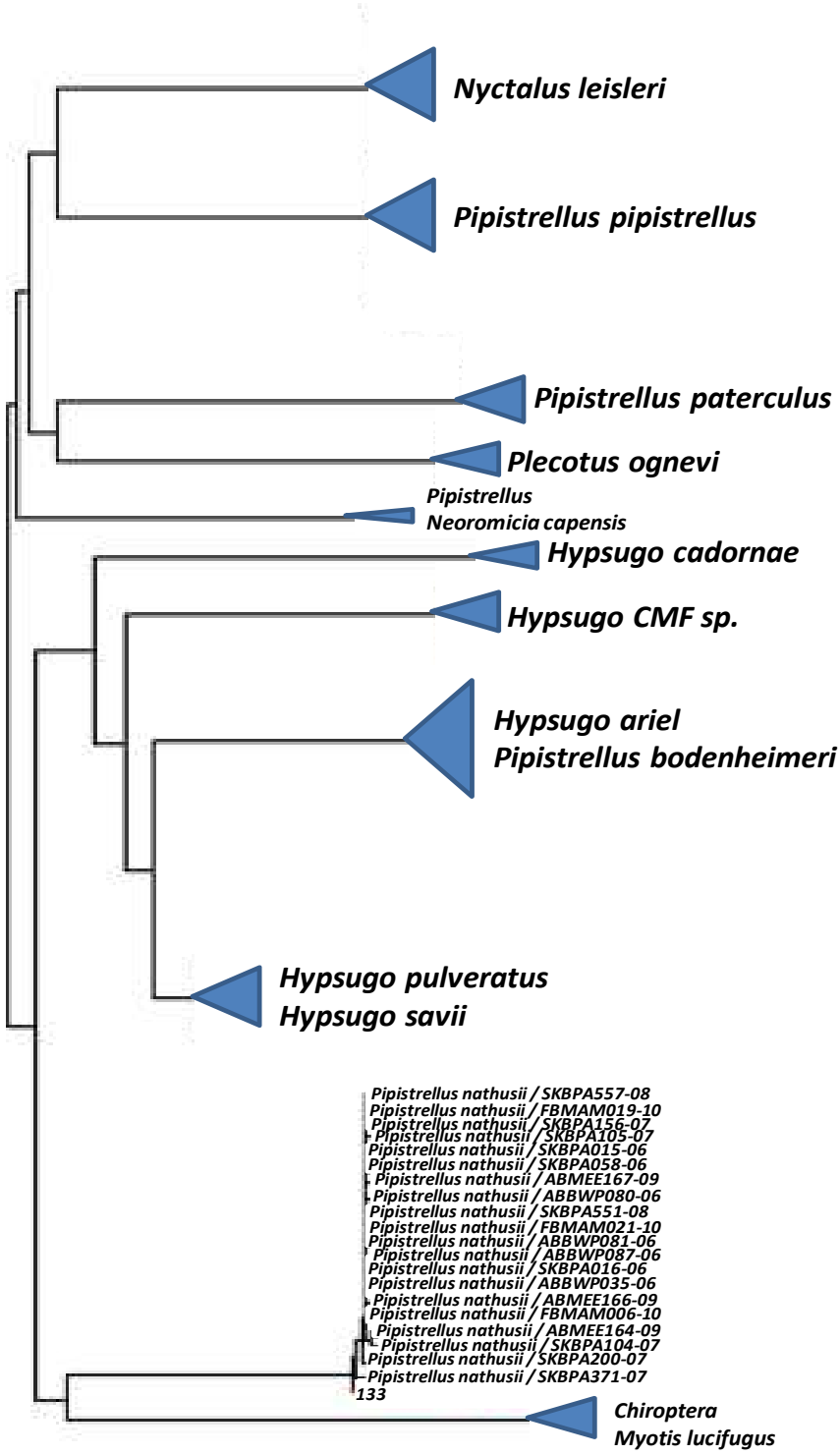

Figure 4.41. Neighbor-joining tree for our *Pipistrellus nathusii* sequences, using sample 133, constructed based on BOLD. The sizes of the triangles are proportional to the number of sequences in BOLD for that species.

4.13. *Pipistrellus pipistrellus*

Three CO1 sequences were analyzed for *Pipistrellus pipistrellus*. The sequences were obtained from three locations; the East Anatolia region (Van), the Black Sea region (Samsun) and the Central Anatolia region (Konya) (Figure 4.42).

Figure 4.42. The sampling locations for *Pipistrellus pipistrellus*. The circles are proportional to the number of individuals. The black color indicates sampling locations for the first group and the white color indicates sampling locations for the second group in the intraspecific trees (Figure 4.43).

Intraspecific trees for *Pipistrellus pipistrellus* are shown in Figure 4.43. All CO1 sequences generated two clades, Group One included samples 13 and 15 whereas Group Two included sample 138.

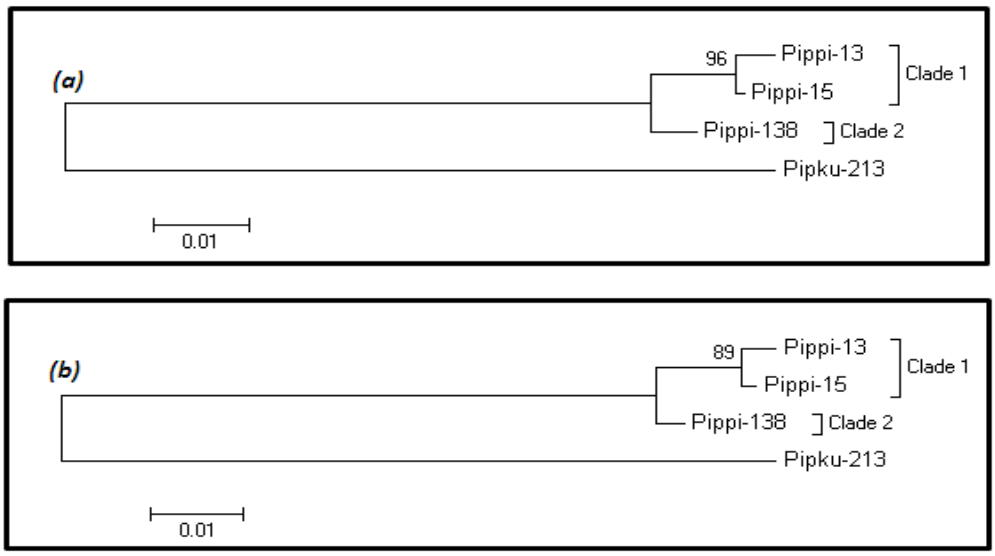

Figure 4.43. Intraspecific trees for *Pipistrellus pipistrellus*. (a) NJ tree and (b) ML tree.

There were three different haplotypes in this species as seen in the haplotype network and the haplotype network table (Figure 4.44 and Appendix B). H2 was found in Samsun. Haplotypes H1 and H3 formed one group, which was separated by eight base pairs from H2 (which corresponded to sample *Pipistrellus pipistrellus*-138 in the trees). H2 was found in the Black Sea region and was separated from the rest of the samples in the intraspecific tree, as shown above.

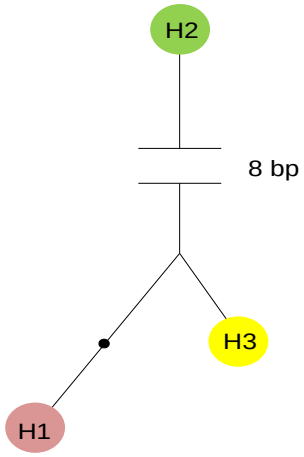

Figure 4.44. Haplotype network for *Pipistrellus pipistrellus.* The sizes of the circles are proportional to the number of individuals. See Table 4.1 for the key to color codes of the geographic positioning of the haplotypes.

Next, we compared the sequences of the individuals from each group to those available in BOLD. From Group One we selected one representative individual, 13, and comparing it with the data from BOLD, the closest match to this sample was *Pipistrellus pipistrellus* with a specimen similarity range of 100-98.1%. Comparing the individual from Group Two, *Pipistrellus pipistrellus* 138, with the matches that were taken from BOLD, the closest match was *Pipistrellus pipistrellus* with a specimen similarity range of 99.5-98.18%.

The neighbor-joining trees for *Pipistrellus pipistrellus*, created with BOLD, using individuals belonging to Groups One and Two, *Pipistrellus pipistrellus* 13 and 138 respectively, are shown in Figures 4.45 and 4.46. In the trees, the barcoded individuals from Turkey clustered closely with other *Pipistrellus pipistrellus* barcodes in BOLD, but in different parts of the trees. There were originally two *Pipistrellus pipistrellus* clades in the

BOLD tree. One of these clades had an individual from St. Katharinan, Germany but we did not have the data on the locations of the other *Pipistrellus pipistrellus* individuals as they were not publicly available. Sample 13 from Van fell onto the clade reciprocal to the one that contained the individual from Germany. On the other hand, sample 138 generated a new clade, reciprocal to the other two *Pipistrellus pipistrellus* clades in the BOLD tree.

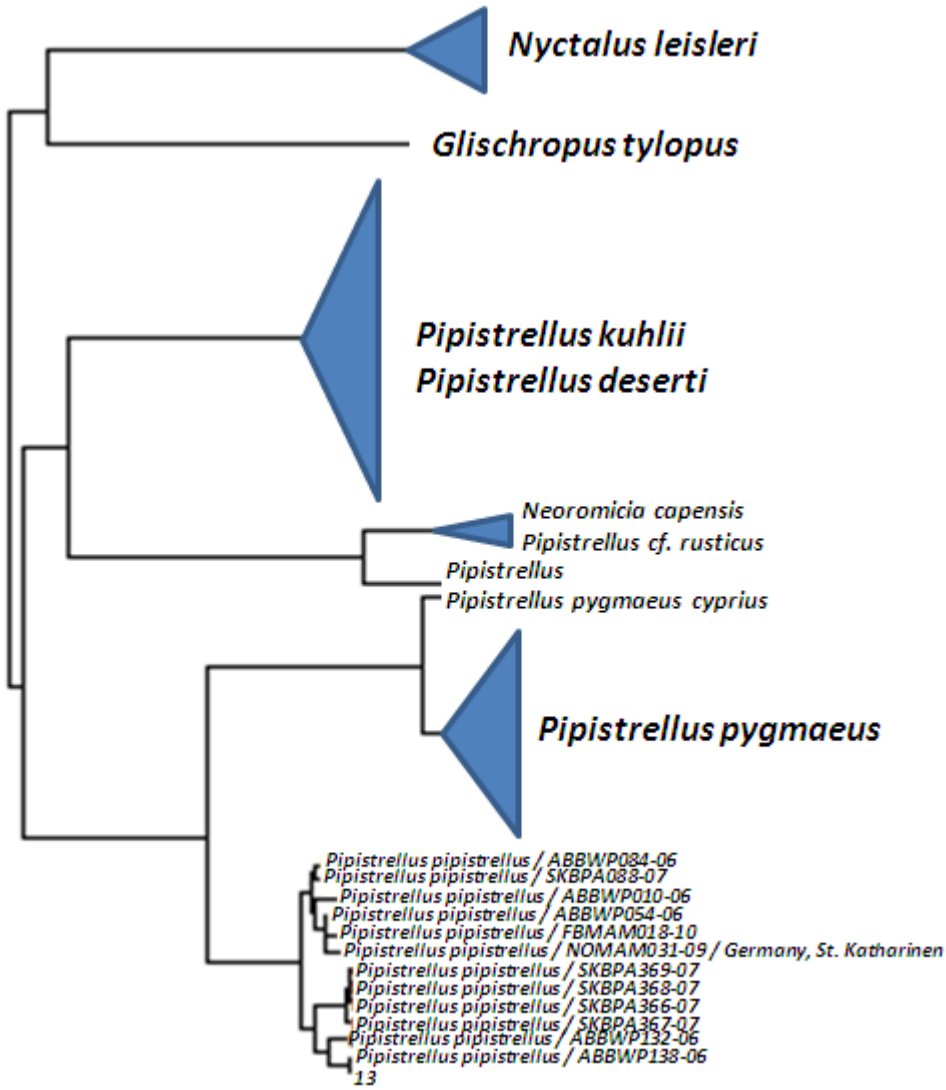

Figure 4.45. Neighbor-joining tree for one of our *Pipistrellus pipistrellus* sequences, sample 13, constructed based on BOLD. The sizes of the triangles are proportional to the number of sequences in BOLD for that species.

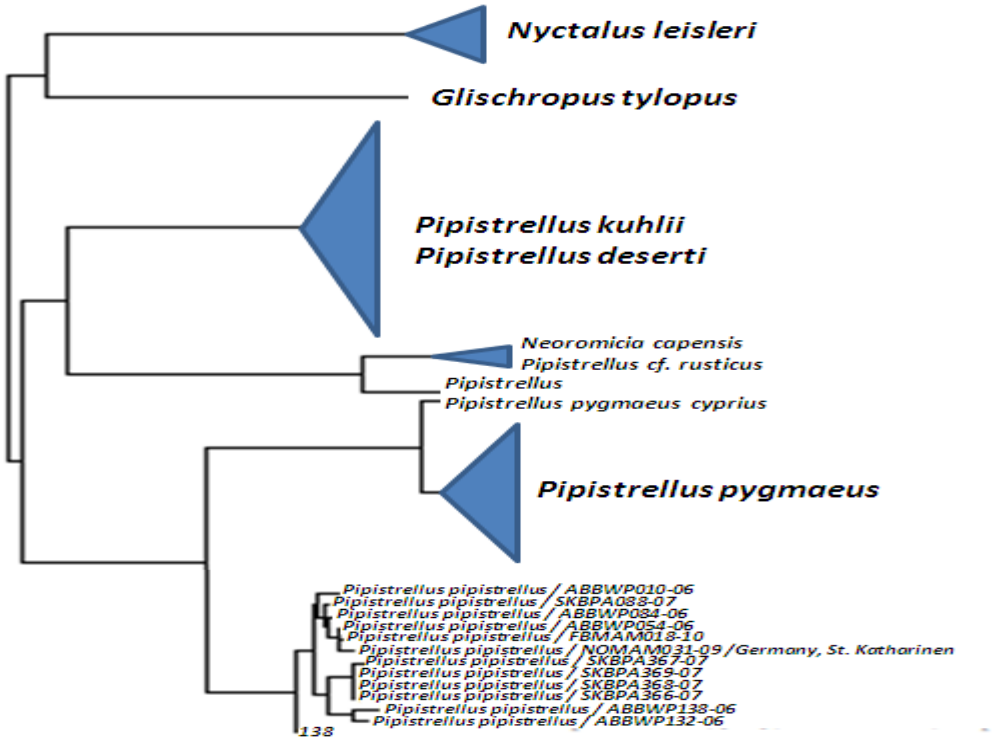

Figure 4.46. Neighbor-joining tree for one of our *Pipistrellus pipistrellus* sequences, sample 138, constructed based on BOLD. The sizes of the triangles are proportional to the number of sequences in BOLD for that species.

4.14. *Pipistrellus pygmaeus*

One CO1 sequence from Turkey was analyzed for *Pipistrellus pygmaeus*. The sample was collected from the Marmara region (Bandırma, Balıkesir) (Figure 4.47). A haplotype network and intraspecific trees could not be prepared as there was only one sample for this species.

Figure 4.47. The sampling location for *Pipistrellus pygmaeus*.

We compared the sequence of our individual (*Pipistrellus pygmaeus* 137) to those available in BOLD. The first closest match to this sample was *Pipistrellus pygmaeus* with a specimen similarity range of 99.83-99.33%, the second was *Pipistrellus pygmaeus cyprius* with a specimen similarity of 98.32% and the third was *Pipistrellus pipistrellus* with a specimen similarity range of 93.14-92.59%.

The neighbor-joining tree for *Pipistrellus pygmaeus*, created with BOLD, using our individual, *Pipistrellus pygmaeus* 137, is shown in Figure 4.48. In the tree, the barcoded individual clustered with *Pipistrellus pygmaeus* barcodes in BOLD, forming a single clade. Two of the BOLD barcodes were from Norway.

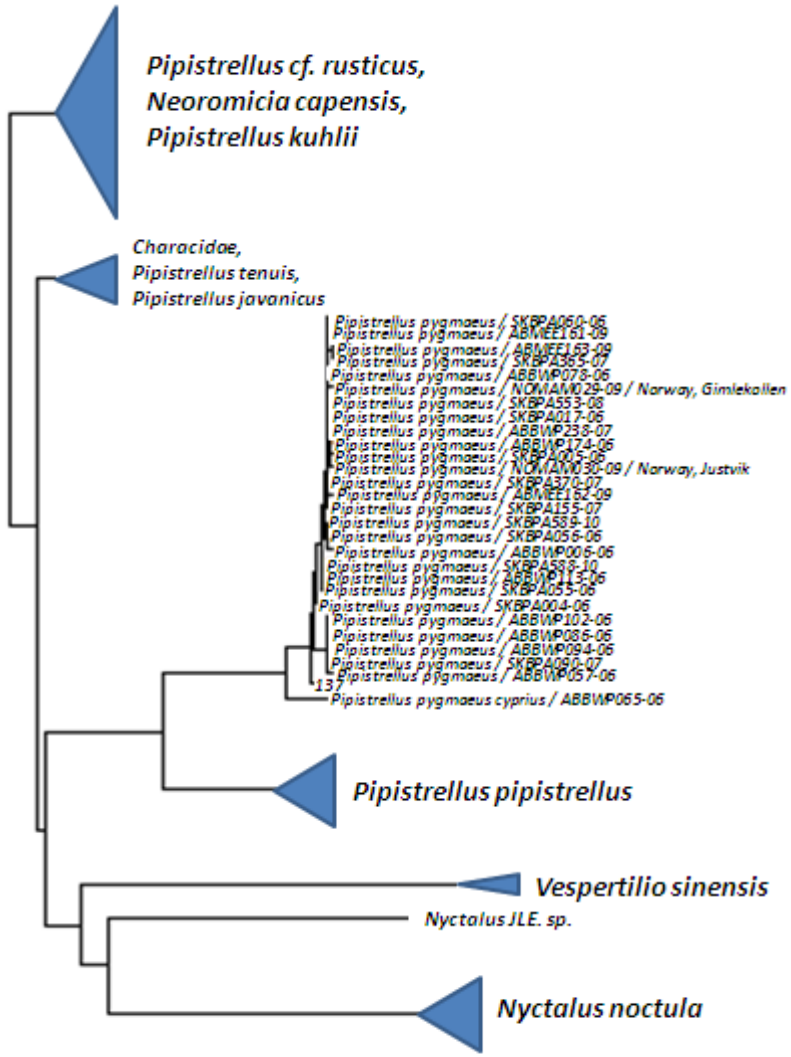

Figure 4.48. Neighbor-joining tree for our *Pipistrellus pygmaeus* sequence, sample 137, constructed based on BOLD. The sizes of the triangles are proportional to the number of sequences in BOLD for that species.

4.15. *Barbastella barbastellus*

Two sequences from Turkey were analyzed for *Barbastella barbastellus*. The samples were collected from the Marmara region (Dupnisa, Kırklareli) and the Black Sea region (Rize) (Figure 4.49). Intraspecific neighbor-joining and maximum-likelihood trees could not be prepared as there were only two samples for this species.

Figure 4.49. The sampling locations for *Barbastella barbastellus*. The circles are proportional to the number of individuals.

Two different haplotypes were observed in this species, as seen in the haplotype network and the haplotype network table (Figure 4.50 and Appendix B). Haplotypes H1 and H2 were differentiated by one base pair. In terms of individual haplotypes, H1 was observed in the Marmara region and H2 was observed in the Black Sea region.

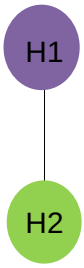

Figure 4.50. Haplotype network for *Barbastella barbastellus*. The sizes of the circles are proportional to the number of individuals. See Table 4.1 for the key to the color-codes of the geographic positioning of the haplotypes.

We compared the sequences of both individuals to those available in BOLD. All the matches obtained from BOLD were from *Barbastella barbastellus*. The closest

matches to sample 18 had a specimen similarity range of 99.83-98.65%. The closest match to sample 19 was *Barbastella barbastellus* with a specimen similarity range of 100-98.82%.

The neighbor-joining tree for *Barbastella barbastellus*, constructed with BOLD is shown in Figure 4.51. The samples that were barcoded from Turkey (18 & 19) fell within the *Barbastella* clade. It should be noted that there was one other clade in this tree, sister to the clade containing our samples.

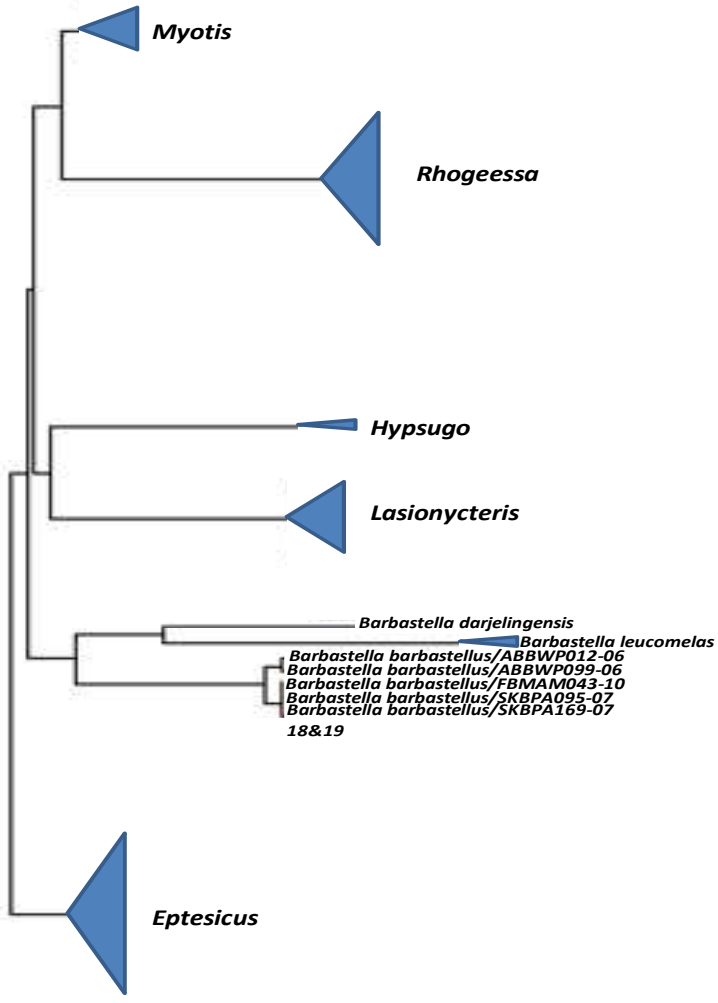

Figure 4.51. The neighbor-joining tree for our *Barbastella barbastellus* sequences (18 & 19) constructed based on BOLD. The sizes of the triangles are proportional to the number of sequences in BOLD for that species.

4.16. *Otonycterus hemprichii*

One CO1 sequence from Syria was analyzed for *Otonycterus hemprichii* (Figure 4.52). A haplotype network and intraspecific trees could not be prepared as there was only one sample for this species.

Figure 4.52. The sampling location for *Otonycteris hemprichii*.

As a first step of analyses, we compared the sequence of our individual to those available in BOLD. The closest match to this sample was *Otonycteris hemprichii* with a specimen similarity range of 100-95.38.

The neighbor-joining tree for *Otonycteris hemprichii*, created with BOLD, is shown in Figure 4.53. In the tree, the barcoded individual from Syria clustered closely with one of the four *Otonycteris hemprichii* clades in BOLD.

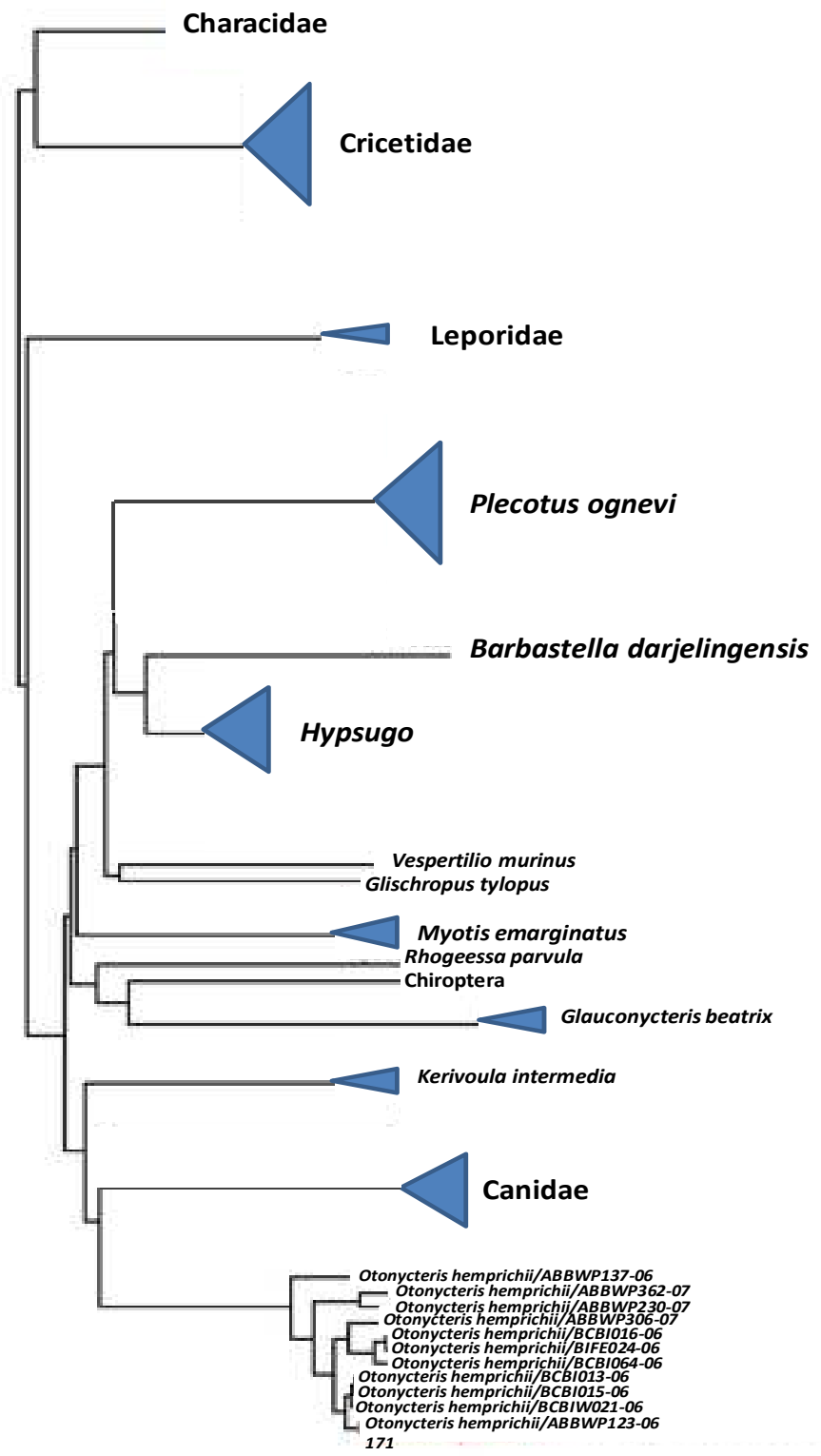

Figure 4.53. Neighbor-joining tree for our *Otonycteris hemprichii* sequence, sample 171, constructed based on BOLD. The sizes of the triangles are proportional to the number of sequences in BOLD for that species.

4.17. *Plecotus kolombatovici*

Four CO1 sequences were analyzed for *Plecotus kolombatovici*. The sequences were obtained from the Central Anatolia region (two from Konya and two from Karaman) (Figure 4.54).

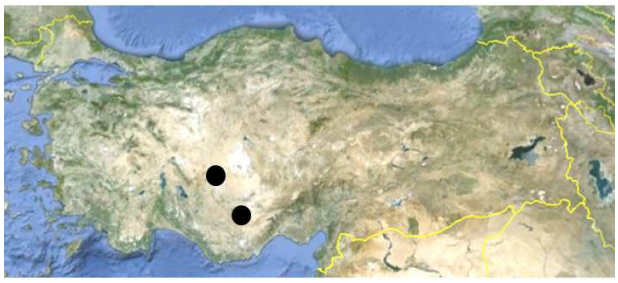

Figure 4.54. The sampling locations for *Plecotus kolombatovici*. The circles are proportional to the number of individuals.

Intraspecific trees for *Plecotus kolombatovici* are shown in Figure 4.55. All CO1 sequences generated one clade but there was some branching between samples 66, 65 and samples 54, 60. Sample 66 and sample 65 were taken from Konya whereas sample 54 and sample 60 were taken from Karaman, so we divided them into two and labelled them as the Konya group and the Karaman group. The Karaman group was different from the Konya group by one base pair (see haplotype network below, Figure 4.56).

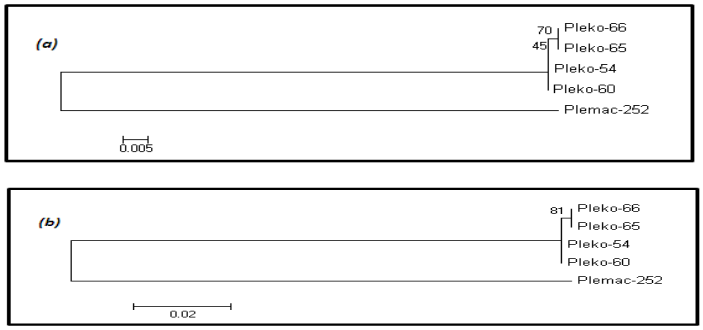

Figure 4.55. Intraspecific trees for *Plecotus kolombatovici*. (a) NJ tree and (b) ML tree.

There were two haplotypes in this species as seen in the haplotype network and the haplotype network table (Figure 4.56 and Appendix B). H1 was separated by one base pair from H2 and found in Konya, whereas H2 was found in Karaman.

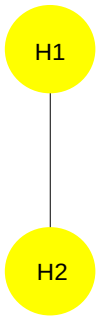

Figure 4.56. Haplotype network for *Plecotus kolombatovici*. The sizes of the circles are proportional to the number of individuals. See Table 4.1 for the key color-codes of the geographic positioning of the haplotypes.

Next, we compared the sequences of the individuals to those available in BOLD. Since there was only one base pair difference between two haplotypes, we selected one representative individual, 65, from Konya and comparing it with the data from BOLD, the closest match to this sample was *Plecotus kolombatovici* with a specimen similarity range of 100-96.52%.

The neighbor-joining tree for *Plecotus kolombatovici*, created with BOLD, using two individuals belonging to Konya and Karaman groups, *Plecotus kolombatovici* 65 and 54, is shown in Figure 4.57. In the tree, the barcoded individuals from Turkey clustered closely with one of the two clades of *Plecotus kolombatovici* barcodes in BOLD.

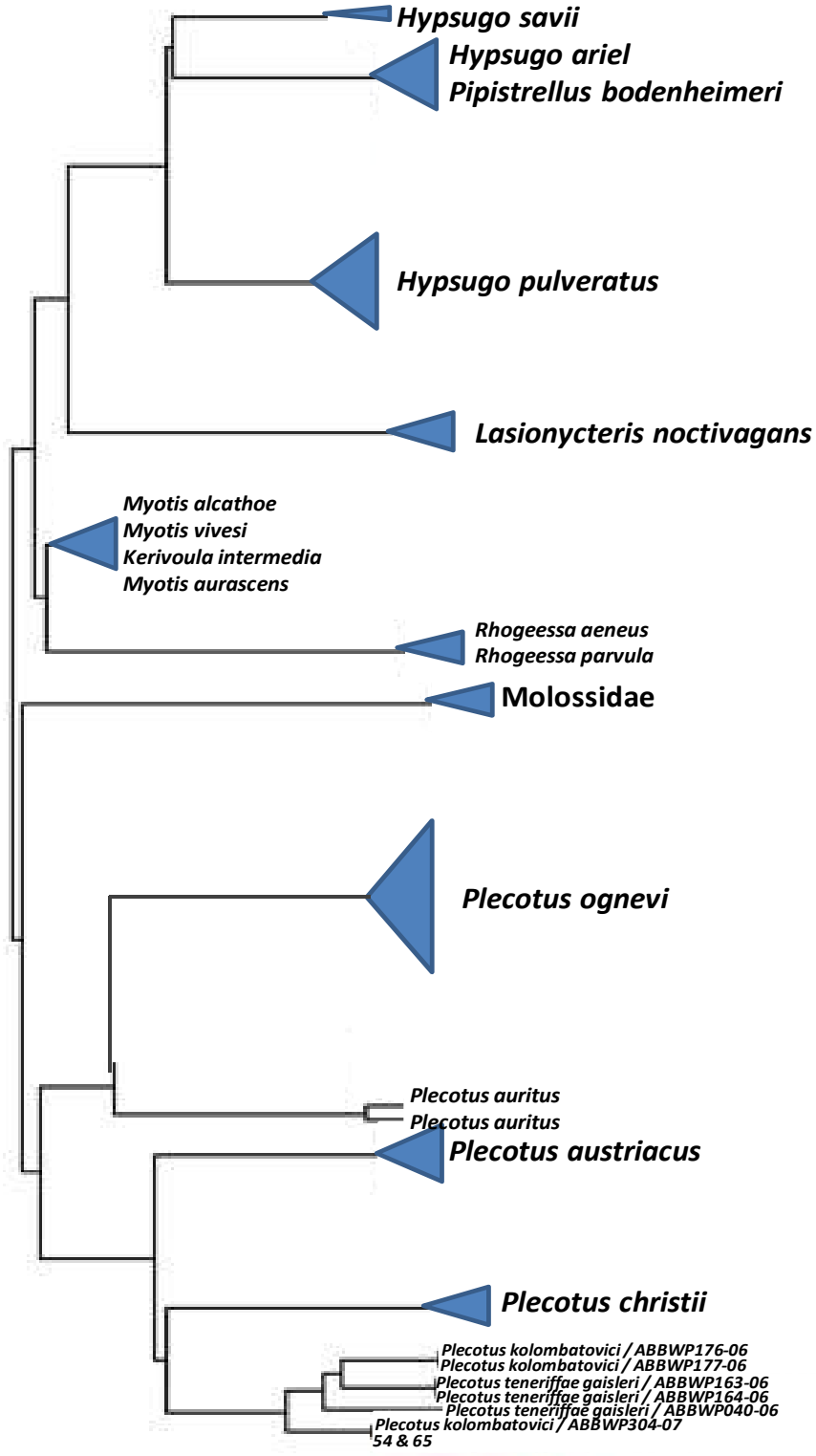

Figure 4.57. Neighbor-joining tree for two of our *Plecotus kolombatovici* sequences, samples 54 and 65, constructed based on BOLD. The sizes of the triangles are proportional to the number of sequences in BOLD for that species.

4.18. *Plecotus macrobullaris*

Eight CO1 sequences were analyzed for *Plecotus macrobullaris*. The sequences were obtained from the Central Anatolia region (one from Nevşehir and three from Kayseri), the Mediterranean region (Antalya) and Iran (Figure 4.58).

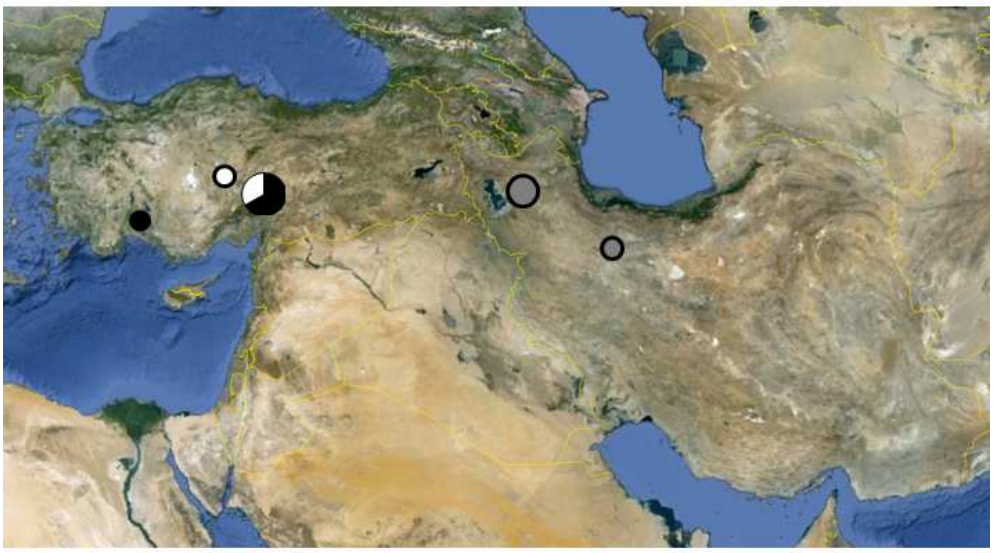

Figure 4.58. The sampling locations for *Plecotus macrobullaris*. The circles are proportional to the number of individuals. The black color indicates sampling locations for the first group, the white color indicates sampling locations for the second group and the gray color indicates sampling locations for the third group in the intraspecific trees (Figure 4.59).

Intraspecific trees for *Plecotus macrobullaris* are shown in Figure 4.59. All CO1 sequences generated three clades, Group One (samples 260, 9, 63) was found in Antalya (the Mediterranean region) and Kayseri (the Central Anatolia region), Group Two (samples 62, 10) in Nevşehir and Kayseri (the Central Anatolia region) and Group Three (samples 259, 252, 258) in Iran.

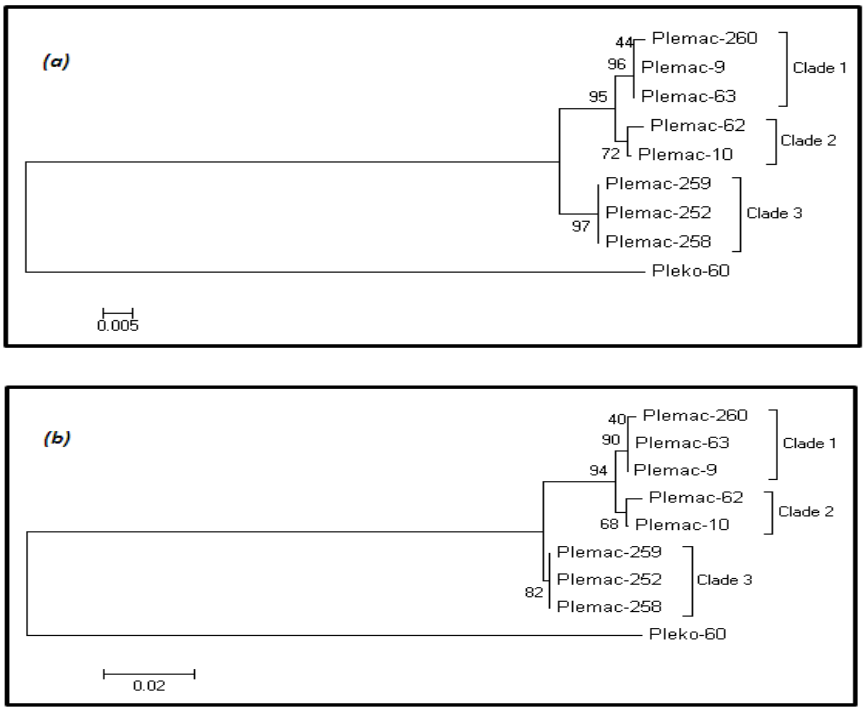

Figure 4.59. Intraspecific trees for *Plecotus macrobullaris*. (a) NJ tree and (b) ML tree.

There were five different haplotypes in this species as seen in the haplotype network and the haplotype network table (Figure 4.60 and Appendix B). H1 was the most common haplotype (found in three individuals), separated by 10 base pairs from the rest of the samples and was found in Iran only. Haplotypes H2, H3, H4 and H5 formed another group, and were found in the Mediterranean and the Central Anatolia regions.

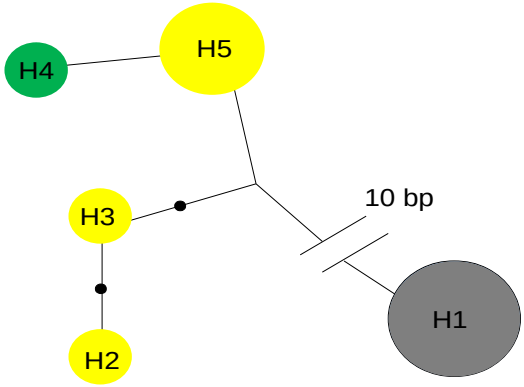

Figure 4.60. Haplotype network for *Plecotus macrobullaris*. The sizes of the circles are proportional to the number of individuals. See Table 4.1 for the key to the color codes of the geographic positioning of the haplotypes.

Next, we compared the individuals from each clade in the intraspecific trees to those available in BOLD. From Group One we selected one representative individual, 260, and comparing it with the data from BOLD, the first closest match to this sample was *Plecotus macrobullaris* with a specimen similarity range of 99.32-98.12%, and the second was *Plecotus macrobullaris alpinus* with a specimen similarity of 96.09%. Comparing the sequence of an individual from Group Two, *Plecotus macrobullaris* 62, with BOLD, the first closest match of *Plecotus macrobullaris* 62 was *Plecotus macrobullaris* again with a specimen similarity range of 99.15-98.12%, and the second was *Plecotus macrobullaris alpinus* with a specimen similarity of 95.75%. Comparing the sequence of an individual from Group Three, *Plecotus macrobullaris* 259, with the two matches that were taken from BOLD, the first closest match of *Plecotus macrobullaris* 259 was *Plecotus macrobullaris* again with a specimen similarity range of 99.83-98.03%, and the second was *Plecotus macrobullaris alpinus* with a specimen similarity of 95.89%.

The neighbor-joining tree for *Plecotus macrobullaris*, created with BOLD, using one individual belonging to Group One, *Plecotus macrobullaris* 260, is shown in Fig 4.61. In the tree, the barcoded individual from Antalya, Turkey, clustered closely with two *Plecotus macrobullaris* barcodes in BOLD. The neighbor-joining tree from BOLD for *Plecotus macrobullaris* 62 is also shown in Figure 4.62. It should be noted that *Plecotus macrobullaris* 62 was in a slightly different position on the tree. The neighbor-joining tree from BOLD for *Plecotus macrobullaris* 259 is shown in Figure 4.63. *Plecotus macrobullaris* 259 fell within the opposite branch but into the same general *Plecotus macrobullaris* clade with all other *Plecotus macrobullaris* CO1 sequences. Hence, our intraspecific trees, haplotype network and BOLD tree were all in conformation.

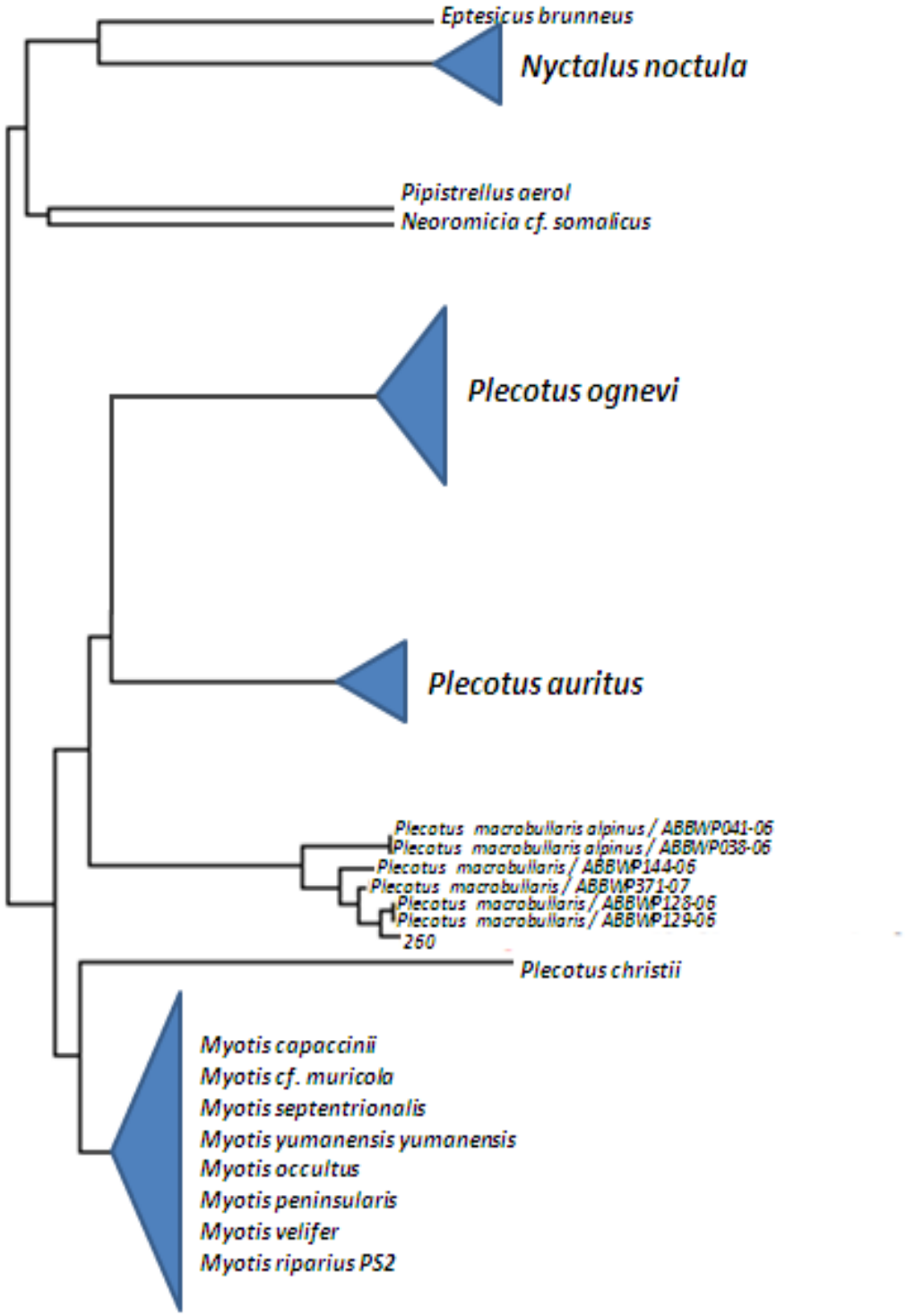

Figure 4.61. Neighbor-joining tree for one of our *Plecotus macrobullaris* sequences, sample 260, constructed based on BOLD. The sizes of the triangles are proportional to the number of sequences in BOLD for that species.

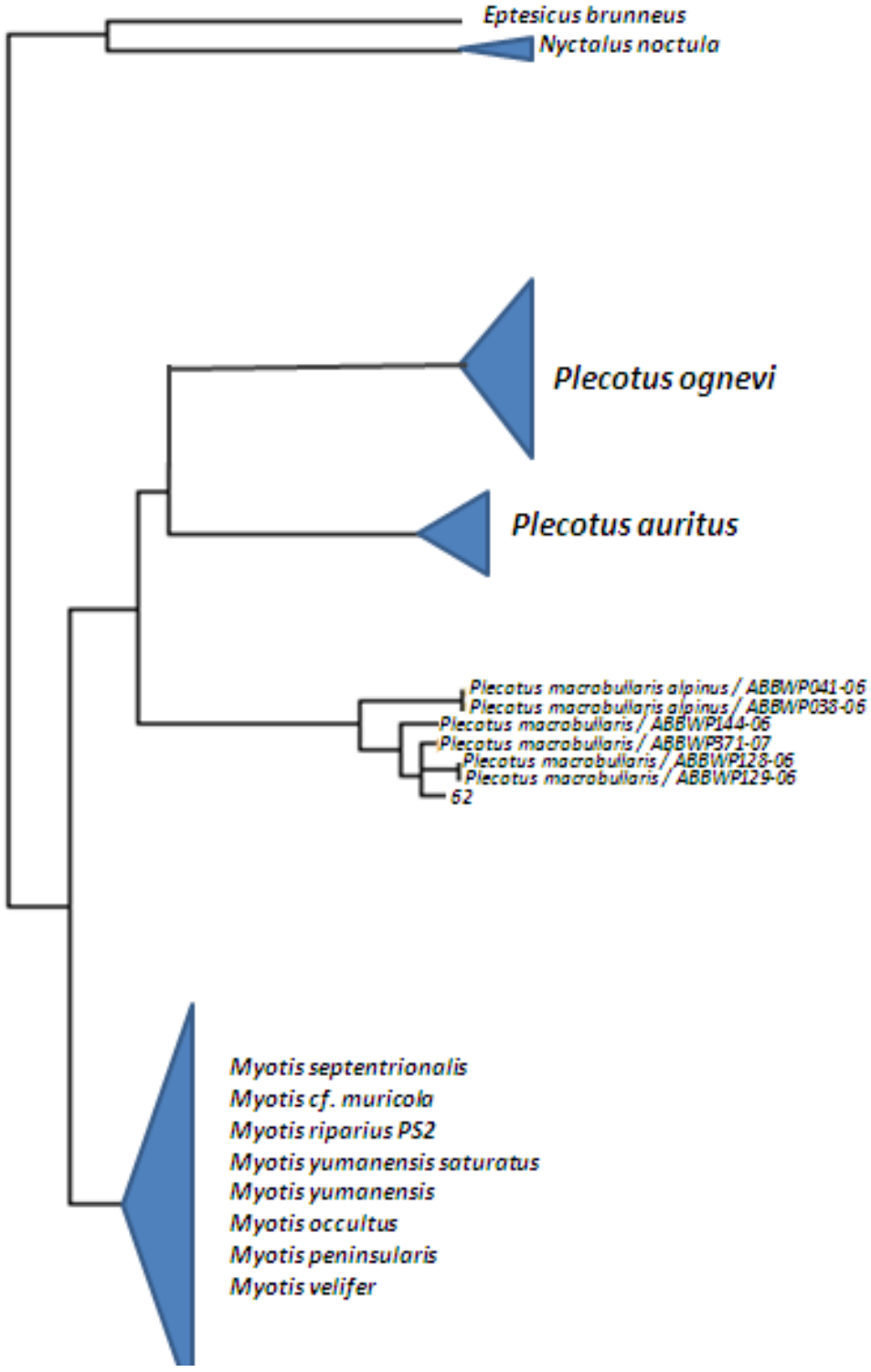

Figure 4.62. Neighbor-joining tree for one of our *Plecotus macrobullaris* sequences, sample 62, constructed based on BOLD. The sizes of the triangles are proportional to the number of sequences in BOLD for that species.

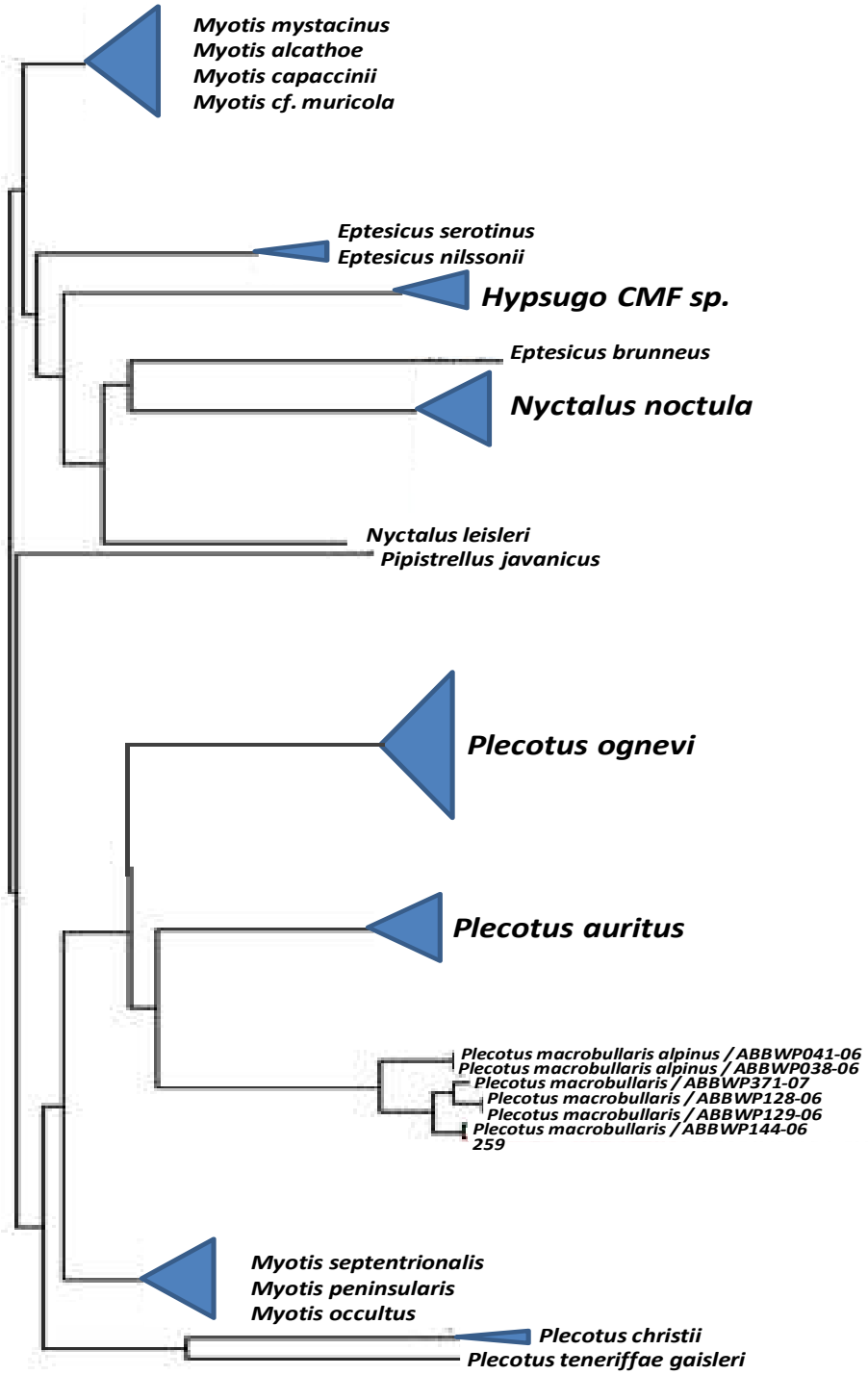

Figure 4.63. Neighbor-joining tree for one of our *Plecotus macrobullaris* sequences, sample 259, constructed based on BOLD. The sizes of the triangles are proportional to the number of sequences in BOLD for that species.

4.19. *Hypsugo savii*

Three CO1 sequences were analyzed for *Hypsugo savii*. The sequences were obtained from the Central Anatolia region (one each from Konya and Karaman) and Iran (Figure 4.64).

Figure 4.64. The sampling locations for *Hypsugo savii*. The sizes of the circles are proportional to the number of individuals. The black color indicates sampling locations for the first group and the white color indicates sampling locations for the second group in the intraspecific trees (Figure 4.65).

Intraspecific trees for *Hypsugo savii* are shown in Figure 4.65. All sequences generated two groups, where *Hypsugo savii* 162 and 248 from the Central Anatolia region clustered together and separately from *Hypsugo savii* 256 from Iran.

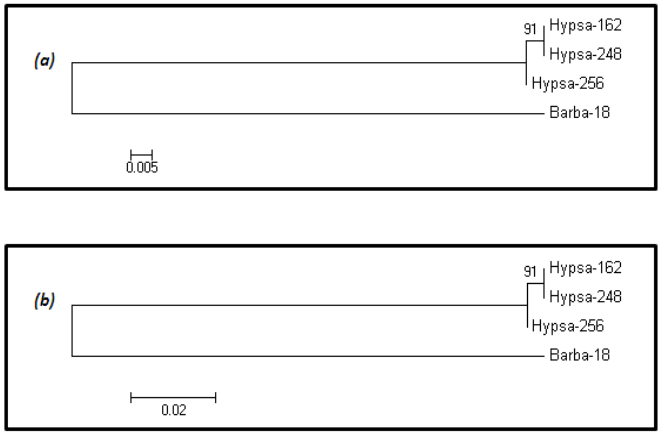

Figure 4.65. Intraspecific trees for *Hypsugo savii*. (a) Neighbor-joining tree and (b) Maximum-likelihood tree.

There were two different haplotypes in this species as seen in the haplotype network and the haplotype network table (Figure 4.66 and Apppendix B), and H1 was separated by two base pairs from H2. Haplotype H1 was found in the Central Anatolia and haplotype H2 was found in Iran.

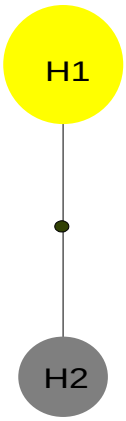

Figure 4.66. Haplotype network for *Hypsugo savii*. The sizes of the circles are proportional to the number of individuals. See Table 4.1 for the key to the color codes of the geographic positioning of the haplotypes.

As a next step, we compared the sequence of the individual 162 to those available in BOLD. Comparing it with the data from BOLD, the only closest match to this sample was *Hypsugo savii* again with a specimen similarity range of 100-91.21%.

The neighbor-joining tree for *Hypsugo savii*, created with BOLD, using individuals 162 and 256, is shown in Figure 4.67. In the tree, the barcoded individuals from the Central Anatolia region and Iran clustered closely with one clade of *Hypsugo savii* barcodes in BOLD. It should be noted that there were three other clades in this tree, one sister to the clade containing our samples.

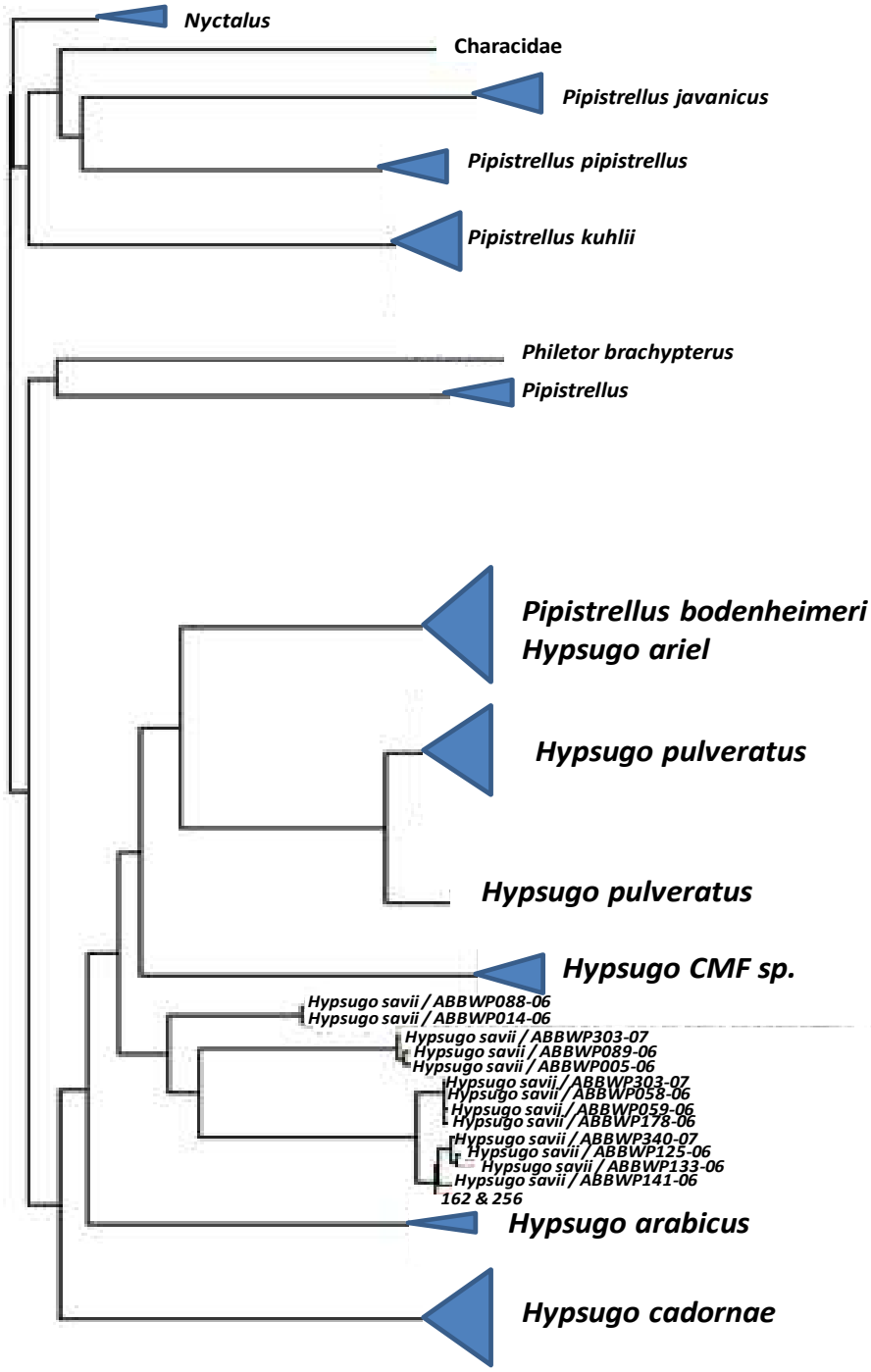

Figure 4.67. Neighbor-joining tree for two of our *Hypsugo savii* sequences, samples 162 and 256, constructed based on BOLD. The sizes of the triangles are proportional to the number of sequences in BOLD for that species.

4.20. *Myotis aurascens*

One CO1 sequence from Iran was analyzed for *Myotis aurascens* (Figure 4.68). A haplotype network and intraspecific trees could not be prepared as there was only one sample for this species.

Figure 4.68. The sampling location for *Myotis aurascens*.

We compared the sequence of our individual, *Myotis aurascens* 257, with the data from BOLD. First closest match to this sample was *Myotis aurascens* with a specimen similarity range of 99.5-97.98%, the second was *Myotis mystacinus* with a specimen similarity range of 91.85-91.09% and the third was *Myotis cf. aurascens* with a specimen similarity range of 91.09-91.03%

The neighbor-joining tree for *Myotis aurascens*, created with BOLD, using *Myotis aurascens* 257 is shown in Figure 4.69. In the tree, the only barcoded individual from Iran clustered closely with one of the two main clades of *Myotis aurascens* barcodes in BOLD.

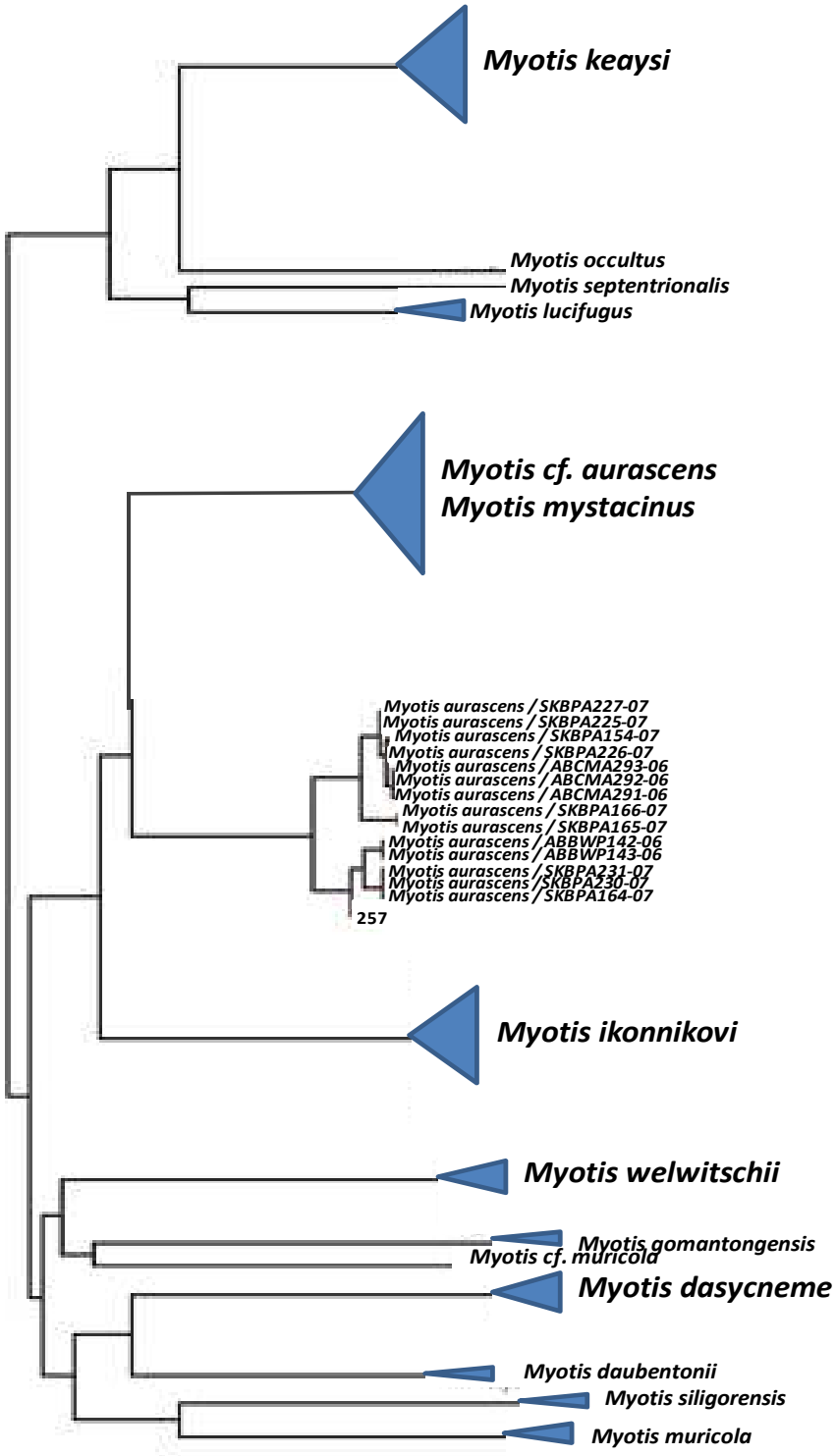

Figure 4.69. Neighbor-joining tree for our *Myotis aurascens* sequence, sample 257, constructed based on BOLD. The sizes of triangles are proportional to the number of sequences in BOLD for that species.

4.21. *Myotis bechsteinii*

One CO1 sequence from Turkey was analyzed for *Myotis bechsteinii*. The sample was collected from the Black Sea region (Artvin) (Figure 4.70). A haplotype network and intraspecific trees could not be prepared as there was only one sample for this species.

Figure 4.70. The sampling location for *Myotis bechsteinii*.

We compared the sequence of our only individual, *Myotis bechsteinii* 4, to those available in BOLD. The closest match to our sample was *Myotis bechsteinii* with a specimen similarity range of 99.83-93.67%.

The neighbor-joining tree for *Myotis bechsteinii*, created with BOLD, using our individual, *Myotis bechsteinii* 4 is shown in Fig 4.71. In the tree, the barcoded individual from Artvin (the Black Sea region) clustered closely with one of the three clades of *Myotis bechsteinii* barcodes in BOLD.

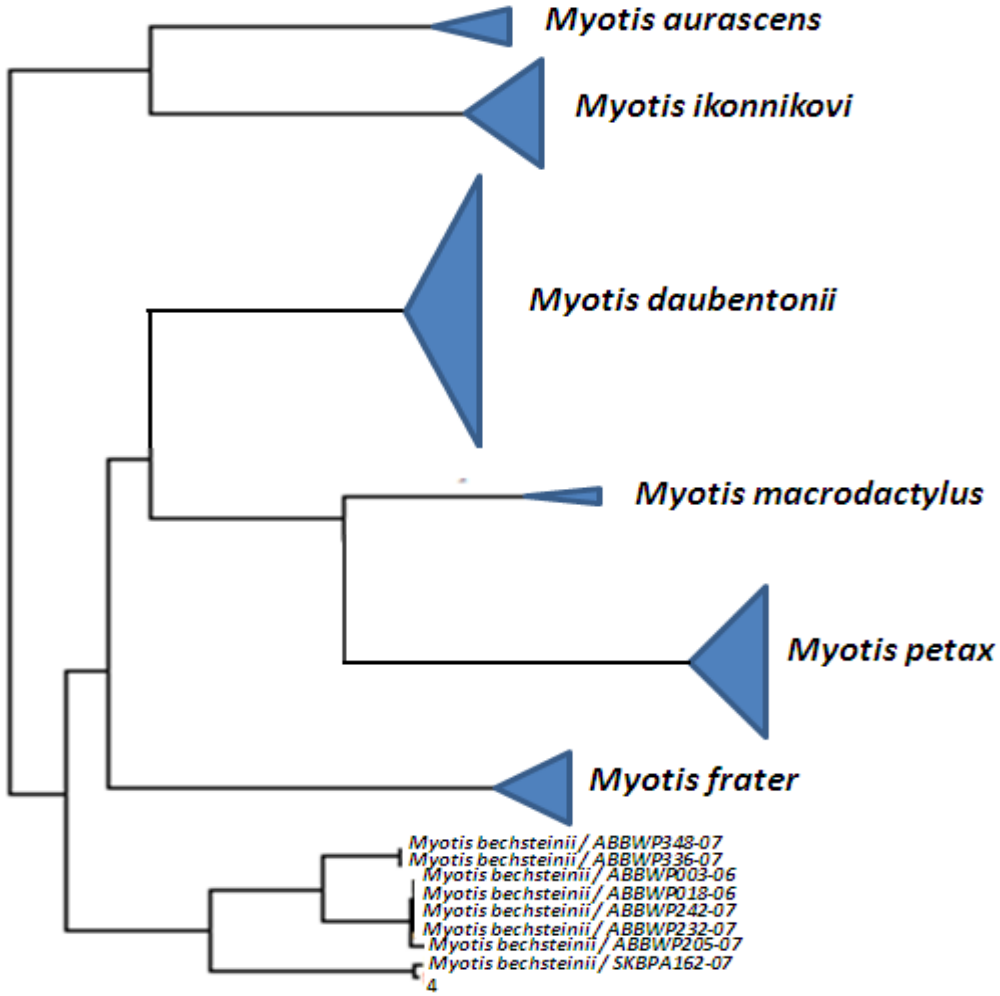

Figure 4.71. Neighbor-joining tree for our *Myotis bechsteinii* sequence, sample 4, constructed based on BOLD. The sizes of triangles are proportional to the number of sequences in BOLD for that species.

4.22. *Myotis blythii - Myotis myotis*

Eighteen CO1 sequences were analyzed for *Myotis blythii – Myotis myotis*. The sequences were obtained from all seven regions of Turkey and Syria. These included one individual from the Marmara region (Kırklareli), three individuals from the Central Anatolia region (Ankara, Kayseri, Yozgat), one individual from the Black Sea region (Artvin), four individuals from the Mediterranean region (two from Osmaniye, two from Mersin), five individuals from the East Anatolia region (two from Bitlis, Erzincan, Van, Malatya), one individual from the Aegean region (Afyon), two individuals from the Southeast Anatolia region (Gaziantep, Urfa) and one individual from Syria (Figure 4.72).

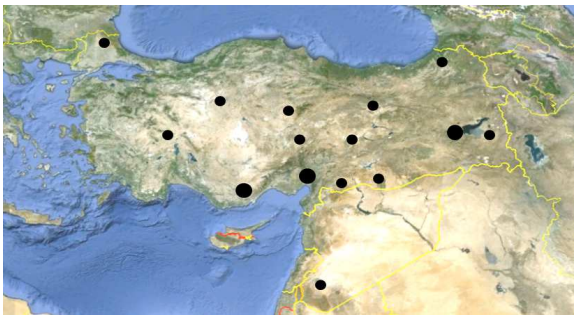

Figure 4.72. The sampling locations for *Myotis blythii-Myotis myotis*. The circles are proportional to the number of individuals.

Intraspecific trees for *Myotis blythii-Myotis myotis* are shown in Figure 4.73. Clades were not clearly separated from each other.

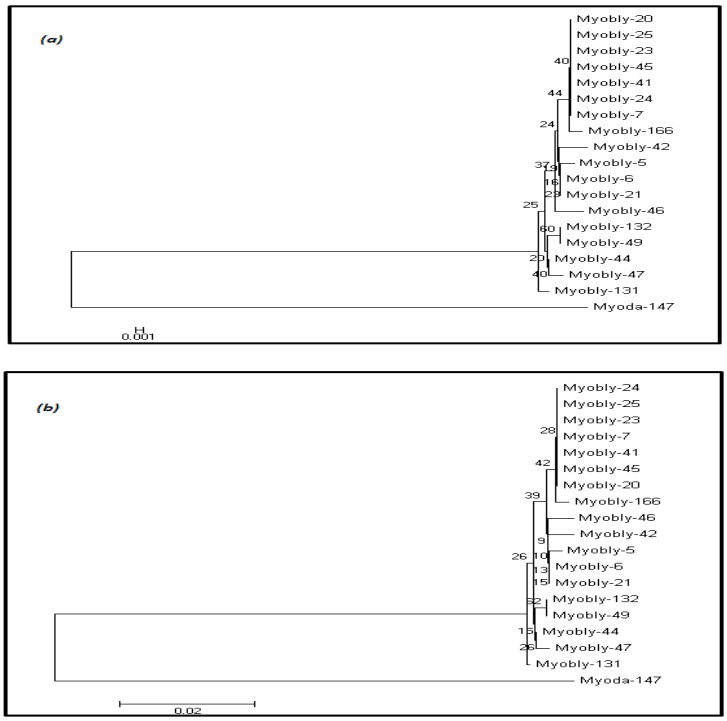

Figure 4.73. Intraspecific trees for *Myotis blythii* and *Myotis myotis*. (a) Neighbor-joining tree and (b) Maximum-likelihood tree. In order to make trees clear, all *Myotis blythii* and *Myotis myotis* samples were coded as Myobly. Myoda (*Myotis daubentonii*) was selected as outgroup.

There were 10 different haplotypes in this species complex as seen in the haplotype network and the haplotype network table (Figure 4.74 and Appendix B). H3 was the most common haplotype (found in seven individuals), and was found in the Mediterranean region, the Central Anatolia region, the Marmara region, the Black Sea region. Since base pair differences were not very high, we could not observe clear groupings between haplotype sets.

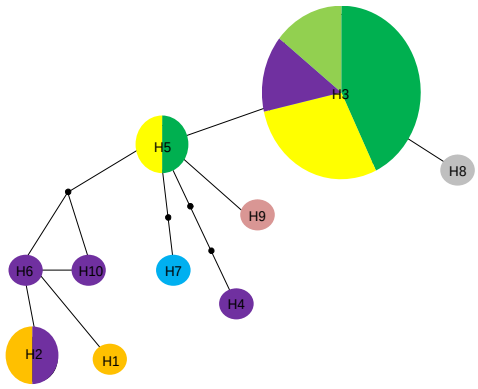

Figure 4.74. Haplotype network for *Myotis blythii-Myotis myotis*. The sizes of the circles are proportional to the number of the individuals. See Table 4.1 for the key to the color codes of the geographic positioning of the haplotypes.

Since there were not many differences between individuals, we chose one individual randomly, *Myotis blythii-Myotis myotis* 44, for comparison of its sequence to those available in BOLD. The first closest match to this sample was *Myotis blythii oxygnathus* with a specimen similarity of 99.67%, the second was *Myotis myotis* again with a specimen similarity of 99.67% and the third was *Myotis blythii omari* with a specimen similarity of 99.67%. This result also showed that there was some disagreement in the nomenclature of *Myotis blythii*, *Myotis myotis* and their subspecies.

The neighbor-joining tree for *Myotis blythii-Myotis myotis*, created with BOLD, using *Myotis blythii-Myotis myotis* 44 is shown in Figure 4.75. In the tree, our barcoded individual clustered closely with one of the three main clades of *Myotis blythii-Myotis myotis* barcodes in BOLD.

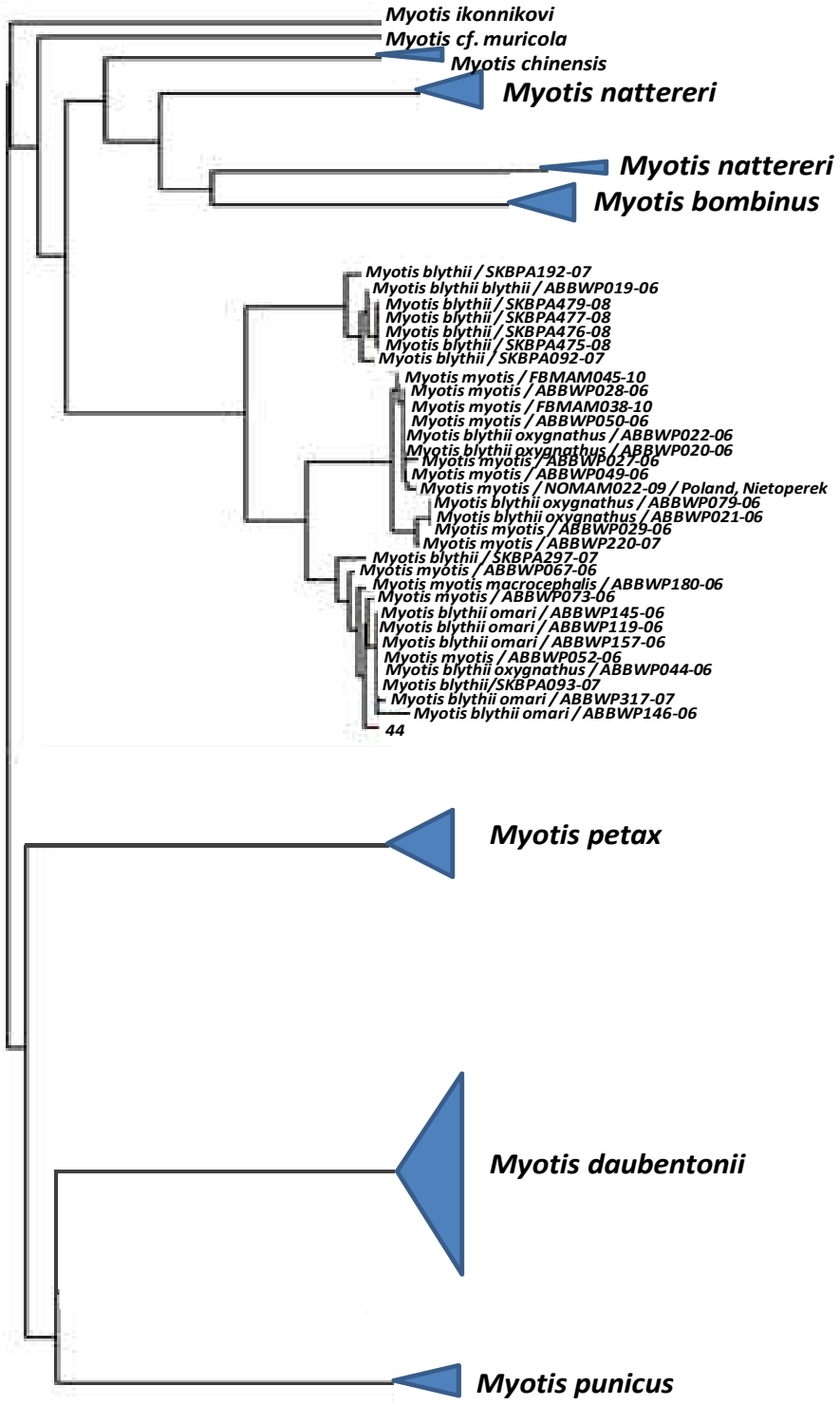

Figure 4.75. Neighbor-joining tree for our *Myotis blythii-Myotis myotis* sequences, using sample 44, constructed based on BOLD. The sizes of the triangles are proportional to the number of sequences in BOLD for that species.

4.23. *Myotis capaccinii*

Eight CO1 sequences were analyzed for *Myotis capaccinii*. The sequences were obtained from the Central Anatolia region (one sample from Nevşehir), the Marmara region (two samples from Kırklareli, one sample from Balıkesir), the East Anatolia region (one sample from Bitlis), and Syria (three samples) (Figure 4.76).

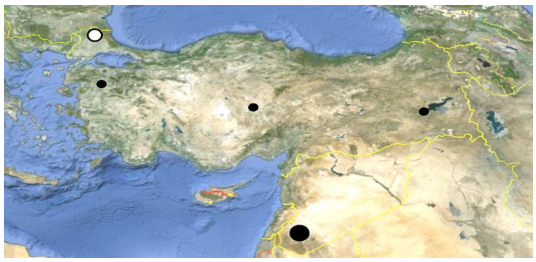

Figure 4.76. The sampling locations for *Myotis capaccinii*. The circles are proportional to the number of individuals. The black color indicates sampling locations for the first group and the white color indicates sampling location for the second group in the intraspecific trees (Figure 4.77).

Intraspecific trees for *Myotis capaccinii* are shown in Figure 4.77. All CO1 sequences generated two clades; six individuals which formed the first group were from Nevşehir, Bitlis, Balıkesir and Syria. Two individuals which formed the second group were both from Kırklareli, Dupnisa. This difference between two clades resulted from a 14 base pair difference between two haplotypes (see haplotype network below, Figure 4.78). Although the two groups had individuals from the same region, there was a high number of base pair difference between two groups.

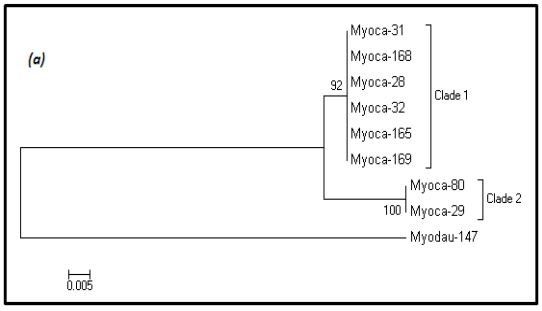

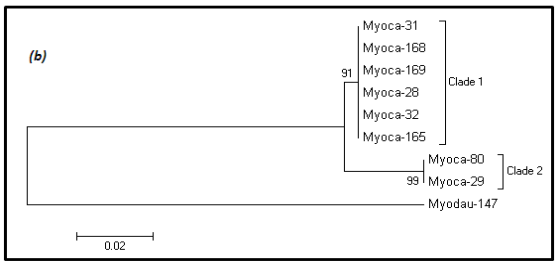

Figure 4.77. Intraspecific trees for *Myotis capaccinii*. (a) NJ tree and (b) ML tree.

There were two different haplotypes in this species as seen in the haplotype network and the haplotype network table (Figure 4.78 and Appendix B). H1 was found in Nevşehir, Bitlis, Balıkesir, and had its highest frequency in Syria within the data set. H1 was separated by 14 base pairs from H2. H2 was found exclusively in Kırklareli, Dupnisa and was separated from the rest of the samples in the intraspecific trees.

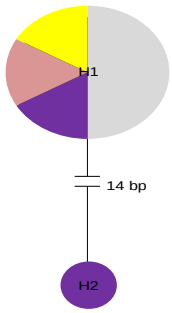

Figure 4.78. Haplotype network for *Myotis capaccinii*. The sizes of the circles are proportional to the number of individuals. See Table 4.1 for the key to the color codes of the geographic positioning of the haplotypes.

Next, we compared the sequences of representative individuals from each clade to those available in BOLD. We selected one individual with haplotype H1, 31, and comparing it with the data from BOLD, the closest match to this sample was *Myotis capaccinii* with a specimen similarity range of 100-97.47%. Comparing an individual with haplotype H2, *Myotis capaccinii* 80, with BOLD, the only match of *Myotis capaccinii* 80 was *Myotis capaccinii* with a specimen similarity range of 100-97.15%.

The neighbor-joining tree for *Myotis capaccinii*, created with BOLD, using one individual belonging to haplotype H1, *Myotis capaccinii* 31, is shown in Figure 4.79. In the tree, the barcoded individual clustered closely with one of the two main clades of *Myotis capaccinii*. The neighbor-joining tree from BOLD for *Myotis capaccinii* 80 is also shown in Figure 4.80. *Myotis capaccinii* 80 fell within the opposite branch but into the same general *Myotis capaccinii* clade.

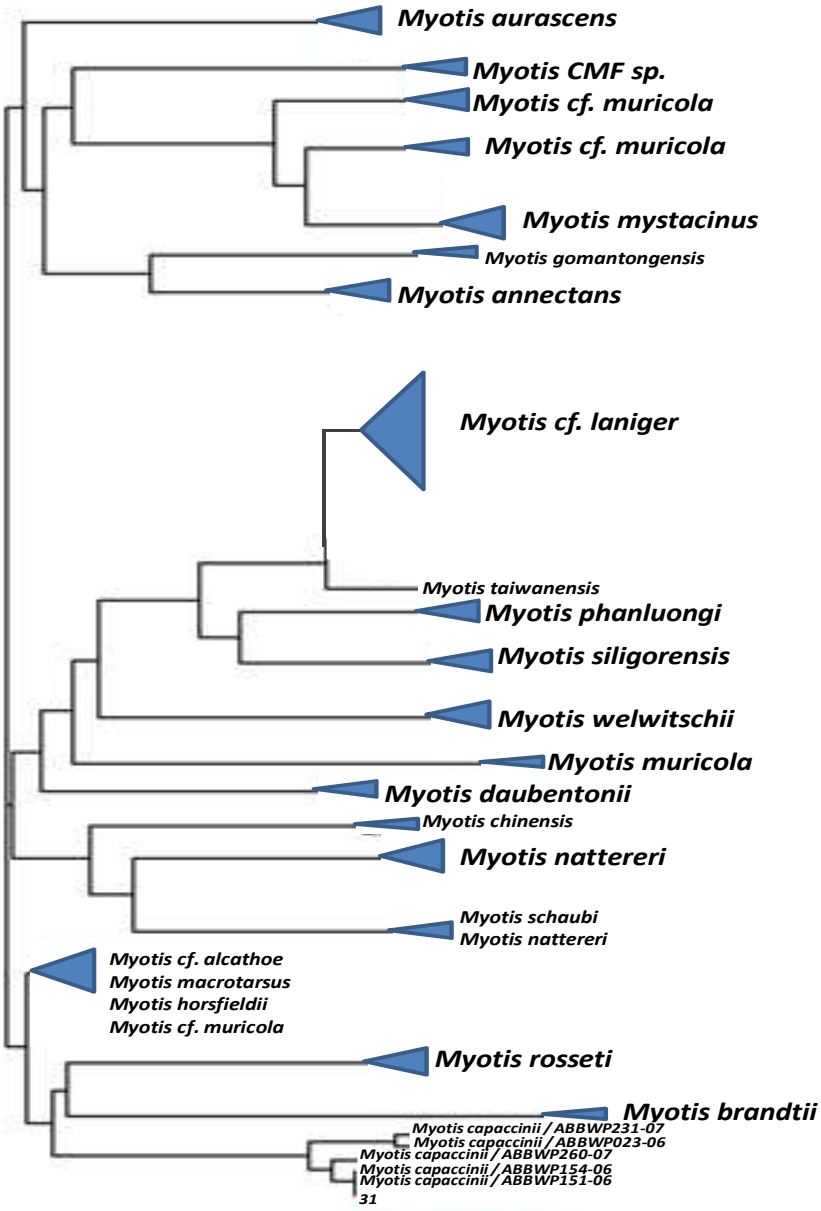

Figure 4.79. Neighbor-joining tree for one of our *Myotis capaccinii* sequences, sample 31, constructed based on BOLD. The sizes of the triangles are proportional to the number of sequences in BOLD for that species.

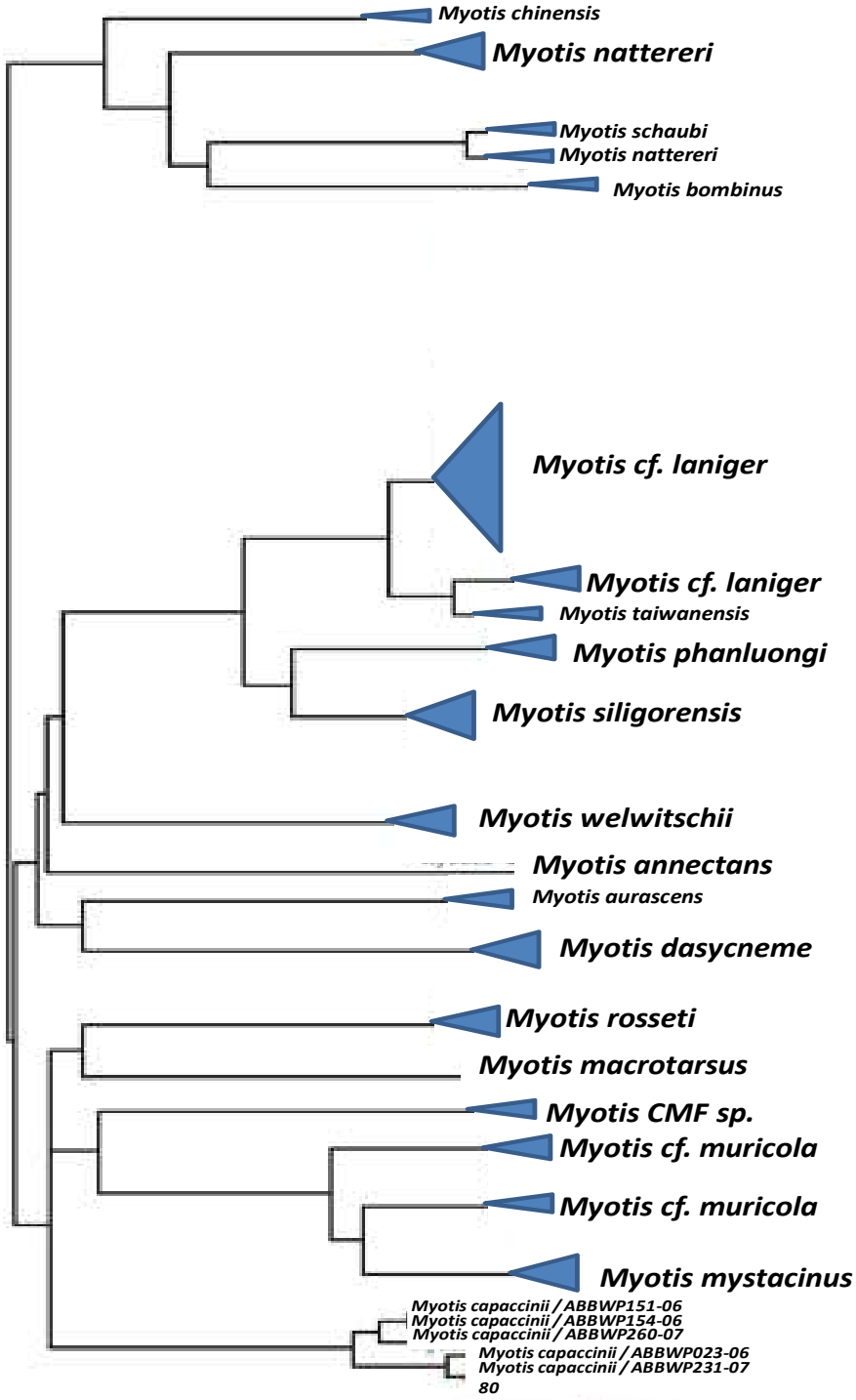

Figure 4.80. Neighbor-joining tree for one of our *Myotis capaccinii* sequences, sample 80, constructed based on BOLD. The sizes of the triangles are proportional to the number of sequences in BOLD for that species.

4.24. *Myotis daubentonii*

Two CO1 sequences from Turkey were analyzed for *Myotis daubentonii*. Both samples were collected from the Black Sea region, Bolu (Figure 4.81). A haplotype network and intraspecific trees could not be prepared as there were only two samples and only one haplotype for this species.

Figure 4.81. The sampling location for *Myotis daubentonii*.

As a first analysis, we compared the haplotype to those available in BOLD. Comparing it with the data from BOLD, the only closest match to this sample was *Myotis daubentonii* with a specimen similarity range of 99.49-97.97%.

The neighbor-joining tree for *Myotis daubentonii*, created with BOLD, using *Myotis daubentonii* 147, is shown in Figure 4.82. In the tree, the barcoded individual from Turkey clustered closely with one clade of *Myotis daubentonii* barcodes in BOLD. It should be noted that there were two other clades in this tree, one sister to the clade containing our sample, and another reciprocally monophyletic to the one comprising our sample and its sister clade.

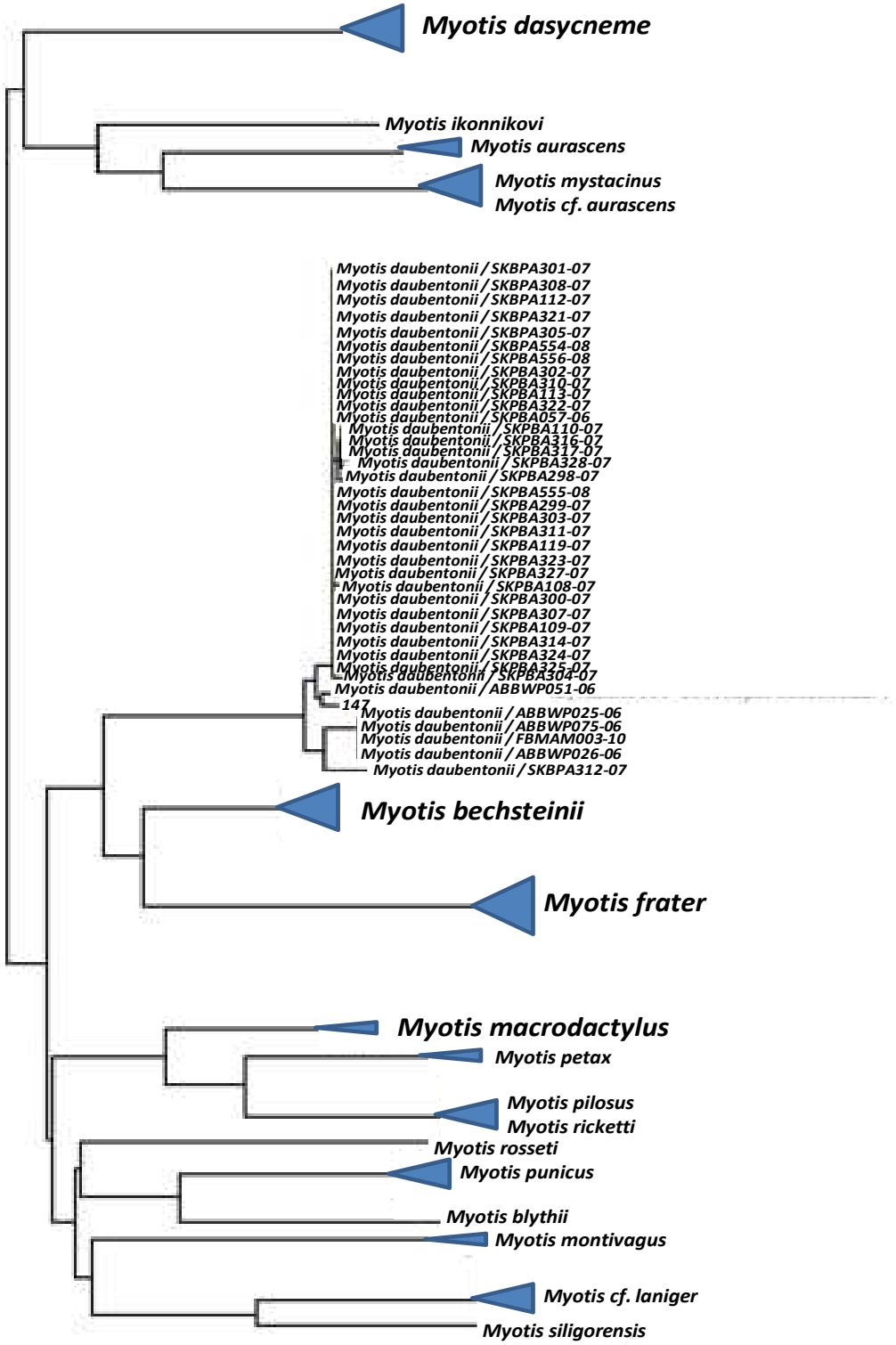

Figure 4.82. Neighbor-joining tree for our *Myotis daubentonii* haplotype, using sample 147, constructed based on BOLD. The sizes of the triangles are proportional to the number of sequences in BOLD for that species.

4.25. *Myotis mystacinus*

Three CO1 sequences were analyzed for *Myotis mystacinus*. The sequences were obtained from three locations; one from the Aegean region (Uşak), one from the Central Anatolia region (Yozgat), and one from the Mediterranean region (Antalya) (Figure 4.83).

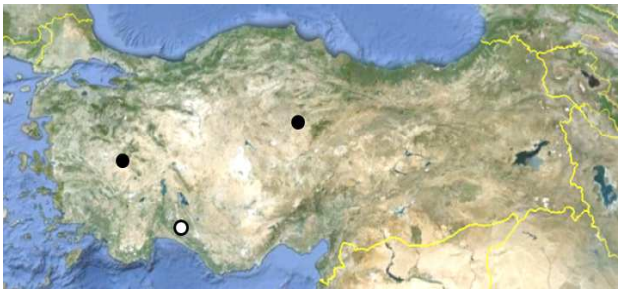

Figure 4.83. The sampling locations for *Myotis mystacinus*. The circles are proportional to the number of individuals. The black color indicates sampling locations for the first group and the white color indicates sampling location for the second group in the intraspecific trees (Figure 4.84).

Intraspecific trees for *Myotis mystacinus* are shown in Figure 4.84. All CO1 sequences generated two clades. Sample 175 was from Uşak and sample 243 from Yozgat and these two samples formed one clade, whereas sample 261 from Antalya fell on a different branch. This was probably due to that haplotype (H3) being different from the rest by four bases (see haplotype network below, Figure 4.85).

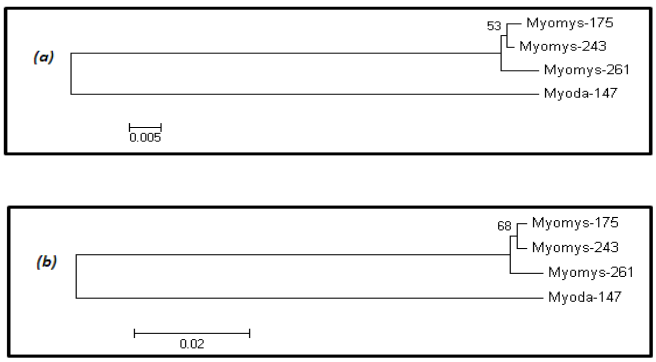

Figure 4.84. Intraspecific trees for *Myotis mystacinus*. (a) NJ tree and (b) ML tree.

There were three different haplotypes in this species as seen in the haplotype network and the haplotype network table (Figure 4.85 and Appendix B). Haplotypes H1 and H2 formed one group, which was separated by four base pairs from H3 (which corresponded to sample 261 in the trees). H3 was found in Antalya (the Mediterranean region) and clustered separately from the other two samples in the intraspecific trees.

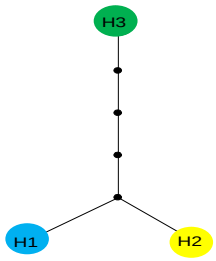

Figure 4.85. Haplotype network for *Myotis mystacinus*. The sizes of the circles are proportional to the number of individuals. See Table 4.1 for the key to the color codes of the geographic positioning of the haplotypes.

As a next step, we compared the sequences of the individuals from each group to those available in BOLD. For H1 and H2, we selected one representative individual, 175, and comparing it with the data from BOLD, the first closest match to this sample was *Myotis mystacinus* with a specimen similarity range of 100-99.67%, the second was *Myotis cf. aurascens* with a specimen similarity range of 99.67-99.66% and the third was *Myotis mystacinus* again with a specimen similarity range of 99.62-99.6%. Comparing the only individual with haplotype H3, *Myotis mystacinus* 261, with the matches to BOLD, the first closest match was *Myotis cf. aurascens* with a specimen similarity of 99.66%, the second was *Myotis mystacinus* with a specimen similarity range of 99.48-99.15%, and the third was *Myotis cf. aurascens* again with a specimen similarity of 99.15%.

The neighbor-joining tree for *Myotis mystacinus*, created with BOLD, using samples 175 and 261, is shown in Figure 4.86. In the tree, the barcoded individuals from Turkey clustered with other *Myotis mystacinus* and *Myotis cf. aurascens* barcodes in BOLD. There was no clear separation between the individuals 175 and 261. The main clade that contained individuals 175 and 261 also included one individual from Veierland,

Norway. There was one other *Myotis mystacinus* individual forming its own clade, sister to the main *Myotis mystacinus* clade.

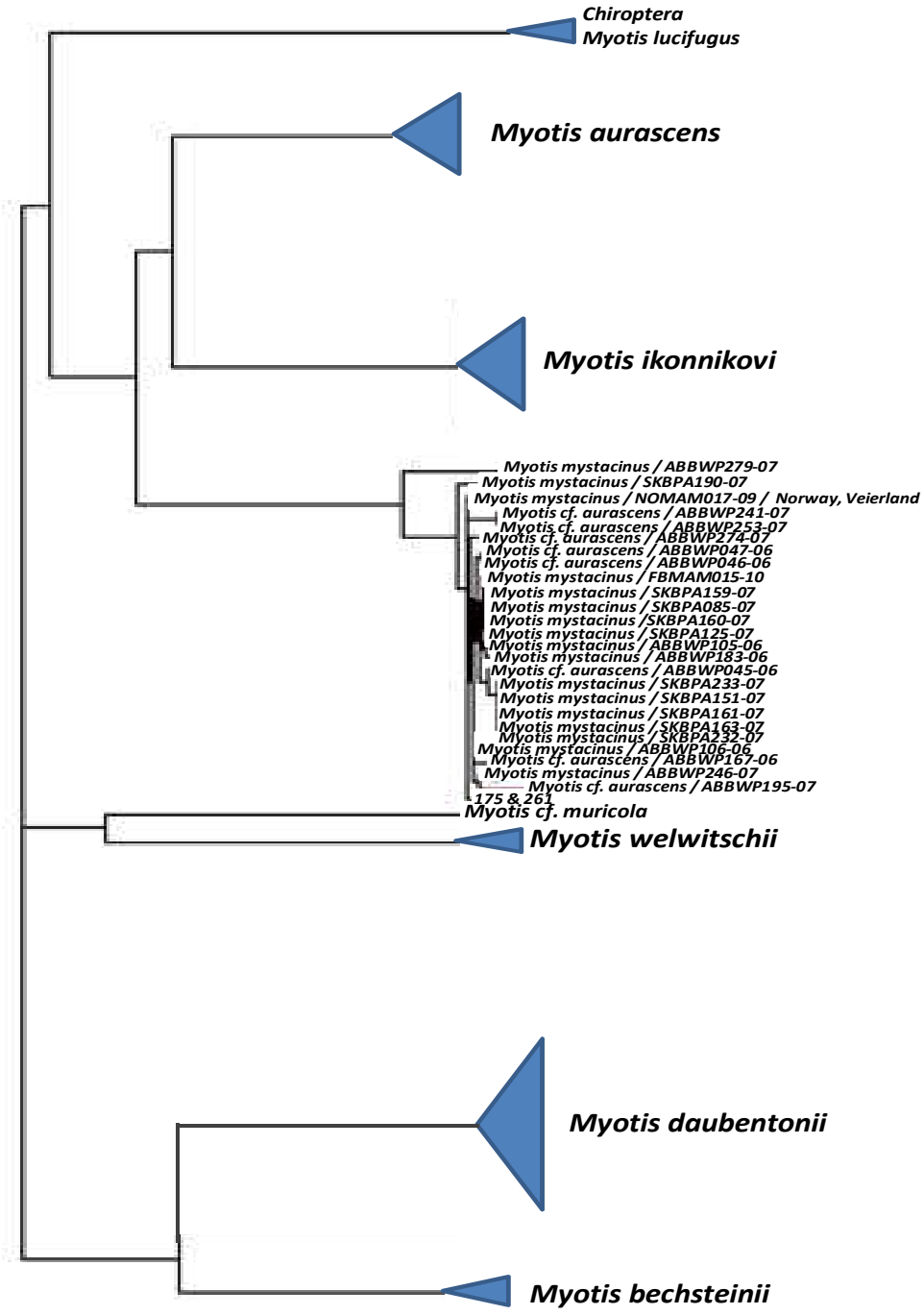

Figure 4.86. Neighbor-joining tree for our *Myotis mystacinus* sequences, sample 175 and sample 261, constructed based on BOLD. The sizes of the triangles are proportional to the number of sequences in BOLD for that species.

4.26. *Miniopterus schreibersii pallidus*

One CO1 sequence from Iran was analyzed for *Miniopterus schreibersii pallidus*. The sample was collected from Ilam, Sarin Ab-Garma (Figure 4.87). A haplotype network and intraspecific trees could not be prepared as there was only one sample for this species.

Figure 4.87. The sampling location for *Miniopterus schreibersii pallidus*.

We compared the sequence of our sample to those available in BOLD. The first closest match to this sample was *Miniopterus schreibersii pallidus* with a specimen similarity of 99.83% and the second was *Miniopterus schreibersii* with a specimen similarity range of 95.69-95.19%.

The neighbor-joining tree for *Miniopterus schreibersii pallidus*, created with BOLD, using our sample, *Miniopterus schreibersii pallidus* M152 is shown in Figure 4.88. In the tree, the barcoded individual from Iran clustered closely with the one barcode, *Miniopterus schreibersii pallidus*, in BOLD, forming a single clade.

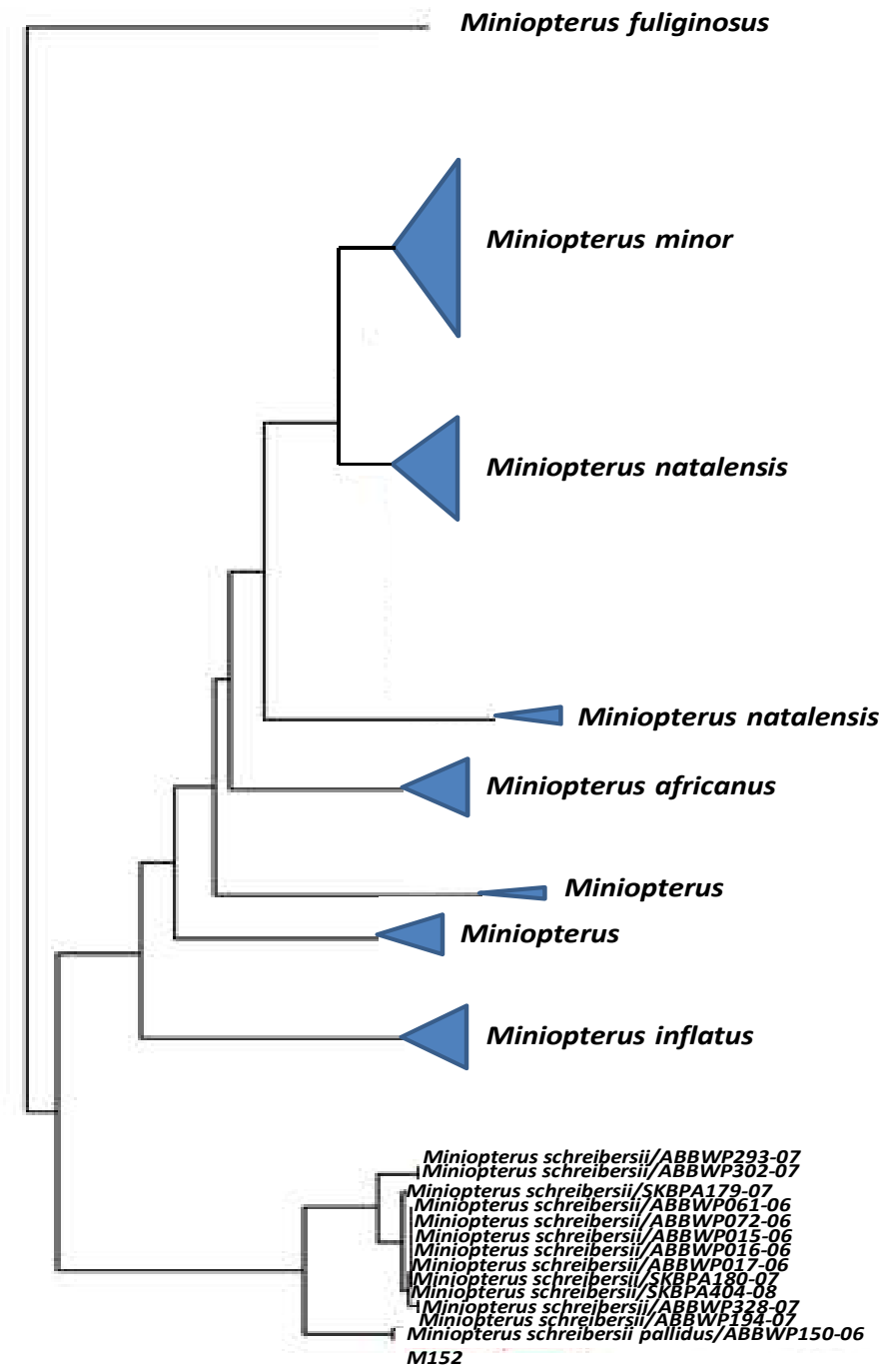

Figure 4.88. Neighbor-joining tree for our *Miniopterus schreibersii pallidus* sequence, sample M152, constructed based on BOLD. The sizes of the triangles are proportional to the number of sequences in BOLD for that species.

5. DISCUSSION

In our study, we analyzed 134 bat tissue samples, six Genbank and six BOLD sequences from a total of 26 species. Samples were taken mainly from Turkey but there were also a few samples from Iran and Syria. The average intraspecific divergence was 1.09%. Intraspecific divergences of *Eptesicus serotinus* and *Tadarida teniotis* had much higher values than the average intraspecific divergence value (4.25% and 9.54%, respectively).

Hebert et al. (2004b) suggests a threshold of ten times the average intraspecific difference for faster discovery of new animal species, and for barcoding to work effectively to discriminate species. However, recently, many authors have discussed the validity of such assumptions. Dasmahapatra and Mallet (2006) argue that the determination of the intraspecific divergence can be biased by the analysis of few individuals per species or by the sampling in a restricted area. Secondly, determination of interspecific divergence may not include the closest relative, and as Meier et al. (2008) also suggest, the use of mean instead of smallest interspecific distances can exaggerate the size of the “barcoding gap”.

We divided the species under investigation into three groups -the first group included the species that formed more than one clade (both in intraspecific trees and in BOLD tree except *Myotis mystacinus*, explained below), the second group included the species that formed one clade (in intraspecific trees) and the third group included the species with one sample only-.

The first group consisted of the following species; *Eptesicus serotinus, Myotis capaccinii, Pipistrellus pipistrellus, Rhinolophus euryale, Rhinolophus ferrumequinum* and *Rhinolophus hipposideros*. Two species, *Plecotus macrobullaris* and *Tadarida teniotis*, formed more than one clade and were included in the first group, however, their patterns do not only reflect the Turkish population, but include samples from a neighboring country (*Plecotus macrobullaris* from Iran) and samples from BOLD and Genbank with locations unavailable to the public (*Tadarida teniotis*). *Myotis mystacinus* was also included in first

group but its division in intraspecific trees resulted in a very complex and structured clade in BOLD.

The second group results need detailed analysis since three different scenarios can be proposed -the first one is that the lack of samples resulted in one clade but does not show the real picture in Turkey (*Barbastella barbastellus, Hypsugo savii, Myotis daubentonii, Pipistrellus kuhlii*). The second one is that although we had enough samples of a particular species, one clade formed because of the genetic complexity of the species (*Myotis blythii/Myotis myotis*). The third one is that there is already a single clade present in Turkey and our samples were adequate to show the real picture (*Nyctalus leisleri, Nyctalus noctula, Plecotus kolombatovici, Pipistrellus nathusii, Taphozous nudiventris*).

Finally, the third group included *Asellia tridens, Miniopterus schreibersii pallidus, Myotis aurascens, Myotis bechsteinii, Nyctalus lasiopterus, Otonycteris hemprichii and Pipistrellus pygmaeus.*

Eptesicus serotinus had an intraspecific divergence value of 4.25%. According to Benda and Horacek (1998), the territory of Turkey may be a zone of transition between two subspecies; *E. s. serotinus* (Northern Turkey) and *E. s. shiraziensis* (Southern Turkey). Our results, including the high intraspecific divergence value, support this expectation. Our single individual from the Black Sea region fell into a separate clade when compared to individuals from southern Turkey in the BOLD tree (Figure 4.28). There were five main clades for *Eptesicus serotinus* in the BOLD tree for this species.

The BOLD tree showed that there were two major clades for *Myotis capaccinii* and we had samples that fell on both clades. Those two groups differed by 16 base pairs from each other, and one group came from Thrace only. According to Benda and Horacek (1998), many authors accepted the presence of *M. c. bureschi* in Thrace. We also agree that one group is highly differentiated genetically when compared with the rest of our *Myotis capaccinii* samples. Our results are in concordance with Bilgin et al. (2008a), who showed the presence of two clades in Turkey, eastern Greece and Bulgaria. It should be noted that IUCN does not mention any differentiation within *Myotis capaccinii*.

There were two main clades in the BOLD tree for *Pipistrellus pipistrellus* and our southern individuals fell into one of these clades, reciprocal to the one including an individual from Germany. Our Black Sea individual formed a new clade. The study of Hulva et al. (2007) on cyt-b of *Pipistrellus* species indicated three main clades for continental *Pipistrellus pipistrellus*, namely the European, Moroccan and Sicilian lineages. Our southern individuals possibly clustered with the Moroccan and Sicilian lineages, since the reciprocal clade consisted of an individual from Germany and thus comprising the European lineage in BOLD. Hulva et al. (2010) showed the presence of three different possible haplotype groups in Turkey. Since our individual from the Black Sea region formed a new clade in the BOLD tree, it is possible that our individual is the first record in BOLD representing one of the haplotype groups mentioned in Hulva et al. (2010). *Pipistrellus pipistrellus* from the Black Sea region was different by eight base pairs from the southern individuals. Benda and Horacek (1998) mention the presence of *P. p. pipistrellus* from Northern and Western Turkey and *P. p. aladdin* from Eastern Turkey and the two clades found in this study support that division.

There was a single clade for *Rhinolophus euryale* in the BOLD tree. Our samples were divided into two groups in intraspecific trees and there was a slight difference in locations of the samples from each group in BOLD tree. The phylogenetic analyses of Bilgin et al. (2008b) of this species showed the presence of two reciprocally monophyletic clades. One of these clades was found in the entire sampling range of the species in their study (southeastern Europe and Anatolia), whereas the other clade was found to the east, and our finding of two groups support the findings of Bilgin et al. (2008b).

Our *Rhinolophus ferrumequinum* samples were divided into two groups and each one corresponded to a different clade in the BOLD tree. Previous research suggests that *R. f. ferrumequinum* is expected to inhabit Thrace while *R. f. irani* Eastern Anatolia (Benda and Horacek, 1998). Our data showed that there was an eight base pair difference between western and eastern populations (Figure 4.9). In a recent study (Bilgin et al. 2009), *Rhinolophus ferrumequinum* showed an east/west division within Anatolia. In that study a zone of overlap between two mtDNA clades was observed in southeastern Anatolia, and the geographic positioning of the phylogeographic break in our study is concordant with that study. Interestingly, there was one record of *Rhinolophus clivosus* among *Rhinolophus*

ferrumequinum barcodes in the BOLD tree, forming its own clade; it is possible that this individual was incorrectly identified in BOLD.

Our intraspecific trees for *Rhinolophus hipposideros* were divided into two main groups. The BOLD tree had four divisions and our samples fell into two different clades in it. Genetic divergence among *Rhinolophus hipposideros* was observed as six base pair differences between our two main groups. Benda and Horacek (1998) state that the systematics of *Rhinolophus hipposideros* in Turkey is very complicated.

Our samples from Turkey and Iran fell into the *Plecotus macrobullaris* clade, but onto different branches within this clade. There were 10 base pair differences between Turkish and Iranian populations. The BOLD tree had two main clades for *Plecotus macrobullaris*, and one of these clades represented *Plecotus macrobullaris alpines* and none of our samples clustered with this subspecies. According to Juste et al. (2004), haplotypes of *Plecotus* from mountains of Iran and Syria were genetically hardly distinct from the European samples and they included *Plecotus alpines* within *Plecotus macrobullaris*. Although our BOLD tree and their phylogenetic tree were in concordance regarding the branching, they concluded that this genetic difference among *Plecotus macrobullaris* was insignificant.

Tadarida teniotis had a high intraspecific divergence of 9.54%. There were two clades present for this species in our intraspecific trees. All the sequences taken from BOLD and Genbank formed one clade whereas the rest of the samples from Turkey formed another clade. Similarly, the BOLD tree had also two main clades for *Tadarida teniotis.* Again, sequences from Genbank and BOLD fell into one of these clades, whereas Turkish samples fell into the other clade. IUCN states that populations in Japan, Taiwan and Korea have been treated as a separate species, *T. insignis* since 2005. An update in the BOLD database is needed regarding IUCN records since it is highly probable that the monophyletic clade reciprocal to the one including Turkish samples is representing *T. insignis*. According to Benda and Horacek (1998), two subspecies names are suggested for Turkish population; *T. t. teniotis* and *T. t. rueppelli*. Further research over the whole species range is necessary to establish the taxonomic status of this species, including the Turkish population.

In our study, *Myotis mystacinus* samples from the Aegean, the Central Anatolia and the Mediterranean regions all fell into the same main group in the BOLD tree. The BOLD tree had one bifurcation for this species and most of the samples fell into the main group. In this group, there was still a high degree of variation. Our samples and one individual from Veierland, Norway fell into the same main group in BOLD. According to Benda and Horacek (1998), morphological studies show that at least three different forms occur in the territory of Turkey; however, our genetic results do not support this notion as samples from the three regions in Turkey mentioned above and Norway are in the same clade.

The second group consists of *Barbastella barbestullus, Hypsugo savii, Myotis daubentonii, Pipistrellus kuhlii, Myotis blythii/Myotis myotis, Nyctalus leisleri, Nyctalus noctula, Plecotus kolombatovici, Pipistrellus nathusii* and *Taphozous nudiventris*.

There was a one base pair difference between the Marmara and the Black Sea region samples of *Barbastella barbastellus*. According to Benda and Horacek (1998), this species might be separated as *Barbastella barbastellus* and *Barbastella leucomelas* in Turkey. Northern individuals are considered as *Barbastella barbastellus* whereas southern species might represent *Barbastella leucomelas*. Unfortunately, both of our samples were taken from north and there was not considerable difference between our *Barbastella* samples. Although *Barbastella barbastellus* and *Barbastella leucomelas* differentiation is not clear according to morphological data, separation can potentially be observed genetically in the BOLD tree (see Figure 4.51 above).

Our *Hypsugo savii* samples were from the Central Anatolia region and Iran, and did not differ significantly based on CO1 data. However, the BOLD tree showed that there were four different clades for this species only. Our samples fell into the same clade on the BOLD tree, suggesting that they represented a single taxon. Benda and Horacek (1998) state that *H. s. savii* and *H. s. caucasicus* are two subspecies that are distributed throughout Turkey, however our two samples do not seem to represent separate taxa.

Myotis daubentonii samples were from the Black Sea region. There were two samples and one haplotype for this species. Benda and Horacek (1998) state that there is a cline increase in size of *Myotis daubentonii* from the west to the east, however they are not sure whether this differentiation is large enough to result in nomenclatoric separation at the level of subspecies. Unfortunately we did not have enough samples to add significantly to this discussion. The BOLD tree showed two main clades for this species and one of these was further divided into two branches. Our haplotype fell onto the smaller branch (Figure 4.82).

Our *Pipistrellus kuhlii* samples from the Southeast Anatolia region fell into the same clade in BOLD. However, it is obvious that this species has some major division genetically that needs to be studied further. There were three main clades for *Pipistrellus kuhlii* in the BOLD tree. Benda and Horacek (1998) conclude that there is a gradual transition between the paler form in the south and a darker one that can be coidentified with the nominotypic form, but whether there is a subspecies differentiation or not is still an open question.

Myotis blythii and *Myotis myotis* were two species we studied together in this project. They had an intraspecific divergence of 0.25% together. This value was relatively low when compared to other species which showed higher levels of intraspecific variation, such as *Eptesicus serotinus* and *Tadarida teniotis*. Although we had 18 samples from all around Turkey, we could not find any pattern that was genetically descriptive. Recent speciation or introgressions of mitochondrial haplotypes are likely explanations for genetically similar and morphologically different species (Mayer et al. 2007). According to Berthier et al. (2006), cryptic hybridization is the case for *Myotis myotis* and *M. blythii*. All our samples had similar haplotypes and they all fell to the same clade in BOLD supporting this scenario.

Nyctalus leisleri samples were taken from the Marmara, the Black Sea and the Mediterranean regions; however, they all had the same haplotype. The BOLD tree had one clade for *Nyctalus leisleri*. Benda and Horacek (1998) state that majority of the East-Mediterranean records come from spring and/or autumn transient period and reflects not a resident population but migrants. They suggest that isolated and non-migrating local

populations need to be studied to understand whether there is more than one nominotypic form of *N. l. leisleri*.

Our samples fell into the one and only *Nyctalus noctula* clade present in BOLD. Benda and Horacek (1998) mention the presence of three different groups, but the samples collected from Anatolia could be migrating individuals, as in the case of *Nyctalus lasiopterus*, so it was not easy to draw a definitive conclusion. Our two samples had a two base pair difference in between, with one sample being from the Thrace and the other from the Mediterranean region. It is worth considering that the two *Nyctalus noctula* individuals in BOLD were from Germany, so this clade including our samples may be representing *N. n. noctula*. The two other subspecies mentioned in Benda and Horacek (1998), are *N. n. lebanoticus* (from Levant) and *N. n. meklenburzevi* (from Central Asia), with the nominotypic form *N. n. noctula* being reported from Europe (including the Balkans).

The BOLD tree had four branches for *Plecotus kolombatovici*. Two of the four branches belonged to *Plecotus teneriffae gaisleri*. Our samples from the Central Anatolia region fell into one of the *Plecotus kolombatovici* branches.

Pipistrellus nathusii samples were taken from the Marmara and the Aegean regions. There was only one clade for *Pipistrellus nathusii* in the BOLD tree, and Benda and Horacek (1998) describe the species as being monotypic. Our genetic conclusions support this idea.

Taphozous nudiventris samples were collected from the Southeast Anatolia region. Our samples fell into one of the two clades of *Taphozous nudiventris* in BOLD. Each BOLD clade was further divided into two groups. IUCN (Bates et al. 2008) also assigns four subspecies to *Taphozous nudiventris*, in concordance with the BOLD tree we obtained.

The third group includes the following species; *Asellia tridens, Miniopterus schreibersii pallidus, Myotis auritus, Myotis bechsteinii, Nyctalus lasiopterus, Otonycteris hemprichii* and *Pipistrellus pygmaeus*.

Asellia tridens samples were from Iran only, but we still included them in our study. IUCN data reveals that *Asellia tridens* has not yet been recorded in Turkey. According to Benda and Horacek (1998), this species can be expected to be found in Turkey since the northern margin of its distributional range is very close to the southern Turkish border. There was a separation in BOLD tree for *Asellia tridens*, so it should be further investigated in its own geographic range to understand whether there is a taxonomic division or not. According to IUCN data (Kock et al. 2008), there are three subspecies of *Asellia* globally.

Miniopterus schreibersii pallidus sample was from Iran. According to Benda and Horacek (1998), there are two subspecies of *Miniopterus schreibersii*. *M. s. schreibersii* inhabits Western Anatolia whereas *M. s. pallidus* inhabits Eastern Anatolia. Since our sample was taken from Iran, our finding confirmed this division. In the BOLD tree, our sample fell within the same clade with *M. s. pallidus*. The rest of *Miniopterus schreibersii* was separated into two clades in the BOLD tree. According to Bilgin et al. (2006), *M. s. schreibersii* and *M. s. pallidus* qualify as two separate phylogenetic species in Anatolia. Furman et al. (2010) later suggested that the species were allopatric and the nominal species' range distribution was limited to Europe and the coastal zones of Asia Minor and that the two forms represented separate species. In the light of these studies, *M. s. pallidus* is granted a full species status, a sister taxon to *M. schreibersii.* Our BOLD tree also supports this sister taxon relationship.

The *Myotis aurascens* sample was also from Iran. This species was formerly included in *Myotis mystacinus*; subsequently it was differentiated on the basis of morphology (Benda and Tsytsulina 2000). Based on the BOLD tree, *Myotis aurascens* itself has many clades that need to be studied further.

Myotis bechsteinii sample was taken from the Black Sea region. There were three clades for *Myotis bechsteinii* in BOLD; however, the geographic variation of this species has not yet been described due to the restricted number of records in Turkey, including this study.

Our *Nyctalus lasiopterus* sample was from the Mediterranean region. There was no separation in BOLD tree for this species. Our sample fell into the same group with all the other *Nyctalus lasiopterus* species. Benda and Horacek (1998) agree with the consideration of this species as monotypic and arrange all its populations under *N. l. lasiopterus.*

Our only *Otonycteris hemprichi* sample was from Syria. The BOLD tree showed that there was one clade for this species, but it had many small branches within. Benda and Gvozdik (2010) state that *Otonycteris hemprichii* (from North Africa and the Middle East) and *Otonycteris leucophaea* (from Central Asia) should be regarded as two separate species. They found three sublineages, each considered to be a separate subspecies within the newly defined *Otonycteris hemprichii*. Both Turkish and Syrian populations are regarded as *Otonycteris hemprichii hemprichii* in their study.

Pipistrellus pygmaeus sample was taken from the Marmara region. This sample fell to the one clade belonging to the same species in BOLD. Hulva et al. (2007) mention this group as exhibiting very low genetic variability across its range. This species was previously considered to be a subspecies of *Pipistrellus pipistrellus*; however, the BOLD tree clearly revealed that two species were genetically very different. There were two samples from Norway in the same clade with *Pipistrellus pygmaeus,* including our sample.

BOLD similarity tables for *Eptesicus serotinus, Myotis mystacinus, Pipistrellus kuhlii* and *Taphozous nudiventris* revealed that although these species matched with their own species first, the second closest match was a different species and was more similar to our individuals than another group of their own species. For example, according to the BOLD similarity table for *Eptesicus serotinus,* this species first matched with *Eptesicus serotinus* with a similarity of 100%. The second match was *Eptesicus nilssonii* with a similarity range of 99.29-97.86% and the third match was again *Eptesicus serotinus* with a specimen similarity range of 93.91-93.57%. Similarly, *Eptesicus bottae* was in the second place in the similarity table for our individuals from Antalya and Syria and for *Myotis mystacinus, Myotis cf. aurascens* was in between. The same pattern was observed for *Pipistrellus kuhlii* and *Taphozous nudiventris* because *Pipistrellus deserti* and an unknown *Taphozous* species were in the second place and was more similar to our samples than

another group of their own species, respectively. This shows that there is an uncertainity regarding these species in BOLD; therefore, identifications should be updated based on the new scientific studies. In addition, the probability of introgression between these species should also not be disregarded.

In conclusion, the DNA barcoding of 26 bat species was performed in this study. The genetic data were also compared with previous studies of Turkish bat fauna, especially at the subspecies level. CO1 barcoding was seen to be effective as an identification tool of bat species. BOLD has a very broad library for Chiroptera, and all our sequences matched with a specific bat species. From a phylogeographic perspective, six species (*Eptesicus serotinus, Myotis capaccinii, Pipistrellus pipistrellus, Rhinolophus euryale, Rhinolophus ferrumequinum and Rhinolophus hipposideros, Myotis mystacinus*) showed the presence of more than one clade for Turkey. These species are good candidates for discovery of cryptic species or subspecies. *Plecotus macrobullaris* samples from Iran differed greatly from Turkish samples of the same species, and the difference was also observed in the BOLD tree. Some of *Tadarida teniotis* sequences were obtained from BOLD and Genbank and these sequences were different from Turkish samples to a large degree, by 63 base pairs. Unfortunately, many of the BOLD and Genbank sequences are not available to the public so we do not know sample locations of these sequences. Seven species (*Asellia tridens, Miniopterus schreibersii pallidus, Myotis aurascens, Myotis bechsteinii, Nyctalus lasiopterus, Otonycteris hemprichii, Pipistrellus pygmaeus*) had only one sample available but we still obtained the results from BOLD and compared our data with previous studies regarding Turkish populations. Ten species (*Barbastella barbastellus, Hypsugo savii, Myotis blythii-Myotis myotis, Myotis daubentonii, Nyctalus leisleri, Nyctalus noctula, Pipistrellus kuhlii, Pipistrellus nathusii, Plecotus kolombatovici* and *Taphozous nudiventris*) clustered in one clade with other sequences in BOLD, and comparisons with previous studies reveal that further studies are needed to get a clearer picture of subspecies distribution for these species in Turkey.

REFERENCES

Bates, P., Benda, P., Aulagnier, S., Palmeirim, J., Bergmans, W., Fahr, J., Hutson, A.M., Amr, Z. & Kock, D., 2008. *Taphozous nudiventris*. In: IUCN 2011. IUCN Red List of Threatened Species. Version 2011.2. <www.iucnredlist.org>. Downloaded on 01 March 2012.

Benda, P., Horacek, I., 1998. Bats (Mammalia: Chiroptera) of the Eastern Mediterranean. Part 1. Review of Distribution and Taxonomy of Bats in Turkey. Acta Societatis Zoologicae Bohemicae, 62: 255-313.

Benda, P., Tsytsulina, K. A., 2000. Taxonomic Revision of *Myotis mystacinus* group (Mammalia: Chiroptera) in the Western Palaearctic. Acta Societatis Zoologicae Bohemicae, 64: 331-398.

Benda, P., Gvozdik, 2010. Taxonomy of the genus *Otonycteris* (Chiroptera: Vespertilionidae: Plecotini) as inferred from morphological and mtDNA data. Acta Chiropterologica, 12(1): 83-102.

Berthier, P., Excoffier L. and Ruedi M., 2006. Recurrent replacement of mtDNA and cryptic hybridization between two sibling bat species *Myotis myotis* and *Myotis blythii*. Proceedings of the Royal Society, 273, 3101-3109.

Bilgin, R., Karataş, A., Çoraman, E., Pandurski, I., Papadotou, E., and Morales J. C., 2006. Molecular taxonomy and phylogeography of *Miniopterus schreibersii* (Kuhl, 1817) (Chiroptera: Vespertilionidae), in the Eurasian transition. Biological Journal of the Linnean Society, 87: 577-582.

Bilgin, R., Karataş, A., Çoraman, E., Morales, J. C., 2008a. The mitochondrial and nuclear genetic structure of *Myotis capaccinii* (Chiroptera: Vespertilionidae) in the Eurasian transition, and its taxonomic implications. Zoologica Scripta, 37(3): 253-262.

Bilgin, R., Furman, A., Çoraman, E., Karataş, A., 2008b. Phylogeography of the Mediterranean Horseshoe Bat, *Rhinolophus euryale* (Chiroptera: Rhinolophidae), in southeastern Europe and Anatolia. Acta Chiropterologica, 10(1): 41-49.

Bilgin, R., Çoraman, E., Karataş, A., Morales, J. C., 2009. Phylogeography of the Greater Horseshoe Bat, *Rhinolophus ferrumequinum* (Chiroptera: Rhinolophidae), in Southeastern Europe and Anatolia, with a specific focus on whether the Sea of Marmara is a barrier to gene flow. Acta Chiropterologica, 11(1):53-60.

Clare, E. L., Burton K. L., Engstrom M. D., Eger J. L. and Hebert P. D. N., 2006. DNA Barcoding of Neotropical Bats: Species Identification and Discovery within Guyana. Molecular Ecology Notes. doi: 10.1111/j.1471-8286.2006.01657.x

Clement, M., Posada D. and Crandall K. A., 2000. TCS: A Computer Program to Estimate Gene Genealogies. Molecular Ecology. 9: 1657-1659.

Cox, A. J. & Hebert, P. D. N., 2001. Colonization, Extinction and Phylogeographic Patterning in a Freshwater Crustacean. Molecular Ecology, 10: 371–386.

Dasmahapatra, K. K., Mallet, J., 2006. DNA barcodes: Recent successes and future prospects. Heredity, 97: 254-255.

Doyle, J. J. & Gaut, B. S., 2000. Evolution of Genes and Taxa: A Primer. Plant Molecular Biology, 42: 1–6.

Fenton, M. B., Acharya L., Audet D., Hickey M. B. C., Merriman C., Obrist M. K., Syme D. M. and Adkins B., 1992. Phyllostomid Bats (Chiroptera: Phyllostomidae) as Indicators of Habitat Disruption in the Neotropics. Biotropica, 24(3): 440-446.

Findley, J. S., 1993. Bats: A community perspective. Cambridge University Press.

Francis, C. M., Borisenko A. V., Ivanova N. V., Eger J. L., Lim B. K., Guille´n-Servent A., Kruskop S. V., Mackie I., Hebert P. D. N., 2010. The Role of DNA Barcodes in Understanding and Conservation of Mammal Diversity in Southeast Asia. Public Library of Science One, 5(9): e12575. doi:10.1371/journal.pone.0012575

Furman, A., Postawa T., Öztunç, T., Çoraman E., 2010. Cryptic diversity of the bent-wing bat, *Miniopterus schreibersii* (Chiroptera: Vespertilionidae), in Asia Minor. BMC Evolutionary Biology, 10:121.

Hajibabaei M, deWaard J. R., Ivanova N. V., 2005. Critical Factors for Assembling a High Volume of DNA Barcodes. Philosophical Transactions of the Royal Society of London. Series B, Biological Sciences, 360: 1959–1967.

Hajibabaei M, Smith M.A., Janzen D.H., Rodriguez J. J., Whitfield J. B., Hebert P. D. N., 2006. A Minimalist Barcode Can Identify a Specimen Whose DNA is Degraded. Molecular Ecology Notes, 6: 959-964.

Hajibabaei, M., Singer G. A. C., Clare E. L. and Hebert P. D. N., 2007. Design and Applicability of DNA Arrays and DNA Barcodes in Biodiversity Monitoring. BMC Biology, 5: 24

Hebert, P. D. N., Cywinska, A., Ball S. L. and deWaard J. R., 2003. Biological Identifications through DNA Barcodes. Proceedings of the Royal Society London, 270, 313–321.

Hebert, P. D. N., Penton, E. H., Burns, J. M., Janzen, D. H., and Hallwachs W., 2004a. Ten Species in One: DNA Barcoding Reveals Cryptic Species in the Neotropical Skipper Butterfly *Astraptes fulgerator*. Proceedings of the National Academy of Science, 101: 41.

Hebert, P. D. N., Stoeckle, M. Y., Zemlak, T. S. and Francis, C. M., 2004b. Identification of birds through DNA barcodes. Public Library of Science Biology, 2(10): e312.

Hulva, P., Benda, P., Hanak, V., Evin, A., Horacek, I., 2007. New mitochondrial lineages within the *Pipistrellus pipistrellus* complex from Mediterranean Europe. Folia Zoologica, 56: 378-388.

Hulva, P., Fornuskova, A., Chudarkova, A., Evin, A., Allegrini, B., Benda, P., and Bryja, J., 2010. Mechanisms of radiation in a bat group from the genus *Pipistrellus* inferred by phylogeography, demography and population genetics. Molecular Ecology, 19(24): 5417-31.

Ivanova, N. V., Dewaard J. R., and Hebert, P. D. N., 2006. An Inexpensive, Automation-friendly Protocol for Recovering High-quality DNA. Molecular Ecology Notes. doi: 10.1111/j.1471-8286.2006.01428.x

Juste, J., Ibañez, C., Muñoz, J., Trujillo, D., Benda, P., Karataş, A., Ruedi, M., 2004. Mitochondrial phylogeography of the long-eared bats (*Plecotus*) in the Mediterranean Palaearctic and Atlantic Islands. Molecular Phylogenetics and Evolution, 31: 1114-1126.

Knowlton, N. & Weigt, L. A. 1998. New Dates and New Rates for Divergence Across the Isthmus of Panama. Proceedings of the Royal Society London, B 265, 2257–2263. (DOI 10.1098/rspb.1998.0568.)

Kock, D., Amr, Z., Mickleburgh, S., Hutson, A.M. & Bergmans, W., 2008. *Asellia tridens*. In: IUCN 2011. IUCN Red List of Threatened Species. Version 2011.2. <www.iucnredlist.org>. Downloaded on 28 February 2012.

Librado, P. and Rozas, J., 2009. DnaSP v5: A software for comprehensive analysis of DNA polymorphism data. Bioinformatics, 25: 1451-1452 | doi: 10.1093/bioinformatics/btp187.

Mayer, F. and von Helversen, O., 2001. Cryptic Diversity in European Bats. Proceedings of the Royal Society, 268: 1825-1832.

Mayer, F., Dietz, C. and Kiefer, A. 2007. Molecular species identification boosts bat diversity. Frontiers in Zoology 4: 4.

Meier, R., Zhang G., and Ali F., 2008. The Use of Mean Instead of Smallest Interspecific Distances Exaggerates the Size of the “Barcoding Gap” and Leads to Misidentification. Systematic Biology, 57(5): 809-813.

Miner, B. G., Sultan S. E., Morgan S. G., Padilla D. K. and Relyea R. A. Ecological Consequences of Phenotypic Plasticity. 2005. Trends in Ecology and Evolution, Vol.20 No.12.

Norrander, J., Kempe, T., and Messing, J., 1983. Construction of improved M13 vectors using oligodeoxynucleotide-directed mutagenesis. http://dx.doi.org/10.1016/0378-1119(83)90040-9

Pfenninger, M. and Schwenk, K., 2007. Cryptic Animal Species are Homogeneously Distributed among Taxa and Biogeographical Regions. BMC Evolutionary Biology, 7: 121.

Saccone, C., DeCarla, G., Gissi, C., Pesole, G. & Reynes, A., 1999. Evolutionary Genomics in the Metazoa: The Mitochondrial DNA as a Model System. Gene, 238: 195–210

Sattler, T., Bontadina, F., Hirzel, A. H. and Arlettaz, R., 2007. Ecological Niche Modelling of Two Cryptic Bat Species Calls for a Reassessment of Their Conservation Status. Journal of Applied Ecology, 44, 1188-1199.

Tamura, K., Peterson, D., Peterson, N., Stecher, G., Nei, M., and Kumar, S., 2011 MEGA5: Molecular Evolutionary Genetics Analysis using Maximum Likelihood, Evolutionary Distance, and Maximum Parsimony Methods. Molecular Biology and Evolution, 28: 2731-2739.

Tanner, D. A., Gonzalez J. M., Matthews R. W., Vinson S. B., Pitts, J. B., 2011. Evolution of the Courtship Display of *Melittobia* (Hymenoptera: Eulophidae). Molecular Phylogenetics and Evolution, 60(2): 219-227.

Wares, J. P., Cunningham C. W., 2001. Phylogeography and historical ecology of the North Atlantic intertidal. Evolution, 55(12): 2455-2469.

Wilson, D.E., Reeder D. M., 2005. Mammal Species of the World: A Taxonomic and Geographic Reference, 3rd edn. Johns Hopkins University Press, Baltimore, Maryland.

APPENDIX A: BAT SPECIMENS AND THEIR LOCATIONS

Table A.1. Bat specimens and their locations.

DNA no.	Species (short)	Species name	District	City	Area
1	Rhife	*Rhinolophus ferrumequinum*		Kars	
2	Rhife	*Rhinolophus ferrumequinum*	Kilis	Gaziantep	
3	Rhife	*Rhinolophus ferrumequinum*		Gaziantep	
4	Myobe	*Myotis bechsteinii*		Artvin	
5	Myobly/Myomyo	*Myotis blythii/Myotis myotis*	Dupnisa	Kırklareli	
6	Myobly/Myomyo	*Myotis blythii/Myotis myotis*		Ankara	
7	Myobly/Myomyo	*Myotis blythii/Myotis myotis*		Artvin	
9	Plema	*Plecotus macrobullaris*		Kayseri	
10	Plema	*Plecotus macrobullaris*		Kayseri	
12	Pipku	*Pipistrellus kuhlii*	İçel	Mersin	
13	Pippi	*Pipistrellus pipistrellus*		Van	
15	Pippi	*Pipistrellus pipistrellus*		Konya	
16	Rhieu	*Rhinolophus euryale*		Zonguldak	
17	Rhieu	*Rhinolophus euryale*	Tarsus	Mersin	
18	Barba	*Barbastella barbastellus*	Dupnisa	Kırklareli	
19	Barba	*Barbastella barbastellus*		Rize	
20	Myobly/Myomyo	*Myotis blythii/Myotis myotis*		Osmaniye	
21	Myobly/Myomyo	*Myotis blythii/Myotis myotis*	Tarsus	Mersin	
23	Myobly/Myomyo	*Myotis blythii/Myotis myotis*		Malatya	
24	Myobly/Myomyo	*Myotis blythii/Myotis myotis*		Kayseri	
25	Myobly/Myomyo	*Myotis blythii/Myotis myotis*		Yozgat	
26	Rhife	*Rhinolophus ferrumequinum*	Koyunbaba	Kırklareli	
27	Rhife	*Rhinolophus ferrumequinum*		Şanlıurfa	
28	Myoca	*Myotis capaccinii*		Nevşehir	
29	Myoca	*Myotis capaccinii*	Dupnisa	Kırklareli	
31	Myoca	*Myotis capaccinii*		Bitlis	
32	Myoca	*Myotis capaccinii*	Havran	Balıkesir	
34	Rhieu	*Rhinolophus euryale*		Balıkesir	
35	Rhieu	*Rhinolophus euryale*	Koyunbaba	Kırklareli	
36	Rhieu	*Rhinolophus euryale*		Hatay	
37	Rhieu	*Rhinolophus euryale*	Tarsus	Mersin	
41	Myobly/Myomyo	*Myotis blythii/Myotis myotis*	Tarsus	Mersin	

42	Myobly/Myomyo	*Myotis blythii/Myotis myotis*	Ağzıkara	Afyon	
44	Myobly/Myomyo	*Myotis blythii/Myotis myotis*		Van	
45	Myobly/Myomyo	*Myotis blythii/Myotis myotis*		Osmaniye	
46	Myobly/Myomyo	*Myotis blythii/Myotis myotis*		Erzincan	
47	Myobly/Myomyo	*Myotis blythii/Myotis myotis*		Bitlis	
49	Myobly/Myomyo	*Myotis blythii/Myotis myotis*		Bitlis	
52	Pipku	*Pipistrellus kuhlii*		Urfa	
53	Pipku	*Pipistrellus kuhlii*		Diyarbakır	
54	Plekolombatovici	*Plecotus kolombatovici*		Karaman	
60	Plekolombatovici	*Plecotus kolombatovici*		Karaman	
62	Plemacrobullaris	*Plecotus macrobullaris*		Nevşehir	
63	Plemacrobullaris	*Plecotus macrobullaris*		Kayseri	
65	Plekolombatovici	*Plecotus kolombatovici*		Konya	
66	Plekolombatovici	*Plecotus kolombatovici*		Konya	
67	Rhieu	*Rhinolophus euryale*	Tarsus	Mersin	
68	Rhieu	*Rhinolophus euryale*		Zonguldak	
69	Rhieu	*Rhinolophus euryale*		Denizli	
70	Rhieu	*Rhinolophus euryale*	Tarsus	Mersin	
71	Rhieu	*Rhinolophus euryale*		Kocaeli	
72	Rhieu	*Rhinolophus euryale*		Sinop	
73	Rhife	*Rhinolophus ferrumequinum*		Van	
74	Rhife	*Rhinolophus ferrumequinum*		Rize	
75	Rhife	*Rhinolophus ferrumequinum*		Hatay	
76	Rhife	*Rhinolophus ferrumequinum*		Niğde	
77	Rhieu	*Rhinolophus euryale*		Hatay	
80	Myoca	*Myotis capaccinii*	Dupnisa	Kırklareli	
81	Rhife	*Rhinolophus ferrumequinum*		Mardin	
98	Nyclei	*Nyctalus leisleri*	Dupnisa	Kırklareli	
101	Nyclei	*Nyctalus leisleri*		Trabzon	
102	Nyclei	*Nyctalus leisleri*		Trabzon	
103	Nyclei	*Nyctalus leisleri*		Trabzon	
131	Myobly/Myomyo	*Myotis blythii/Myotis myotis*	Nizip	Gaziantep	
132	Myobly/Myomyo	*Myotis blythii/Myotis myotis*	Viranşehir	Urfa	
133	Pipnathusii	*Pipistrellus nathusii*	Manyas	Balıkesir	Kuş cenneti
135	Tapnu	*Taphozous nudiventris*	Nizip	Gaziantep	
136	Rhife	*Rhinolophus ferrumequinum*	Epcik	Niğde	
137	Pippyg	*Pipistrellus pygmaeus*	Bandırma	Balıkesir	
138	Pippi	*Pipistrellus pipistrellus*	Bafra	Samsun	
139	Rhihi	*Rhinolophus hipposideros*		Ordu	

140	Tadte	*Tadarida teniotis*	Kahta	Adıyaman	
141	Tapnu	*Taphozous nudiventris*	Nizip	Gaziantep	
143	Tadte	*Tadarida teniotis*	Selime	Aksaray	
144	Rhihi	*Rhinolophus hipposideros*	Epcik	Niğde	
147	Myoda	*Myotis daubentonii*	Çepni	Bolu	
149	Pipnathusii	*Pipistrellus nathusii*	Manyas	Balıkesir	Kuş cenneti
153	Tadte	*Tadarida teniotis*	Birecik Köprüsü	Urfa	
161	Rhihi	*Rhinolophus hipposideros*		Antalya	
162	Hypsa	*Hypsugo savii*		Konya	
163	Epser	*Eptesicus serotinus*		Suriye	
165	Myoca	*Myotis capaccinii*		Suriye	
166	Myobly/Myomyo	*Myotis blythii/Myotis myotis*		Suriye	
168	Myoca	*Myotis capaccinii*		Suriye	
169	Myoca	*Myotis capaccinii*		Suriye	
171	Othe	*Otonycteris hemprichii*		Suriye	
174	Rhife	*Rhinolophus ferrumequinum*	Kilitbahir	Çanakkale	
175	Myomys	*Myotis mystacinus*	Banaz	Uşak	
177	Tapnu	*Taphozous nudiventris*	Nizip	Gaziantep	
182	Rhihi	*Rhinolophus hipposideros*	Sındırgı	Balıkesir	
184	Rhife	*Rhinolophus ferrumequinum*	Sındırgı	Balıkesir	
188	Rhihi	*Rhinolophus hipposideros*	Hafik	Sivas	
190	Rhihi	*Rhinolophus hipposideros*	Yaylabaşı	Erzincan	
191	Rhihi	*Rhinolophus hipposideros*		Urfa	
195	Rhihi	*Rhinolophus hipposideros*		Zonguldak	
196	Rhihi	*Rhinolophus hipposideros*		Zonguldak	
197	Rhihi	*Rhinolophus hipposideros*		Zonguldak	
199	Nycnoc	*Nyctalus noctula*		Kırklareli	
200	Rhieu	*Rhinolophus euryale*		Kocaeli	
202	Rhife	*Rhinolophus ferrumequinum*		Karabük	
203	Epser	*Eptesicus serotinus*		Zonguldak	
204	Rhihi	*Rhinolophus hipposideros*		Bartın	
205	Rhife	*Rhinolophus ferrumequinum*		Zonguldak	
207	Pipnathusii	*Pipistrellus nathusii*		Afyon	
208	Rhihi	*Rhinolophus hipposideros*	Ayancık	Sinop	
211	Rhihi	*Rhinolophus hipposideros*	Maçka	Trabzon	
213	Pipku	*Pipistrellus kuhlii*	Nizip	Gaziantep	
217	Pipku	*Pipistrellus kuhlii*	Eski Kale	Mardin	
219	Pipku	*Pipistrellus kuhlii*	Türkoğlu	Kahramanmaraş	
223	Pipku	*Pipistrellus kuhlii*	Kahta	Adıyaman	

224	Pipku	*Pipistrellus kuhlii*	Ceylanpınar	Şanlıurfa	
226	Pipku	*Pipistrellus kuhlii*	Kilis	Gaziantep	
228	Pipku	*Pipistrellus kuhlii*	Börgenek Köyü	Adıyaman	
230	Pipku	*Pipistrellus kuhlii*		Iğdır	
231	Myoda	*Myotis daubentonii*	Traverten Mağ	Bolu	
235	Rhihi	*Rhinolophus hipposideros*	Çaybaşı	Bursa	
243	Myomys	*Myotis mystacinus*	Hacıbekirçiftliği köyü	Yozgat	
245	Rhihi	*Rhinolophus hipposideros*	Saray Köyü, Yenice	Karabük	
248	Hypsa	*Hypsugo savii*	Ermenek	Karaman	
251	Nycnoc	*Nyctalus noctula*		Osmaniye	
252	Plemacrobullaris	*Plecotus macrobullaris*	Zencan	Iran	
255	Aselia	*Asellia tridens*	Ilam	Iran	
256	Hypsa	*Hypsugo savii*		Iran	
257	Myoaur	*Myotis aurescens*		Iran	
258	Plemacrobullaris	*Plecotus macrobullaris*		Iran	
259	Plemacrobullaris	*Plecotus macrobullaris*	Zencan	Iran	
260	Plemacrobullaris	*Plecotus macrobullaris*	Elmalı	Antalya	
261	Myomys	*Myotis mystacinus*	Beşkonak	Antalya	
263	Aselia	*Asellia tridens*	Ilam	Iran	
265	Nyclei	*Nyctalus leisleri*		Antalya	
269	Epser	*Eptesicus serotinus*	Elmalı	Antalya	
270	Epser	*Eptesicus serotinus*	Beşkonak	Antalya	
271	Nycla	*Nyctalus lasiopterus*	Elmalı	Antalya	
M152	Minsc	*Miniopterus schreibersii pallidus*	Ilam	Iran	Sarin Ab-Garma

APPENDIX B: HAPLOTYPE NETWORK TABLES

Table B.1. Haplotype network table for *Rhinolophus euryale.*

Haplotype	Number of individuals	Code for the individuals as seen in the intraspecific trees (Figure 4.3)
H1	1	77
H2	7	68-71-69-16-200-35-34
H3	2	67-70
H4	1	72
H5	2	17-37
H6	1	36

Table B.2. Haplotype network table for *Rhinolophus ferrumequinum.*

Haplotype	Number of individuals	Code for the individuals as seen in the intraspecific trees (Figure 4.8)
H1	1	2
H2	1	3
H3	4	26-174-205-202
H4	2	27-75
H5	3	1-74-81
H6	1	73
H7	2	136-76
H8	1	184

Table B.3. Haplotype network table for *Rhinolophus hipposideros.*

Haplotype	Number of individuals	Code for the individuals as seen in the intraspecific trees (Figure 4.12)
H1	7	245-195-208-204-196-235-197
H2	3	188-190-139
H3	1	161
H4	1	144
H5	1	182
H6	1	191
H7	1	211

Table B.4. Haplotype network table for *Tadarida teniotis.*

Haplotype	Number of individuals	Code for the individuals as seen in the intraspecific trees (Figure 4.21)
H1	6	ABBM293-ABBM310-ABBM311-HM541963-HM541964-HM541965
H2	2	153-143
H3	1	140

Table B.5. Haplotype network table for *Eptesicus serotinus.*

Haplotype	Number of individuals	Code for the individuals as seen in the intraspecific trees (Figure 4.26)
H1	4	ABBM280-BM084-HM540267-HM540268
H2	2	ABBM380-HM540269
H3	2	269-270
H4	1	203
H5	1	163

Table B.6. Haplotype network table for *Nyctalus noctula.*

Haplotype	Number of individuals	Code for the individuals
H1	1	199
H2	1	251

Table B.7. Haplotype network table for *Pipistrellus kuhlii.*

Haplotype	Number of individuals	Code for the individuals as seen in the intraspecific trees (Figure 4.37)
H1	7	52-53-213-226-230-217-224
H2	1	12
H3	2	223-228
H4	1	219

Table B.8. Haplotype network table for *Pipistrellus pipistrellus.*

Haplotype	Number of individuals	Code for the individuals as seen in the intraspecific trees (Figure 4.43)
H1	1	13
H2	1	138
H3	1	15

Table B.9. Haplotype network table for *Barbastella barbastellus.*

Haplotype	Number of individuals	Codes for the individuals as seen in BOLD tree (Figure 4.51)
H1	1	18
H2	1	19

Table B.10. Haplotype network table for *Plecotus kolombatovici.*

Haplotype	Number of individuals	Code for the individuals as seen in the intraspecific trees (Figure 4.55)
H1	2	65-66
H2	2	54-60

Table B.11. Haplotype network table for *Plecotus macrobullaris.*

Haplotype	Number of individuals	Code for the individuals as seen in the intraspecific trees (Figure 4.59)
H1	3	252-258-259
H2	1	62
H3	1	10
H4	1	260
H5	2	9-63

Table B.12. Haplotype network table for *Hypsugo savii.*

Haplotype	Number of individuals	Code for the individuals as seen in the intraspecific trees (Figure 4.65)
H1	2	162-248
H2	1	256

Table B.13. Haplotype network table for *Myotis blythii-Myotis myotis.*

Haplotype	Number of individuals	Code for the individuals as seen in intraspesific trees (Figure 4.73)
H1	1	131
H2	2	132-49
H3	7	20-41-24-23-45-7-25
H4	1	46
H5	2	6-21
H6	1	44
H7	1	42
H8	1	166
H9	1	5
H10	1	47

Table B.14. Haplotype network table for *Myotis capaccinii.*

Haplotype	Number of individuals	Code for the individuals as seen in the intraspecific trees (Figure 4.77)
H1	6	28-31-32-165-168-169
H2	2	29-80

Table B.15. Haplotype network table for *Myotis mystacinus.*

Haplotype	Number of individuals	Code for the individuals as seen in the intraspecific tree (Figure 4.84)
H1	1	175
H2	1	243
H3	1	261